Characterization of the murine pulmonary phagocytic network during *Aspergillus fumigatus* infection

Inaugural-Dissertation
zur
Erlangung des Doktorgrades

Dr. rer. nat.

der Fakultät für
Biologie

an der

Universität Duisburg-Essen

vorgelegt von

Pegah Seddigh

aus Tehran, Iran

June 2016

Die der vorliegenden Arbeit zugrunde liegenden Experimente wurden am Institut für Experimentelle Immunologie und Bildgebung der Universität Duisburg-Essen durchgeführt.

1. Gutachter: Prof. Dr. Matthias Gunzer
2. Gutachter: Prof. Dr. Karl Sebastian Lang

Vorsitzender des Prüfungsausschusses: Prof. Dr. Markus Kaiser

Tag der mündlichen Prüfung: 02.09.2016

Publications during thesis

Professional articles

Hasenberg A, Hasenberg M, Männ L, Neumann F, Borkenstein L, Stecher M, Kraus A,Engel DR, Klingberg A, **Seddigh P**, Abdullah Z, Klebow S, Engelmann S, Reinhold A, Brandau S,Seeling M, Waisman A, Schraven B, Göthert JR, Nimmerjahn F, Gunzer M. **Catchup: a mouse model for imaging-based tracking and modulation of neutrophil granulocytes Nat Methods**. 12(5):445-52. doi: 10.1038/nmeth.3322. Epub 2015 Mar 16

Poster presentations

Title of the posters: Characterization of the murine pulmonary phagocytic network during *Aspergillus fumigatus* infection

Medizinisches Forschungszentrum (MFZ), Science day, Essen, Germany, 2013, 2014, 2015

BIOME Graduate School of Biomedical Science, retreat, Essen, Germany 2015

4th European Congress of Immunology (ECI), Vienna, Austria, 2015

44th Annual Meeting German Society for Immunology (DGFI), Bonn, Germany, 2014

43rd Annual Meeting German Society for Immunology (DGFI), Mainz, Germany, 2013

BIOME Graduate School of Biomedical Science, retreat, Hamminkeln, Germany 2012

Oral presentations

Title of the talks: Characterization of the murine pulmonary phagocytic network during *Aspergillus fumigatus* infection

International Leibniz Research School for Microbial and Biomolecular Interactions (ILRS), Annual Symposium, Jena, Germany, 2013, 2014 and 2015

The Centre for Medical Biotechnology (ZMB), lunch seminar, Essen University, Germany, 2013, 2014, 2016

BIOME Graduate School of Biomedical Science, Essen University hospital, Germany, 2013 and 2014

Winter seminar, Medicine faculty of university hospital Essen, Pichl, Austria, 2015

To my dear parents

Abbreviation

°C	Degree Celsius
µg	Microgram
µl	Microliter
µm	Micrometer
A	
A.	*Aspergillus*
Ab	Antibody
ABPA	Allergic Bronchopulmonary Aspergillosis
CAN	Acetonitrile
ACQ	6-Aminoqinolyl-N-Hydroxysuccinimidyl-carbamote
AEC	Alveolar epithelial cell
AF	Alexa Fluor
AP	Alkaline phosphatase
APC	Antigen presenting cell
APC	Allophycocyanin
APS	Ammonium persulfate
AMM	*Aspergillus* minimal medium
ASA	Amino acid analysis
B	
BAL	Bronchoalveolar lavage
BADJ	Bronchoalveolar duct junction
BASC	Bronchoalveolar stem cell
BCIP	5-Bromo-4-chloro-3-indolyl phosphate
Bl6	C57BL/6

BM	Bone marrow
BSA	Bovine serum albumin
C	
C3	Complement component 3
CD	Cluster of Differentiation
c-DNA	Complementary DNA
CDP	Common dendritic cell progenitors
CFU	Colony-forming unit
CHAPS Propanesulfonic Acid	3- ((3-Cholamidopropyl)dimethylammonio)-1-
CHI3L1	Chitinase-3-like protein 1
CLR	C-type lectin receptor
Cre	Cyclization recombinase
D	
DAPI	4',6-diamidino-2-phenylindole
DC	Dendritic cell
2-D DIGE electrophoresis	Two-dimensional fluorescence difference gel
dd H_2O	Double-distilled water
DMB	1,2-diamino-4,5-methylendioxybenzene
DMEM	Dulbecco's Modified Eagle Medium
DNA	Deoxyribonucleic acid
DNase	Deoxyribonuclease
DTT	Dithiothreitol
E	
ECL	Enhanced chemiluminescence
EDTA	Ethylenediaminetetraacetic acid
ELISA	Enzyme-linked immunosorbent assay
EpCAM	Epithelial cell adhesion molecule

ESI	Electrospray ionization
F	
FDR	False discovery rate
FITC	Fluorescein isothiocyanate
G	
G	Gauge
G	G-force
GAPDH	Glyceraldehyde 3-phosphate dehydrogenase
G-CSF	Granulocyte-colony stimulating factor
GFP	Green fluorescent protein
GM-CSF	Granulocyte-macrophage colony-stimulating factor
H	
HCD	Higher-energy collisional dissociation
HCL	Hydrogen chloride
HPLC	High Performance Liquid Chromatography
I	
I3P	Indole-3-pyruvate
IA	Invasive Aspergillosis
ICAM-1	Intercellular Adhesion Molecule 1
IFN	Interferon
Ig	Immunoglobulin
IL	Interleukin
IL4i1	Interleukin 4-induced 1
Inf	Infected
IP	Intraperitoneal
IPG strip	Immobilized pH gradient
IEF	Isoelectric focusing
ITAM	Immunoreceptor tyrosine-based activation like motif
IV	Intravenous

K	
KIC	α-ketoisocaproate
KIV	α-Ketoiso valerate
KMV	α-keto-β-methyl-n-valeric acid
k.o.	Knock out
L	
LCMS	Liquid chromatography mass spectrometry
Lcn 2	Lipocalin-2
LFA-1	Lymphocyte function-associated antigen-1
LoxP	Locus of crossing (x) over, bacteriophage P1
M	
MAC-1	Macrophage-1 antigen
MACS	Magnetic cell separation
MHC	Major Histocompatibility complex
m/z	Mass/Charge
MP	Multiphoton
mRNA	Messenger RNA
MYD88	Myeloid Differentiation Primary Response 88
N	
NBT	Nitroblue Tetrazolium
NET	Neutrophil extracellular traps
NF-κB	Nuclear factor 'kappa-light-chain-enhancer' of activated B-cells
n.s	Not significant
NZW	New Zealand White
O	
OPD	O-phenylendiamine
P	
PAMP	Pathogen-associated molecular patterns

PBS	Phosphate-buffered saline
PCA	Principal Component Analysis
PCR	Polymerase chain reaction
PE	Polyethylene
PE	Phycoerythrin
PECAM	Platelet endothelial cell adhesion molecule
PE-Cy7	Phycoerythrin-Cyanine7
PFA	Paraformaldehyde
Phepyr	Phenylpyruvate
PMT	Photomultiplier tube
ProSp-C	Pro surfactant protein-C
PRR	Pattern recognition receptors
PSI	Pounds per square inch
PSM	Peptide spectrum matches
PVDF	Polyvinylidene difluoride
Q	
qPCR	quantitative PCR
R	
RCF	Relative centrifugal force
Relm-alpha	Resistin-like molecule-alpha
Retnla	Resistin like alpha
RNA	Ribonucleic acid
RP-HPLC	Reversed phase HPLC
ROS	Reactive oxygen species
SFTPD	Surfactant protein D
RPM	Round per minute
RPMI	Roswell Park Memorial Institute medium
RT	Room temperature
S	

SDS	Sodium dodecyl sulfate
SEM	Scanning electron microscopy
SLE	Systemic lupus erythematous
T	
TAE	Tris-acetate-EDTA
TBS	Tris-buffered saline
TCR	T-cell receptor
tdTomato	Tandem dimer Tomato
TEMED	Tetramethylethylenediamine
TFA	Trifluoroacetic acid
TLR	Toll like receptor
TMEM173	Stimulator of interferon genes protein
TNF-α	Tumor necrosis factor-alpha
U	
UV	Ultraviolet
V	
V	Voltage
VLA-4	Very late antigen-4

List of figures

List of tables

Table of contents

Zusammenfassung

Aspergillus fumigatus ist ein ubiquitärer, luftübertragener Schimmelpilz, der eine weit verbreitete Gefahr für immunsupprimierte Patienten darstellt und in der Lage ist, die invasive Aspergillose (IA) hervorzurufen, ein Krankheitsbild mit hoher Sterblichkeitsrate. In immunkompetenten Individuen hingegen wird diese Infektion sehr effizient mit Hilfe der phagozytotischen Eigenschaften verschiedener Zelltypen des Immunsystems, wie beispielsweise Alveolarmakrophagen, Neutrophile Granulozyten und Dendritische Zellen, bekämpft. Möglicherweise spielen jedoch neben den drei oben genannten professionellen Phagozyten, auch „unprofessionelle“ phagozytotische Zellen, wie die alveolaren Epithelzellen des Typs I und II (AEC) eine zentrale Rolle für die Bewältigung der Pilzinvasion. Obwohl bereits viele Studien die Interaktion zwischen professionellen Phagozyten und *A. fumigatus* detailliert analysiert haben, konzentrieren sich nur wenige Arbeiten auf die Interaktion des Pilzes mit alveolaren Epithelzellen. Aus diesem Grund wurde im Rahmen dieser Arbeit mit der Analyse der Proteomregulation der AECII nach pulmonaler *A.fumigatus* Infektion begonnen. Zuerst wurde ein Protokoll zur negativen, magnetischen Isolierung muriner AECII mit einer Reinheit von über 90% erfolgreich etabliert. Mit Hilfe dieser Methode wurden dann AECII aus infizierten Mauslungen isoliert und ihr Proteom im Vergleich zu AECII aus nicht infizierten Tieren mittels Flüssigchromatographie/Massenspektrometrie (LCMS) analysiert. Aus der sich ergebenden Liste signifikant regulierter Proteine wurde das Protein mit der deutlichsten Hochregulierung für weitere Untersuchungen im Rahmen von *A.fumigatus* Infektionen ausgewählt. Durch weitere experimentelle Ansätze, wie qRT-PCR, Western Blot und Immunhistochemie konnte zunächst die deutliche Hochregulierung des Proteins bestätigt werden. Anschließend wurde ein Mausmodel mit *knock-out* für das entsprechende Protein verwendet, um seine Bedeutung unter Infektionsbedingungen zu untersuchen. Aus Parametern wie Überlebensrate, Kolonie bildenden Einheiten (CFUs), Neutrophilenrekrutierung in die Lunge infizierter Tiere und TNF-α-Sekretions-Level in Proben aus der bronchoalveolaren Lavage, konnten keine Unterschiede in dieser Mauslinie im Vergleich zu Wildtypmäusen festgestellt werden. Die Rolle und Bedeutung weiterer

vielversprechenden Proteine aus der in dieser Arbeit erstellten Liste sollten daher in künftigen Arbeiten charakterisiert werden

Einen weiteren zu untersuchenden Zelltyp in dieser Studie stellten die Neutrophilen Granulozyten dar, da sie in Bezug auf Anzahl und Funktion die wichtigsten Zellen im Verlauf einer *A.fumigatus*-Infektion der Lunge sind. Darüber hinaus ist Neutropenie die häufigste Todesursache bei Patienten mit invasiver Aspergillose . Das Ziel in diesem Teil der Studie war es, die Neutrophilen Granulozyten aus verschiedenen Stellen der Maus zu isolieren. Zu diesem Zweck mussten Protokolle etabliert werden für die Isolierung von Neutrophilen aus dem Knochenmark, Blut und bronchoalveolarer Lavage (BAL) von *A. fumigatus* infizierten Tieren . Die neue „Catchup“ Mauslinie mit transgenen tdTomato exprimierenden Neutrophilen stellte hierfür das perfekte Werkzeug dar. Nach der Isolierung von Neutrophilen wurde ihre Proteinzusammensetzung mittels LCMS charakterisiert. Über 3000 Proteine wurden detektiert und mittels Hauptkomponentenanalyse untersucht. Diese Daten zeigten, dass die Neutrophilengruppe aus der BAL-Isolation mit unmittelbarem Kontakt zu Pilzsporen die deutlichsten Änderungen bezogen auf die Proteinmenge aufweist. Diesem Ergebnis folgend sollten sich künftige Untersuchungen, wie z.B. die Charakterisierung von Phänotypen in entsprechenden *knock out* Mäusen, auf Proteine konzentrieren, die in dieser experimentellen Gruppe deutlich reguliert waren.

1 Abstract

Aspergillus fumigatus is a ubiquitous, airborne mold and a common threat for immunosuppressed patients as it can induce invasive aspergillosis, characterized by a tremendously high mortality rate. Immunocompetent individuals on the other hand, encounter this infection very efficiently due to the phagocytic action of different immune cell types such as alveolar macrophages, neutrophil granulocytes and dendritic cells we believe, that beside these professional phagocytes, “unprofessional” phagocytic cells, such as alveolar epithelial type I and II cells (AEC) also constitute a central element for encountering fungal invasion.

Although many studies have deeply analyzed the interaction between professional phagocytes and *A. fumigatus,* just few works have concentrated on the fungal interaction with alveolar epithelial cells. With this ground, we started with analyzing the proteome regulation of AECII after pulmonary *A. fumigatus* infection. We started with the successful establishment of a negative, magnetic isolation protocol to isolate primary murine AECII with purity greater than 90 %. Using this method, we isolated AECII from infected murine lungs and characterized their proteomic constitution by liquid chromatography mass spectrometry (LCMS) in comparison to AECII from uninfected animals. From the resulting list of significantly regulated proteins the protein with the highest up-regulation was chosen for further investigation in the context of an *A. fumigatus* infection. By additional experimental approaches, such as qRT-PCR, Western Blot and Immunohistology we could first of all confirm the initially detected high level of up-regulation. Subsequently, we employed a knock-out mouse model for the protein to investigate its significance under infection conditions. Addressing different parameters, such as survival, colony forming units (CFU), Neutrophil recruitment to the lungs of the infected animals and TNF- α secretion level in bronchoalveolar lavage fluid, we unfortunately could not find a different behavior of this mouse strain, compared to wildtype animals. Hence, future work should characterize the role and importance of further promising proteins from the generated list of this work.

The next cell type to investigate in this study was neutrophil granulocytes as they are known to be the major immune cells in number and function for facing *A. fumigatus* infection inside the lung. Additionally, neutropenia is the main cause

of death for IA patients. The aim for this part of the study was to isolate neutrophil granulocytes from different sites of the same mouse. In other words, protocols for neutrophil isolation of bone marrow, blood and bronchoalveolar lavage (BAL) of *A. fumigatus* infected animals had to be set up. The novel “Catchup” mouse line with transgenic tdTomato expressing neutrophils was the useful tool to perform this task. After neutrophil isolation, they were further investigated in protein level by LCMS. Over 3000 proteins were detected and analyzed in a principal component plot. According to this data the neutrophil group isolated from BAL with direct contact to fungal spores indicated the most variance in protein abundancies. With this hint further investigation on the expressed proteins from this experimental group should be performed such as looking for phenotypes in the knock out mice for the most relevant regulated proteins during *A. fumigatus* infection.

2 Introduction

2.1 Airway infections

Infectious diseases are caused by a variety of bacteria, viruses, fungi or parasites (Zumla et al., 2016). Their infectious mechanisms, which are characteristic for each pathogen include their tropism, their route of infection, the pathogenesis mechanisms and their replication and life cycle systems.(Murphy et al., 2012) In the airways, epithelial cells, mucosal layers and cilia are the first physical barriers that pathogens have to succumb before they can enter into deeper lung tissues Phagocytes of the innate immune system, like macrophages are the next line of defense, and later the adoptive immune response. In case that the immune system cannot properly suppress the pathogens they replicate extensively and spread into different organs (Khan et al., 2016). Severeness and symptoms of an infection depend on the location in which the pathogen resides. *Streptococcus pneumoniae* is a good example. It causes pneumonia in the lung, while in the blood leads to pneumococcal sepsis, in the middle ear it causes Otitis media, Meningitis in the brain and bacteremia by invading into the brain (Daniels et al., 2016). Among all these sites, the respiratory tract is one of the most common targets for different types of infections. The wo main types of infections are upper respiratory tract infection, which occur in the nose, sinuses and throat and lower respiratory tract infections, which take place in the airways and lungs (Lee et al., 2016). *Aspergillus fumigatus (A. fumigatus)* is an example for the latter. Daily and repeated exposures to this mold do not cause serious diseases in healthy individuals. However, immunosuppressed patients can suffer from severe Aspergillosis and eventually death (Ben-Ami et al., 2010).

2.1.1 *A. fumigatus*

A. fumigatus is a saprophytic fungus with its natural niche in soil, which is absolutely necessary for carbon and nitrogen recycling. This mold can be found on organic debris and is one of the most ubiquitous fungi in the world (Haines, 1995). *A. fumigatus*' spores are 2-3 µm in diameter and are called conidia. This word roots in the Greek word Konis which means dust. Conidia are extremely light and airborne. We inhale via nose or mouth a huge amount of conidia with our breathing

air. Afterwards, conidia reside in the alveoli and cause strong immune responses. Surveys have shown that each human is in contact with some hundreds of these conidia per day (Chazalet et al., 1998) but the innate immune system of a healthy individual can efficiently keep them in check. Initially, *A. fumigatus* was known as a pathogen responsible for farmer's lung disease, which is an allergic reaction to conidia in case of unusually heavy contact with organic debris; *A. fumigatus* can trigger Invasive Aspergillosis (IA) which is a life threatening disease in individuals receiving immunosuppressive drugs due to solid organ transplantation or under leukemic treatment. (Rogers, 1995). During the last 10 years, *A. fumigatus* has become the most extensive airborne fungal pathogen and is roughly responsible for more than 90 % of human fungal infections (Andriole, 1993)

2.1.1.1 *A. fumigatus* reproduction life cycle

A. fumigatus has an asexual reproduction cycle. Conidia scatter around by air and. find the best conditions to grow in the human body, in terms of temperature, humidity and amount of supplied oxygen. What makes conidia sustainable to environment is especially their tolerance to high temperature. If they enter a location with favorable conditions for growth, haploid hyphae begin to form one of their diversions called foot cells. Foot cells swell in the next step and a vesicle called conidiophore shapes.

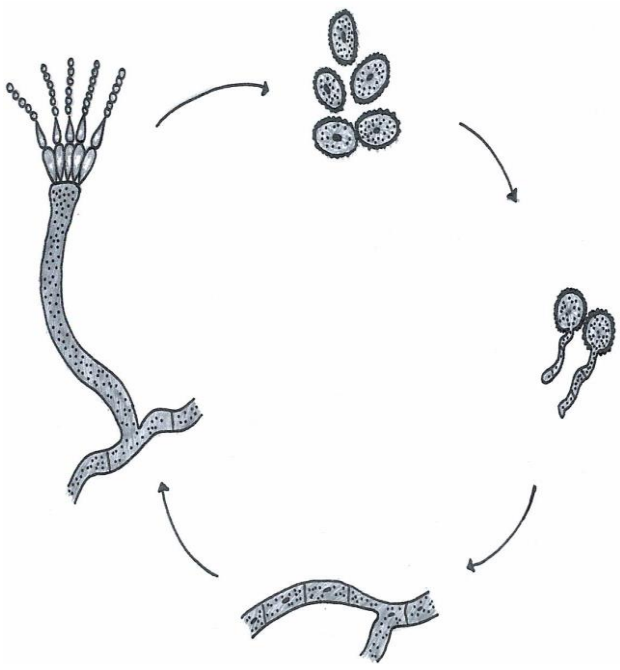

Figure 2.1 *A. fumigatus* asexual life cycle Conidia place in a humid location. Germinates and produces hypha. Hypha's foot cells swell and create conidiophore

Via a number of mitotic divisions conidia are formed (Fig 2.1) (Kwon-Chung et al., 1992).

For a eukaryotic fungus, like *A. fumigatus* it is known that sexual reproduction is a common alternative way to reproduce. Scientists taking this fact into account, quite recently have started

investigating *A. fumigatus*' sexual life cycle. Performing genome sequencing, they discovered that genes for sexual reproduction like putative pheromones, receptors and signaling proteins are present within the fungal DNA, which indicates a sexual life cycle (Dyer et al., 2005). Moreover, recently, productive mating of *Aspergillus fumigatus* has been shown in the laboratory (O'Gorman et al., 2009). Although an asexual life cycle is still counted as the main, faster and less complicated reproduction process for *Aspergillus*, Sexual reproduction can increase the chance of survival of the species (Ene et al., 2014).

2.1.1.2 Invasive Aspergillosis

Although *A. fumigatus* can cause infection in the skin, peritoneum, eyes, bones, kidneys and gastrointestinal tract, the main sight of infection for this mold is the respiratory tract. Within the respiratory tract, the specific location of the infection and the severity of the spreading of the mycelium are the two determining factors for the type of the disease (Latgé, 1999). Invasive Aspergillosis (IA) is a highly lethal form of *Aspergillus* infection, which is most critical for immunosuppressed individuals such as acute leukemia patients, bone marrow and solid transplant recipients and AIDS patients (Ribaud et al., 1994) (Brown et al., 1998). There are four main types of IAs in immunocompromised patients according to the location of the infection: 1) pulmonary aspergillosis (most common), 2) tracheobronchitis, 3) rhinosinusitis and 4) disseminated disease usually in the brain (Denning, 1998). Although many different methods for the detection of IA have been proposed so far, there is still remaining difficulty in the diagnosis process. Up to now, tissue histopathological tests are the most definite diagnostic method as the clinical symptoms such as fever, chest pain and weight loss are relatively nonspecific (Boon et al., 1991). CT scan is another approach for the detection of IA. With this method a classic "halo" is the characteristic for hemorrhagic necrosis of the tissue (Caillot et al., 1997). Some other approaches are microscopy, detection of *A. fumigatus* in serum, culture of the sputum or bronchoalveolar lavage (BAL) from the patients, nasal swabs and specimens from bronchoscopy trials and last but most specific, quantification of serum antigens by ELISA (Horvath et al., 1996; Nalesnik et al., 1980) (Martino et al., 1989) (Denning, 1998; Latge, 1995)

2.2 Immune responses to *A. fumigatus*

As the whole respiratory tract is exposed to the environment, different types of pathogens such as A. fumigatus' conidia can enter and settle in this organ. Therefore, different strategies evolved to fight pathogens in the lung (Newton et al., 2016). In the first place, inhaled pathogens and allergens are inhibited via a process in this physical barrier called mucociliary clearance. Ciliated cells, Goblet cells (mucus secreting), Basal cells and Clara cells are the main cell types, which are involved in this process. The efficiency of the system depends on the cilia beat speed and mucus production (Gohy et al., 2016). Bronchial epithelial cells secret mucins, cytokines and chemokines (Holgate, 2007). On the other hand, the epithelium produces a chemical barrier against pathogens such as antimicrobial substances (Hupin et al., 2013). The next strategy to encounter inhaled pathogens represents phagocytosis via lung resident phagocytosing cells (Fig 2.2).

A. fumigatus is detected by phagocytes of the innate immune system via the receptor Dectin-1. Beta-1, 3-glucan is the carbohydrate epitope of the fungus that is recognized by Dectin-1 (Drummond et al., 2011). This receptor is a member of the big family of C-type lectin receptors (CLR) that bind to carbohydrates. C stands for calcium, since the binding requires calcium. Dectin-1 is a transmembrane receptor with a cytoplasmic and an extracellular domain (Brown et al., 2001). The cytoplasmic domain carries an immunoreceptor tyrosine-based activation like motif (ITAM),which is phosphorylated after the ligation of the extracellular domain (Ariizumi et al., 2000). This event leads to NF-κB activation and eventually production of ROS and pro inflammatory cytokines such as TNF-α and IL-12. This activation results in the recruitment of more immune cells (Gross et al., 2006). After the recognition of the antigen from *A. fumigatus* by Dectin-1 the phagocytosis process proceeds (Michael K. Mansour et al., 2012).

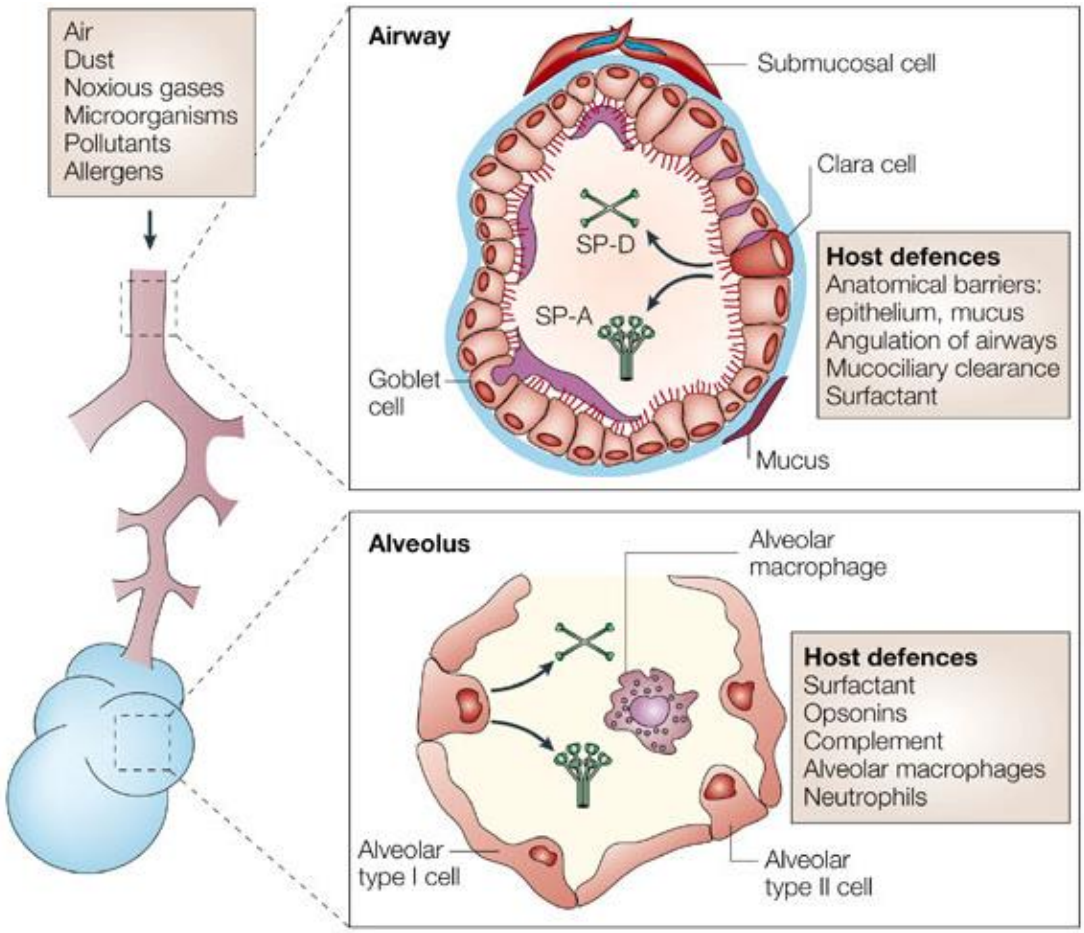

Figure 2.2 Different strategies used against invading pathogens inside the lung
Pathogen clearance inside the lung starts with a physical and anatomical barrier called mucociliary clearance by ciliated cells, Goblet cells, Basal cells and Clara cells. It continues with chemical barriers such as mucus and cytokine secretion by epithelial cells. In case the clearance was not performed efficiently, innate immune phagocytes come to play an important role (Wright, 2005).

2.2.1 Phagocytosis and phagocytes of the innate immune system during *A. fumigatus* infection

Phagocytosis is one of the most important cellular functions of the innate immune system. During this process pathogens, foreign particles or apoptotic cells are engulfed and digested by innate immune cells in vesicles within their cytoplasm (Fig 2.3). Macrophages, neutrophil granulocytes and dendritic cells are so called professional phagocytes (Alberts, 2002). As soon as pathogens encounter phagocytes, they are engulfed by projection of pathogen's membrane. This protrusion of the membrane is called pseudopodia. With this process a vesicle called phagosome forms. In the phagosome, pathogen components stimulate the

toll like receptors (TLRs) and this leads to the expression of a number of genes. An important gene being expressed resulting from TLR stimulation is myeloid differentiation primary response gene 88 (MYD88) (Xiang et al., 2015). Consequently, NFκB and other signaling pathways are activated and inflammatory cytokines become induced. It is known that in the absence of TLR2, TLR4 or MYD88 due to impaired phagosome maturation, phagocytosis of different bacteria diminishes (Takeda et al., 2005). After formation of the phagosome the intracellular degradation of the microbial components occurs. This task is done by fusion of the phagosomes with the lysosomes (Gordon, 2016). Lysosomes are one of the cell's organelles that contain about 50 different kinds of enzymes for the breakdown of biological polymers such as lipids, carbohydrates, nucleic acids and proteins. Some examples of lysosomal enzymes are sulfatases, proteases and glycosidases. Lysosomes appear as globular shaped vacuoles with an acidic pH that differ in size depending on the digested material. Phagosomes fused with lysosomes form an enormous organelle called phagolysosome (Cooper et al., 2013). Resulting debris from the digestion process become either exocytosed or, in case of small molecular fragments, are presented to T cells of the adoptive immune system via the Major Histocompatibility Complexes (MHC) (Kindt et al., 2007). In the next pages all phagocytes of the innate immune system with crucial roles in clearing an *A. fumigatus* infection are explained in detail.

2.2.1.1 Monocyte/Macrophages

Monocytes from blood immigrate into different tissues in both health and disease (Nichols et al., 1971). Based on the conditions of the tissue, such as growth factors and cytokine levels monocytes differentiate either into macrophages or dendritic cells (Geissmann et al., 2010). However, in the course of a pro-inflammatory reaction this process escalates (Guilliams et al., 2014). Two main groups of monocytes exist: Ly6C^{hi} and Ly6C^{low} in mice and their equivalent in humans CD14^{hi} and CD14^{low}. In the bone marrow, macrophages and dendritic cell precursors (MDPs) give rise to Ly6C^{hi} monocytes which are the most abundant type of monocyte (Ginhoux et al., 2014). These cells exit the bone marrow and are recruited into inflamed tissues, which is mediated via the CC-chemokine receptor 2 (CCR2) (Si et al., 2010). Recruitment of monocytes occurs in different steps including rolling, adhesion and transmigration, which is only possible with the expression of special molecules on their surfaces. For instance, in mice, Ly6C^{hi} monocytes express L-selectin, lymphocyte function-associated antigen-1 (LFA-1), Macrophage receptor-1 (MAC-1), platelet endothelial cell adhesion molecule (PECAM) and very late antigen 4 (VLA-4) (Shi et al., 2011). According to the tissue in which monocytes reside, different types of macrophages are generated. Alveolar macrophages, which can develop from both peripheral monocytes and resident progenitors represent an important example. GM-CSF is the key growth factor for these macrophages, which is essential for their stability, activity and maturation (Gordon et al., 2005). Central nervous system macrophages, splenic macrophages, Kupffer cells (liver), Osteoclasts (Bone) and Histocytes (interstitial connective tissue) represent other examples (Murray et al., 2011b).

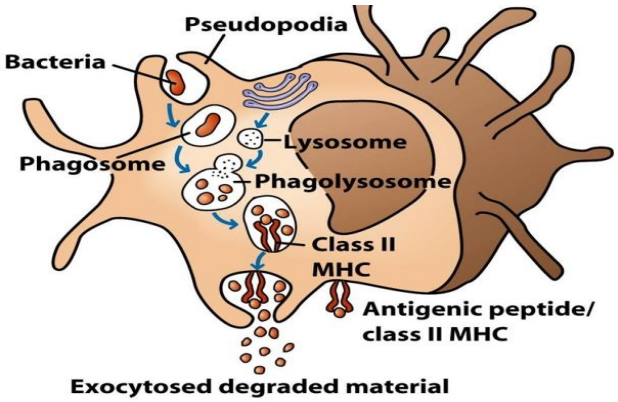

Figure 2.3 Conventional phagocytosis, Macrophages recognize the PAMPs (pathogen associated molecular patterns) by their pattern recognition receptors (PRRs), extend their pseudopods, engulf and eventually digest the pathogen through phagocytosis process (Kindt et al., 2007).

2.2.1.2 Neutrophil Granulocytes

In contrast to macrophages that live relatively long, granulocytes are short lived. The name granulocyte roots in the fact that these cells contain granules in their cytoplasm (Summers et al., 2010). Neutrophils, eosinophils and basophils are the three different types of granulocytes. Among them, neutrophils are the most frequent cells and the first line of defense during an immune response (Sheshachalam et al., 2014). Recruitment of the neutrophils from blood into infected tissue occurs via process called extravasation (Middleton et al., 2002). To reach the infection, neutrophils rapidly pass through small blood vessels, whereas at the site of infection the vessels expand so that the neutrophils can interact with adhesion molecules on the surface of the vascular endothelium. The expression of the adhesion molecules is massively increased during an infection to speed up the extravasation process (Muller, 2013). The first adhesion molecule that neutrophils bind is P-selectin, followed by E-selectin, which is expressed a few hours later (Kelly et al., 2007). The adhesion molecules bind to special glycoproteins such as sialyl Lewis X (sLeX) on the surface of the neutrophils. Next, the interaction between LFA-1 (Leukocyte integrin) and ICAM-1 (adhesion molecules on the endothelium) tightens the bound between neutrophils and endothelium (Carlos et al., 1994). With this, neutrophils can squeeze between the endothelial cells and enter the basement membrane; this process is called “extravasation”. Finally, a chemokine gradient leads the “extravasated” neutrophils to the spot of the infection. One of these chemokines is CXCL8 which is secreted from the resident macrophages in the infected tissue that has previously encountered and engulfed a pathogen. Tumor necrosis factor-α (TNF-α) and Interleukin-1 β additionally activate endothelial cells and this leads to more

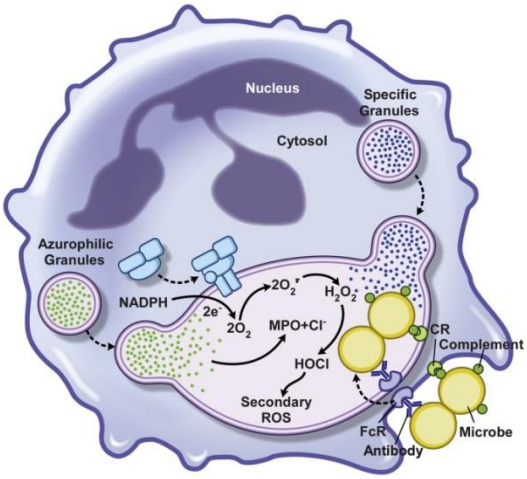

Figure 2.4 The strategies that prompt neutrophil phagocytosis On the one hand, Neutrophil’s pathogen uptake occurs not only by PAMP recognition but also by opsonization and on the other hand Azurophilic granule’s enzymes and reactive oxygen species production by NADPH-dependent oxidase complex elevates their lethal potential (Kobayashi et al., 2015)

neutrophil recruitment due to enhanced expression of adhesion proteins (Middleton et al., 2002). Due to the fact that neutrophil recruitment occurs fairly fast upon inflammation and they act as phagocytic effector cells, neutropenia (absence of the neutrophils) can cause death during many different types of infection (Murphy et al., 2012). Neutrophil phagocytosis occurs upon the recognition of PAMPs by PRRs such as TLRs and CD14 (Aderem, 2003). In addition to this, a mechanism called opsonization helps neutrophils in pathogen identification. Opsonization includes the binding of an Opsonin, e.g. an antibody, to the surface of the pathogen. Since neutrophils possess Fc receptors, which can bind to antibodies, pathogen recognition and phagocytosis can be accelerated (Ricevuti et al., 1993).As soon as the pathogen is taken up by pseudopodia a phagosome forms and fuses with a lysosome to form a phagolysosome (Braem et al., 2015). At this point, neutrophils have other mechanisms for pathogen digestion compared to other phagocytes and those are Azurophilic granules (Wysocka et al., 2001).

Neutrophils contain three different types of granules. The primary or azurophilic granule, known as peroxidase positive, contains numerous enzymes such as Defensins, Cathepsins, Proteinase-3, Elastase, Azurocidin, Lysozyme, and bactericidal permeability-increasing protein (Soehnlein et al., 2009). Azurophilic granule's fusion with phagolysosome assists the pathogen digestion process. Specific granules (secondary granules) containing Alkaline phosphatase, Lysozyme, NADPH oxidase and Collagenase and tertiary granules containing Cathepsin and Gelatinase are the other two types of granules (Borregaard et al., 1997).

Another strategy used by neutrophils to enhance pathogen clearance is reactive oxygen species (ROS). A multicomponent protein complex located on the membrane called NADPH-dependent oxidase which produces hydrogen peroxide, superoxide anions and hypochlorous acid. These various oxygen metabolites are highly toxic for the pathogens (Fig 2.4) (Kobayashi et al., 2015).

Besides phagocytosis, Neutrophil Extracellular Traps (NET) represent another strategy for neutrophils to encounter pathogens. During NETosis neutrophils release their chromatin via disruption of their nuclei and plasma membranes, which is of course lethal for them. By this way they can put the pathogens in a chromatin

trap which is lethal for the pathogens due to antibacterial properties of the released chromatin (Mantovani et al., 2011).

2.2.1.3 Dendritic cells

The extended dendrite shape of these leukocytes gives them their name. As explained earlier, monocytes differentiate to macrophages or dendritic cells (Geissmann et al., 2010). Although monocytes and DCs have the same precursor some established surface markers exist to distinguish these two cell types, despite their close relation (Murray et al., 2011a). Monocyte and dendritic cell progenitor cells generate common dendritic cell progenitors (CDPs). CDPs are precursors for intestinal $CD103^+$ dendritic cells. On the other hand, in the intestine $Ly6C^{hi}$ monocytes differentiate to $CD11b^+$ $CD11c^+$ dendritic cells that also express CX_3CR1. In the absence of $CD11c^+$ dendritic cells, $Ly6C^{hi}$ monocytes are recruited. Thay proliferate considerably to fill this gap (Rivollier et al., 2012).

In the lung, $Ly6C^{hi}$ monocytes are precursors of $CD103^+$ dendritic cells, while $Ly6C^{low}$ monocytes produce $CD11b^+$ dendritic cells (Jakubzick et al., 2008). Dendritic cells like macrophages and neutrophil granulocytes take up pathogens and activate T-lymphocytes by a process called antigen presentation (Savina et al., 2007). Dendritic cells maturate after they encounter the first pathogen and perform phagocytosis. In the next step, dendritic cells migrate via lymphatic vessels to lymph nodes and present antigens from the pathogen via their MHC molecules to T-cells, which leads to their activation. Therefore dendritic cells are known as bridging cells between the innate and adoptive immune system (Fig 2.5) (Heath et al., 2001). There are two different types of MHC molecules, class I and II. The two classes of MHCs differ in the constitution of their subunits and other than this, MHC molecules present different peptides to different T-lymphocytes.

MHC class I presents the peptides from cytosol to CD8 T-cells whereas MHC class II presents pathogen peptides generated in intracellular vesicles to CD4 T-cells (Murphy et al., 2012).

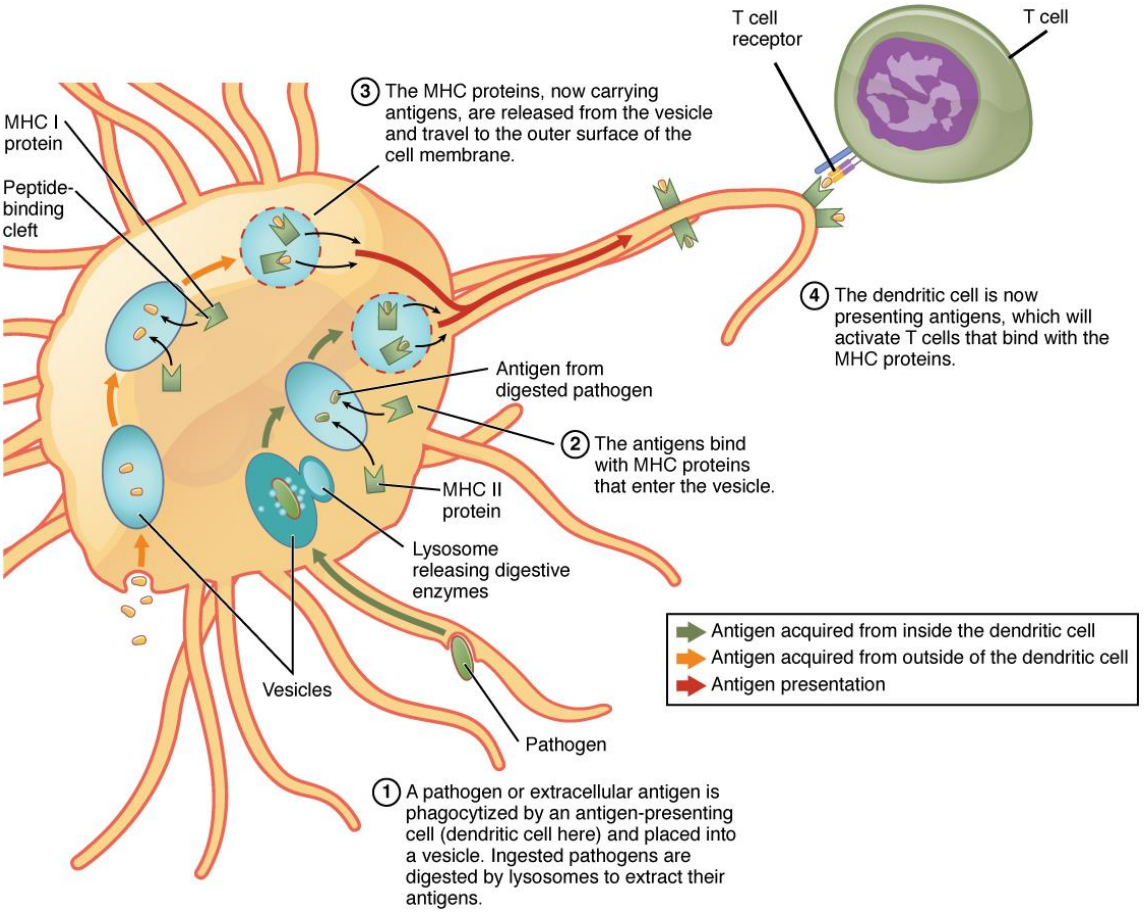

Figure 2.5 Dendritic cells phagocytose pathogens and present antigens to T-cells in the lymph nodes. Dendritic cells take up pathogens or remaining antigens from pathogens and present them with MHCII and MHCI respectively, to T-cells after the digestion process of phagocytosis is fulfilled (Betts et al., 2013).

Presentation of the collected antigens by dendritic cells stimulates adoptive immunity in which the main players are T-lymphocytes. Naïve CD4 T-cells proliferate and differentiate to effector T-cells, upon activation in a lymph node via an antigen presenting cell that carries the specific antigen on its MHC-II (Golubovskaya et al., 2016). In the thymus two different types of T cells develop: CD4 T-cells and CD8 T-cells (Geginat et al., 2015). All types of T-cells express the T-cell receptor (TCR). CD8 T-cells are activated via the antigens presented by MHCI, whereas CD4 T-cells are primed via MHC II. CD8 T-cells, which become cytotoxic T-cells after activation, recognize and kill viruses or parasites infected cells. CD4 T cells differentiate into different subsets. Among them the most prominent are Th1, Th2, Tfh, Th17 and Treg cells. Each of them has different functions in immunity. T helper cells, as their name conveys, fulfill different important

purposes for the immune system, such as B-cells antibody production and growth, macrophages bactericidal activity and neutrophil response enhancement. CD4 T-cells also give rise to regulatory T-cells with the crucial aim of immune suppression. An outstanding feature of T cells is the generation of immunological memory. Memory T-cells are long lived cells generated from the initial T-cell response. Upon a second encounter with the same antigen, they are more rapidly activated than the first time and help the body to protect itself from known invaders much more efficiently (Murphy et al., 2012; Zhu et al., 2008).

2.2.1.4 Alveolar epithelial cells (AEC)

Through breathing many liters of air reach the alveoli via the upper respiratory tract and prior to any other cell type they encounter epithelial cells. Clearly, these cells are the first wall of defense to keep airborne pathogens out. Therefore, beside the main roles AECs play for gas exchange, there are studies indicating AECs participation in innate immunity upon pathogen encounter. Alveoli are covered by two types of epithelial cells, AEC type I and type II. AECI are squamous and cover 95% of the surfaces in the lung (Chen et al., 2004). These epithelial cells are very fine and fragile. They are located adjacent to pulmonary capillaries and this proximity makes the gas exchange possible (Rozycki, 2014).

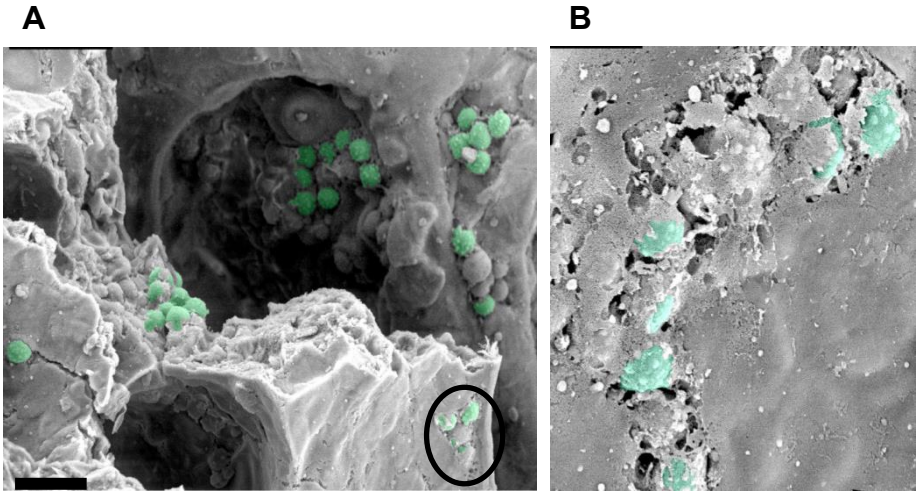

Figure 2.6 AECI takes up *A. fumigatus conidia* A. Electron microscopy image of an *A. fumigatus* infected murine lung. Each cavity corresponds to an alveolus. Inside each alveolus is mainly covered by AECI (grey). Conidia are visualized in green. The scale bar indicates 10 µm. B. AECI takes up conidia (Hasenberg, M, Gunzer, M, Unpublished data).

AECI cover most of the alveolar space, therefore the chance of conidia encountering with this cell type is extremely high. Electron microscopic images of an *A. fumigatus* infected murine lung indicate uptake of the spores by cells covering the alveoli (Fig 2.6).

AECII are cuboidal and occupy only 5% of the lung's total surface, but they are not very different from AECI in number. The main role for AECII is secretion of surfactant proteins to bring down the tension and prevent alveolar collapse (Corti et al., 1996). On the other hand, during *A. fumigatus* infection, several studies show the interaction of AECII and the fungus spores (Chen et al., 2004).

Moreover, internalization of conidia by the AECII cell line A549 has been reported (Fig 2.7) (Paris et al., 1997). This internalization has been interpreted as fungal escape from the professional phagocytes. With this strategy conidia find a favorable niche inside the epithelial layer to evade the immune system.

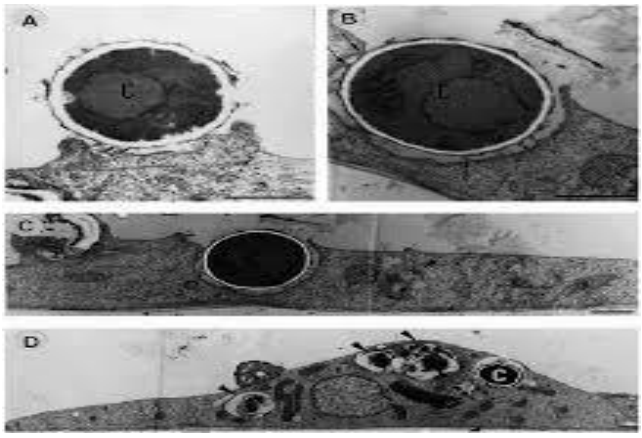

Figure 2.7 The transmission electron micrographs of human alveolar epithelial cell line (A549), 6 hours after co-incubation with *Aspergillus fumigatus* conidia (A) Conidia are sticking to AECII. (B) & (C) AECII engulf conidia by its pseudopodia. (D) An AECII in culture. Arrows show the lamellar bodies that secrete surfactant protein (Paris et al., 1997).

It has been shown that conidia can survive in A549 cells and can germinate in acidic phagosomes. However germination of the internalized conidia is postponed versus extracellular conidia (Paris et al., 1997; Wasylnka et al., 2002). It has also been shown that AECII express MHCII on their surface and can present antigen to CD4 T cells. In addition there is data in the literature that indicates induction of regulatory T-cells by antigen presenting AECII (Gereke et al., 2009).

2.2.2 Phagocytic network during an *A. fumigatus* infection

The phagocytic network, as its name indicates, is the matrix of different phagocytosing cell types in which each cell individually and in communication with

other cells performs the immune response to eliminate *A. fumigatus* infection inside the lung. The members of the phagocytic network during an A. fumigatus infection include alveolar macrophages, neutrophil granulocytes, dendritic cells, AEC type I and II cells. The first three cell types were previously described as professional phagocytes and the two latter are the so called non-professional phagocytes (Fig.2.8) (Rabinovitch, 1995).

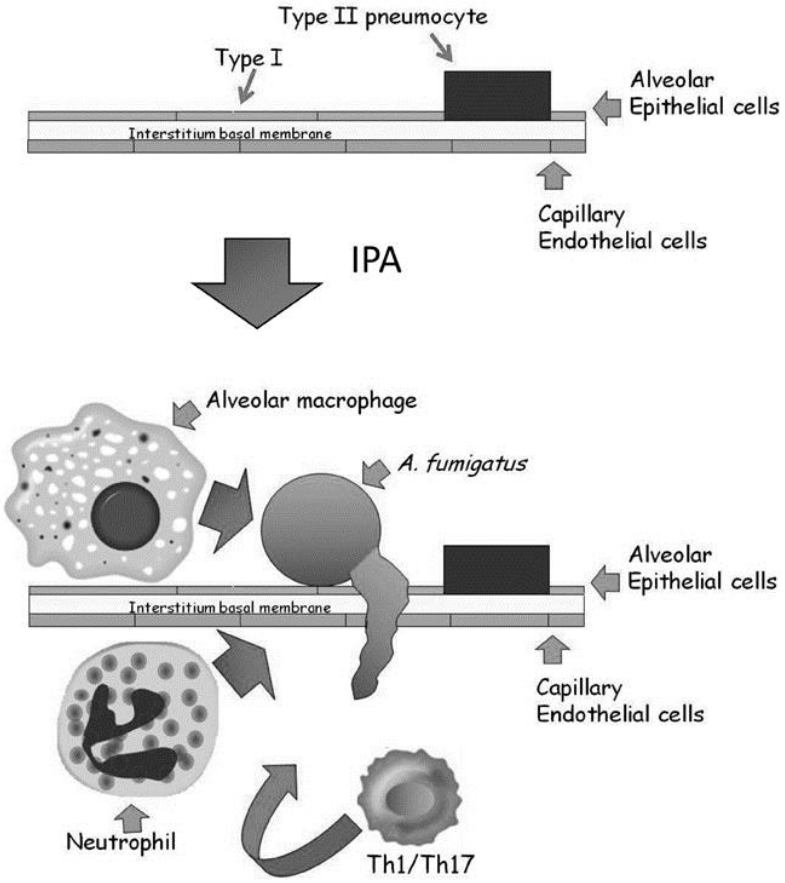

Figure 2.8 Schematic image of the innate immune response during *A. fumigatus* infection As soon as *A. fumigatus'* conidia enter alveoli they encounter alveolar epithelial cells and alveolar macrophages. Next, neutrophil granulocytes get recruited to the lung. Monocytic dendritic cells also get enrolled into fungal clearance and present antigen to T-cells (Osherov, 2012).

It has been reported that phagocytes of the innate immune system are the main cell types which clear the inhaled conidia from the lungs (Margalit et al., 2015). However, the first cells, which encounter the inhaled conidia, are epithelial cells. It has been reported that these cells besides secreting cytokines and surfactants are able to take up conidia (Paris et al., 1997). Next, alveolar macrophages start

clearing up the pathogen and within a few hours after the infection neutrophil granulocytes are recruited into the lung as well (Sibille et al., 1990). Later on, dendritic cells also start the phagocytosis of pathogens and present antigens to T cells of the adoptive immune system (Neyt et al., 2013).

2.2.3 Proteome analysis of the phagocytes during *A. fumigatus* infection

Proteome analysis is the investigation of the whole set of proteins expressed by a cell under special circumstances such as an infection. Proteins, as important elements for metabolism, growth, defense and death on the cellular level are essential molecules in living organisms and their comprehensive analysis has been a revolutionary breakthrough in discovering new biological pathways. (Lominadze et al., 2006). Although many researchers have focused on proteome analysis of the phagocytes in different contexts during the past years, the interaction of the innate immune phagocytes and *A. fumigatus* during an infection has remained an unmet need for a profound understanding of these interactions on the molecular level.

2.2.3.1 Mass spectrometry (MS) for protein characterization

MS is a method for characterization of the proteins by first ionizing the given sample and then measuring the masses within the sample. Finally the analyzed mass to charge ratio results in a plot called the mass spectrum which is used for identification of the proteins (Price, 1991). Among the different existing ionization techniques for MS analysis, electrospray ionization (ESI) and matrix–assisted laser desorption/ionization (MALDI) are the two most popular approaches (Beavis et al., 1989; Fenn et al., 1989).

Over the years, a broad range of experimental techniques for protein analysis of different types of samples such as tissue, cultured cells or body fluids have been developed (Megger et al., 2013). Two-dimensional (2-D) electrophoresis as a method for protein separation and quantification was first introduced about 40 years ago. As the name conveys the principle of this technique is based on protein separation in two dimensions: First the isoelectric focusing, and secondly separation of the proteins by size using sodium dodecyl sulfate (SDS) polyacrylamide gel

electrophoresis (PAGE). The protein spots of interest on the 2D gel can be extracted and identified by MS.(O'Farrell, 1975). This type of proteome analysis in which proteins are intact until the ionization step for MS measurement is called Top-down analysis. In contrast, in a so called bottom up approach, proteins undertake proteolytic digestion prior to MS analysis. Liquid chromatography mass spectrometry (LCMS) is one example for a bottom up experimental analysis. In this technique proteins undergo digestion (usually by the enzyme trypsin) as the first step. In the next step Liquid Chromatographic analysis of the peptides leads to a physical separation. The peptides then automatically transfer to a coupled mass spectrometer for mass analysis (Pitt, 2009).

2.2.3.2 Primary cell isolation

In order to be able to study the cells in different contexts such as phagocytes during an interaction with *A. fumigatus* infection, these cells must be enriched from affected tissues. Generally two main techniques for primary cell purification exist: positive and negative selection. Positive cell selection is a process with which the population of interest is purified via binding to an antibody that can specifically recognize the antigens on the surface of this population. Eventually, the labeled population can be purified either by flow cytometry or immune magnetic separation. In contrast, negative isolation technique purifies the target population by labeling all the non-wanted populations and leaving the population of interest untouched (Hasenberg et al., 2011). Since antibody labeling can lead to activation of different biological pathways inside a cell, this process can be a reason for differential expression of the proteins in the target population (Pitsillides et al., 2011). Therefore a positively enriched primary cell population is not a suitable target for proteome analysis, whereas the untouched, purified primary cell population resulting from negative isolation is an ideal sample for proteomics studies.

Aims

The first aim of this thesis was the development of a useful isolation method for non-professional phagocytes (Alveolar epithelial type I and II) during an *A. fumigatus* infection and their characterization on the protein level by liquid chromatography mass spectrometry (LCMS). AECs were chosen for investigation, since these cells can potentially act as important members of the innate immune system during fungal infection. So far no investigated on the proteome of primary AECs following *A. fumigatus* infection exist while the proteome of A549 cell line during the *H1N1 influenza A* virus infection has been studies. To obtain a reliable list of regulated proteins, the cell isolation technique had to be optimized in a way that the target cells remained untouched and as little activated as possible. To achieve this goal immune magnetic based negative isolation protocols for the purification of AECI and II had to be set up. The second aim of this thesis was the molecular characterization of murine neutrophil granulocytes upon *A. fumigatus* infection. Neutrophils were aimed to be isolated from the bone marrow, blood and lung of the same animal. These cells were chosen because of their importance in clearance during fungal infection and the lack of knowledge on differences in the proteome between resting and activated cells. After setting up proper isolation protocols, LCMS analysis was supposed to be performed and among all the regulated proteins the one with most relevance should be selected for further investigation regarding their role during *A. fumigatus* infection. Furthermore, knowing all the regulated proteins of the mentioned phagocytes of the network should suggest probable pathways for the communication of the phagocytes.

3 Material

3.1 Animals

Mice, both male and female, were used for experiments between 8 and 15 weeks after birth.

C57Bl/6J mice were purchased from Harlan Laboratories or were bred in the mouse facility of the University Essen, Germany.

C57BL/6-*Ly6gtm2621(Cre-tdTomato)Arte* or the so called Catchup mice were bred in the mouse facility of the University Essen, Germany. This mouse line is a novel transgenic strain, which expresses tdTomato under Ly6G promoter together with Cre recombinase. Therefore the neutrophils glow in red and Homozygous Catchup mouse is deficient for Ly6G (Hasenberg et al., 2015).

New Zealand White (NZW) mice were purchased from Jackson Laboratory.

IL4i1 k.o. mice were kindly bred and gifted by Dr. Valérie- Molinier- Frenkel and Dr. Flavia Castellano, French Institute of health and medical research Créteil, France (Cousin et al., 2015). This mouse line originates from The Texas A&M Institute for Genomic Medicine (TIGM), Texas, United States.

All animal experiments were performed according to local and European regulations.

3.2 *A. fumigatus*

Wild type *A. fumigatus* strain ATCC46645 was used throughout the project.(Hearn et al., 1980).

Transgenic tdTomato and GFP expressing *A. fumigatus* strains were generated and kindly provided by Prof. Dr. Sven Krappmann. Both strains express the respective fluorescent proteins in the cytoplasm under control of the GAPDH promoter (Krappmann et al., 2005)

3.3 Kits

Kits used for cellular and molecular experiments, such as Western blot, qPCR and ELISA are listed in Table 2.1.

Table 3.1 Commercial kits used throughout this project

Product	Manufacturer	Catalog no.
Cytofix/Cytoperm Fixation/Permeabilization kit	Becton Dickinson BD	554714
DNeasy Blood and Tissue kit	Qiagen	69504
RNeasy mini kit	Qiagen	74104
QuantiTect reverse transcription kit	Qiagen	205310
One step RT-PCR kit	Qiagen	210210
BCA kit	Thermo Fischer	23225
SuperSignal WestDura Extended Duration Substrate	Thermo scientific	34075
RAPIGEST SF surfactant kit	Waters	186001861
Bradford kit	BIO-RAD	500-0201
Mouse TNF-alpha Quantikine ELISA Kit	R&D systems	MTA00B

3.4 Primary Antibodies

In Table 3.2 primary antibodies used for AECII negative isolation, flow cytometry, immunohistochemistry and Western blot are listed below.

Table 3.2 Primary antibodies used in flow cytometry measurements

Product	Isotype	Conc. mg/ml	Manufacturer	Conj.	Clone	Catalog#
α-CD11b	IgG2b,k	0.5	Biolegend	Biotin	M1/70	101204
α-CD11c	IgG	0.5	Biolegend	Biotin	N418	117304
α-F4/80	IgG2a,k	0.5	Biolegend	Biotin	BM8	123106
α-T1 α	IgG	0.5	Biolegend	Biotin	8.1.1	127404
α-CD31	IgG2a,k	0.5	Biolegend	Biotin	390	102404
α-CD45	IgG2b,k	0.5	Biolegend	Biotin	30-F11	103104
α-CD19	IgG2a,k	0.5	Biolegend	Biotin	6D5	115504
α-Sca-1	IgG2a,k	0.5	Biolegend	Biotin	D7	108104
α-CD11b	IgG2b	0.2	BD Biosciences	V450 Horizon	M1/70	560455
α-CD11c	IgG	0.2	Biolegend	APC	N418	117318
α-F4/80	IgG2a	0.5	eBioscience	FITC	BM8	11-4801
α-T1 α	IgG	0.2	Biolegend	FITC	8.1.1	127408

α-CD31	IgG2a,k	1	Biolegend	PE	MEC 13.3	553369
α-CD45	IgG2b	0.2	BD Biosciences	PE-Cy7	30-F11	552848
α-CD19	IgG2a	0.2	BD Biosciences	APC	6D5	550992
α-Sca-1	IgG2a,k	0.2	eBioscience	PE-Cy7	D7	25-5981
α-EpCAM	IgG2a, k	0.2	BioLegend	APC	G8.8	118214
α-CD74	IgG2b	0.5	BD Biosciences	FITC	Ln-1	555318
α-ProspC	poly	1	Merck Millipore	Unconj.	Poly	AB3786
α-IL4i1*	IgG	0.9	----------	Unconj	------	---------

*IL4i1antibody was a kind gift from Dr. Valérie- Molinier- Frenkel and Dr. Flavia Castellano, French Institute of health and medical research Créteil, France. This antibody has been produced by this group and has not been purchased from a company.

3.5 Secondary antibodies

In table 3.3 Secondary antibodies used in immunohistochemistry and flow cytometry are listed.

Table 3.3 Secondary antibodies

Product	Manufacturer
Goat anti rabbit Alexa Fluor 488	Invitrogen
Biotinylated Goat Anti-Rabbit	Vector laboratories
Streptavidin, Alexa Fluor® 488 conjugate	Thermo fisher
Anti-Rabbit IgG, HRP-linked antibody	Cell signaling technology

3.6 Buffers, solutions and media

Table 3.4 Commercial media

Product	Manufacturer
Dulbecco/Vogt modified Eagle's minimal essential medium(DMEM)	Gibco
Roswell Park Memorial Institute medium (RPMI)	Sigma

Table 3.5 Handmade media

Name	Composition
***Aspergillus* minimal media (AMM)**	D(+) Glucose solution (50% w/v) 20 ml AMM stock solution (50X) 20 ml $MgSO_4$ solution in dH_2O(1M) 2 ml Hunter's trace elements solution 1 ml dH_2O 957 ml (for solid medium 30 g Agar/ liter)
50x AMM solution **(Used for making AMM)**	$NaNO_3$ 297.47 g KCl 26.10 g KH_2PO_4 74.85 g dH_2O fill up to 1000 ml
HSL1 **(Used for making Hutner's trace elements solution)**	$FeSO_4.7H_2O$ 1 g EDTA Disodium Salt (Dihydrate) 10g dissolve both one after the other in 50 ml dH_2O adjust pH with KOH pellets to 5.5 fill up to 80 ml with dH_2O
HSL2 **(Used for making HSL3)**	$(NH_4)6Mo_7O_{24}.4H_2O$ 0.22g dH_2O fill up to 5 ml
HSL3 **(Used for making Hutner's trace elements solution)**	$ZnSO_4.1H_2O$ 2.75 g H_3BO_3 2.20 g $MnCl_2.4H_2O$ 1 g $CoCl_2.6H_2O$ 0,32 g $CuSO_4.5H_2O$ 0.32 g HSL2 5 ml dH_2O to 75 ml
Hunter's trace elements solution **(Used for making AMM)**	Mix HSL1 and HSL3 adjust pH to 6.5 fill up to 200 ml filter through 0.2 µl filter unit

Table 3.6 Handmade buffers and solutions

Name	Composition
phosphate buffered saline(PBS) pH:7.4	NaCl 136.9 mM KCl 2.7 mM Na_2HPO_4 8.1 mM K_2HPO_4 1.47 mM
magnetic activated cell sorting buffer (MACS)	PBS FCS (1 %) EDTA 1.6 mM
erythrolysis buffer	NH_4Cl 155 mM $KHCO_3$ 10 mM Na-EDTA 0.1 mM
ketamine/ xylazine	Ketamine 4 ml (50 mg/ml) Xylazine 1 ml (2 %) NaCl Solution (0.9 %) 5 ml
TPNE buffer	NaCl 300 mM Triton X-100 (1% v/v) EDTA 2 mM in PBS pH 7.4
Western blot AP-buffer	Tris-HCl 100mM, pH 9.5 NaCl 100mM $MgCl_2$ 5mM ddH_2O to 1 liter
Western blot buffer A	1.5 M Tris-HCl pH 8.8 0.4% SDS
Western blot buffer B	Tris-HCl 0.5 M, pH 6.8 0.4% SDS

Name	Composition
Western blot transfer buffer	Tris 25 mM, pH 8.0 Glycerol 192 mM Methanol (20% v/v)
Tris-buffered saline (TBS)	Tris 30 mM NaCl 150 mM pH 7.5
TBS-Tween	TBS 0.1% TWEEN 20
2-D gel sample buffer	CH_4N_2O 4.2 g CH_4N_2S 1.52 g CHAPS 0.2 g zwittergent 3-10 0.1 g ampholyte 80 µl ultrafiltered H_2O to 10 ml
10x SDS electrophoresis running buffer	Glycine 1.92 M Tris-HCl 333mM SDS 1%
SDS electrophoresis running buffer	Tris 21.2 g $C_3H_8O_3$ 100.8 g 10% SDS 70.0 ml
IPG strip Equilibration buffer	Glycerol (87% v/v) 172.5 ml CH_4N_2O 180.2 g Tris-HCl, pH 8.8 25 ml, SDS 4 g bromophenol blue 1% (w/v) 1 ml ultrafiltered dH_2O to 500 ml
rehydration buffer	CH_4N_2O 10.5 g CH_4N_2S 3.8 g

Name	Composition
	CHAPS 0.5 g zwittergent 3-10 -0.25g bromophenol blue (1%) 50 µl ultrafiltered dH_2O to 25 ml
lysis buffer for genotyping	NaCl 200 mM Tris-HCl 100 mM, pH 8.5 SDS 0.2% EDTA 5mM ddH_2O 42ml
***A. fumigatus* lysis buffer**	5ml Tris-Hcl (1M), pH7.2 1.46 g EDTA 3g SDS 1 ml Beta- betamercaptoethanol dd H_2O to 100 ml
lysis buffer for DIGE	CH_4N_2O 4.2 g CH_4N_2S 1.52 g CHAPS 36.3 mg zwittergent 0.1 g ddH_2O to 10 ml (dissolve in 37°C) store at -20°C
50x Tris, Acetate, EDTA (TAE) buffer	2.42 g Tris base 57.1 ml acetate 100ml 0.5 M EDTA, pH8.0 ddH_2O to 1 liter
heparin solution	28 mg heparin in 1 ml NaCl solution 0.9%
fixing solution for silver gel staining	Ethanol 40% (v/v) CH_3COOH 10% (v/v)

Name	Composition
	500 µl 37% (v/v) formaldehyde per liter
washing solution for silver gel	Ethanol 30% (v/v)
thiosulfate solution for silver gel	$NA_2S_2O_3$ 0.02% (w/v)
silver nitrate solution for silver gel	$AgNO_3$0.2% w/v 75 µl 37% (v/v) formaldehyde per 100 ml
developing solution for silver gel	Na_2CO_3 3% (w/v) $NA_2S_2O_3$ 0.0004 % (w/v) 500 µl 37 % (v/v) formaldehyde per liter
stop solution for silver gel	EDTA 50 mM

3.7 Chemicals, enzymes and beads

Table 3.7 chemicals, enzymes and beads

Product	Manufacturer	Cat. number
Low melting agarose	Sigma	A-4018
Dispase	BD biosciences	354235
Deoxy ribonuclease I	Sigma Aldrich	D4263
Anti-biotin micro-bead	Miltenyi biotec	130-090-485
MACSQuant calibration beads	Miltenyi Biotec	130-093-607

4x Laemmli Sample Buffer	BIO-RAD	161-0747
Precision Plus Protein All Blue Standards	BIO-RAD	350000383
Tween 20	Carl Roth	9127.1
Bovine serume albomine	Sigma	A9418
DAPI Fluoromount-G	SouthernBiotech	0100-20
Xylazine	CEVA	6324464.00.00
Ketamine	Inresa	32696.01.00
Ammonium Persulfate (APS)	Carl Roth	9592.1
Seasand	Carl Roth	8441.1
PFA	Sigma	P6148
Agarose	Carl Roth	6352.4
D(+)-Glucose	Carl Roth	X997.2
MgSO4	Sigma	M2643
NaNO3	Carl Roth	8601.2
KCl	Sigma	P9541

KH2PO4	Sigma	P5655
FeSO4.7 H_2O	Sigma	F8263
EDTA Disodium Salt (Dihydrate)	Sigma	E6758
(NH4)6Mo7O24.4 H_2O	Sigma	431446
ZnSO4.1 H_2O	Sigma	96495
H3BO3	Sigma	B6768
MnCl2.4 H_2O	Sigma	203734
CoCl2.6 H_2O	Sigma	C8661
CuSO4.5 H_2O	Sigma	C8027
Urea	Sigma	51459
5x PCR- Mastermix	BioBudget	80-62001000
Betamercaptoethanol	Sigma	M6250
EDTA	Sigma	E6758
HCl	Sigma	H9892
Triton-x100	Carl Roth	3051.3
SDS	Carl Roth	2326.2

Glycine	Carl Roth	3908.2

3.8 Tools and devices

Devices related to 2D-DIGE experiments such as IPGphor II manifold ceramic tray, Ettan IPGphor II platform, Ettan Daltsix casting chamber, Ettan Daltsix electrophoresis unit and Typhoon scanner were kindly offered by Prof. Axel Brakhage, Hans Knöll Institute (HKI), Molecular and Applied Microbiology Department, Jena, Germany. Devices related to LCMS such as UltiMate 3000Nano LC and Qexactive MS were provided to useby Prof. Barbara Sitek inRuhr University, Medical Proteomics Department, Bochum, Germany. Devices related to Immunohistochemistry paraffin sample preparation and sectioning, such as Spin tissue processor, tissue embedder and microtome were provided to use by Prof. Andrea Vortkamp, Department for Developmental Biology, Essen University, Germany. Image quant for quantification of chemiluminescent Western blots was performed in the laboratory of Prof. Dominik Boos, Department of Molecular Genetics, Essen University, Germany. Imaging Center Essen (IMCES) provided support for using their microscopes, flow cytometer and Fluorescence-activated cell sorter.

Table 3.8 tools and devices used throughout the experiments

Product	Manufacture	Cat. number/Comments
PE tube 50ml	CELLSTAR	227261
PE tube 15 ml	Falcon	352096
PE tube 1.5 ml **Pipette tip**	Eppendorf	All different sizes
Intracan-W **(Intravenous catheter)**	Braun	4254090B
96 well rounded bottom plate	Carl Roth	9291.1

Product	Manufacture	Cat. number/Comments
C-tube	Miltenyi Biotec	130-093-237
10 cm Petri dish	VWR	25384-088
HistoBond (Microscope slides)	Marienfeld superior	0810001
PVDF-membrane	Thermo scientific	88518
Fine dosage syringe **I ml syringe** **2 ml syringe** **10 ml syringe**	Braun Braun Terumo Syringe BD Discardit II	9161502 9161406V SS+T02S1
Ls magnetic column	miltenyi biotec	130-042-401
Mini-PROTEAN Tetra System	Bio-Rad	SDS Page and Blotting
Power Pac Basic	BIO-Rad	Power supply for SDS and Agarose gel
UltiMate 3000Nano	Dionex, Idstein, Germany	LC
Qexactive	Thermo Fischer scientific	MS
spectrometer	Molecular Devices	SpectraMax M5^{e}
spin tissue processor	Thermo scientific	STP 120
tissue embedder	Leica	EG1150
Microtome	Thermo scientific	HM 340 E

Product	Manufacture	Cat. number/Comments
wide field microscope	Leica	DMI6000
2-photon microscope	Leica	SP8 MP confocal
gentleMACS Dissociator	Miltenyi Biotec	130-093-235
Petriturn-M	Schuett biotec	
incubator	Thermo scientific	Model 4352
PCR machine	peQSTAR	96 Universal Gradient
qPCR machine	QIAGEN	Rotor-Gene Q
Centrifuge	Eppendorf	5810 R & 5430 R
Imagequant LAS-4000	Sigma Aldrich	Gel documentation

3.9 Software and data bases

Software related to LCMS data analysis such as Progenesis, Proteome Discoverer and Mascot were an offer of Prof. Barbara Sitek, Ruhr University, Medical Proteomics Department, Bochum, Germany. The software related to 2D-DIGE data analysis called Delta 2D was provided by Prof. Axel Brakhage, HKI, Molecular and Applied Microbiology, Jena, Germany. IMARIS and FACSDiva software usage were kindly supported by IMCES team, University hospital Essen, Germany.

Table 3.9 Software and data bases

Product	Manufacturer	Version/released
MACSQuantify	Miltenyi Biotec	Ver.2.6
Flowjo	Flowjo	Ver.10
IMARIS	Bitplane	Ver.8.2
Progenesis QI *for proteomics*	Nonlinear Dynamics Ltd	ver. 2.0.5387.52102, Newcastle upon Tyne, GB
Proteome Discoverer	Thermo Fisher Scientific	1.4
UniProtKB/Swiss-Prot database		Release 2015_11 of 11.11.2015; 549,832 entries
Mascot	Matrix Science, London, UK	Ver.2.5
Delta 2D	Decodon	Ver.4.3.2
BD FACS Diva	Becton Dickinson	Ver.8

4 Experimental methods

4.1 Intratracheal intubation

C57Bl/6 mice were anesthetized by 100 µl / 20 g mouse weight ketamine/xylazine solution (Inresa Arzneimittel GmbH, Freiburg im Breisgau, Germany/Ceva, Düsseldorf, Germany). The mouse was fastened via the teeth on a special stage and the tongue was pulled aside by a laryngoscope. A 22 G Intravenous (IV) catheter (B. Braun medical Ltd, Sheffield, UK) was placed into the trachea and 50 µl *A. fumigatus* conidia with the concentration of $1x10^8$ /ml was instilled into the lung.

4.2 AECII isolation

The mouse was sacrificed by CO_2 asphyxiation and a long cut along the ventral midline of the body was made. The skin together with the peritoneum was cut. Then the mouse got exsanguinated by cutting the left and right jugular veins as well as the right and left renal arteries. The diaphragm got carefully punctured and the ribs got removed. With a 22G IV catheter and a 10 ml syringe filled with cold phosphate buffered saline (PBS), the right ventricle of the heart was punctured and the lungs were perfused until they were free of blood. The salivary glands and the muscles surrounding the trachea were removed. 2 ml dispase (BD biosciences, San Jose, United states) was instilled inside the lung using a catheter and a 2 ml syringe. Next, 0.5 ml 1% low melting agarose was injected into the lung and the lung was covered by a tissue and on top of it ice so that the low melting agarose (Sigma Aldrich, Missouri, United States) solidifies and does not let the enzyme out of the lung. The lungs got dissected and incubated at room temperature for 45 min in a 15 ml PE tube containing 2 ml dispase so that the tissue digestion takes place. The lungs were then removed and trachea, Bronchi and intralobar bronchioles were cut removed as much as possible. This step is especially important to remove several different cell populations, which could be a reason for contamination

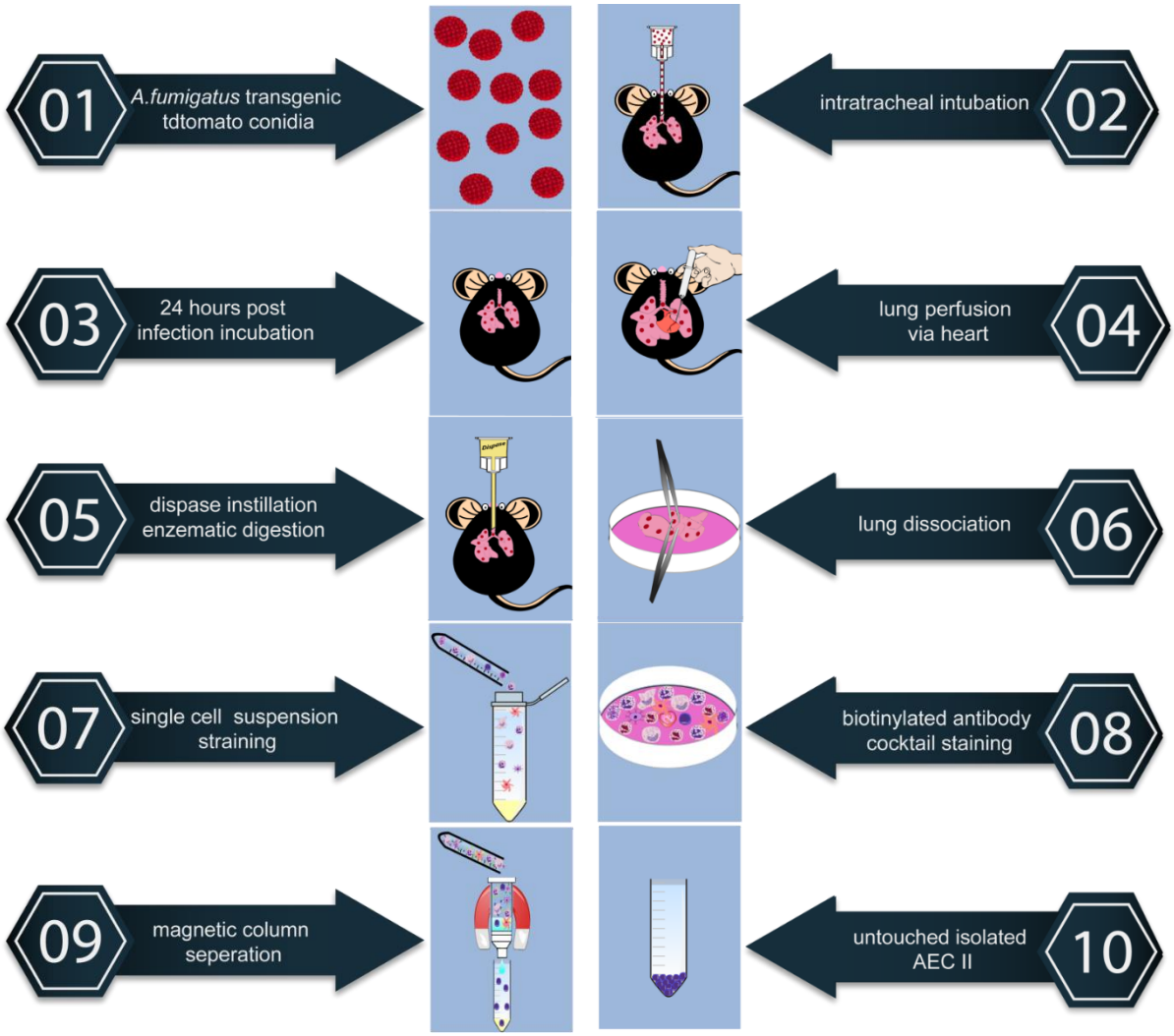

Figure 4.1 AECII negative isolation by immune magnetic approach The Lung tissue was digested by dispase and dissociated by forceps. The formed single cell suspension was put through filters of different pore sizes. After erythrocyte lysis the cells were stained by the designed biotinylated antibody mixture (Table 5.1). Next, anti-biotin microbeads were added to the cells and after incubation the cells were put through magnetic column. AECII got collected from the column.

Then the tissue was transferred into a dish containing 7 ml DMEM medium and 100 µl DNase (660 Kunitz unit) was added on top. Using forceps the lung tissue was completely disintegrated and incubated for 10 minutes at room temperature with gentle rocking. Afterwards, the cell suspension was filtered through 100 µm, 70 µm and 30 µm and 20 µm cell strainers. After centrifugation at 250 G, 4 °C for 15 minutes, the pellet was re-suspended in 2 ml erythrocyte lysis buffer. After incubation on ice for 5 minutes the erythrocyte lysis process was stopped by 10 ml cold PBS or DMEM medium. After another round of centrifugation at 270 G, 4 °C for 10 min the pellet was re-suspended in the designed biotinylated antibody mixture

for performing the negative isolation. The antibody mixture contained 5 µl (2 µg) of each of the following antibodies in 460 µl PBS : α-CD11b to label monocytes and macrophages, α-CD11c against dendritic cells, α-CD19 for B cells, F4/80 for macrophages, α-CD31to label endothelial cells, α-CD45 against all leukocytes, α-Sca-1 for bronchoalveolar stem cells (BASCs) (Raiser et al., 2009) and T1α to label AEC I. Then, the cells were incubated with the antibody mixture for 15 min at 4°C,washed with 10 ml cold MACS buffer and centrifuged at 4°C, 270 G for10 min. Afterwards the pellet was re-suspended in 300 µl MACS buffer and 200 µl anti-biotin microbeads was added and incubated at 4 °C for 15 min. The cells were washed with 10 ml MACS buffer and pelleted at 4°C, 270 G for10 min. Finally, the suspension was run through LS magnetic column and the column was washed 3 times with 3 ml MACS buffer. All the labeled cells were bound to the column and the unlabeled cells passed through. The negatively isolated AECII were collected in a 15 ml PE tube and centrifuged at 4°C, 250 G for 10 min. (Fig4.1).

4.3 Whole lung flow cytometry

C57Bl/6 mice were sacrificed by CO_2 exsanguination. The skin and peritoneum were cut open and salivary glands removed. With 10 ml ice cold PBS the lung lobes were perfused via the right ventricle of the heart. A 22 G IV catheter was inserted into the trachea and 2 ml dispase was instilled into the lung. Then, the trachea was tied by a piece of yarn and the lung got dissected from the mouse. The lung was incubated in 2 ml dispase for 45 minutes at room temperature. The lung was dissociated with two forceps and incubated in 7 ml DMEM medium together with DNAse (660 Kunitz unit) in room temperature for 10 minutes on a shaker. The whole lung's single cell suspension was purified via cell strainers of 40, 70 and 100 µm pore size and centrifuged for 10 minutes at 4°C and 250 G. The pellet was re-suspended in erythrocyte lysis buffer and incubated on ice for 10 minutes. After another round of centrifugation, the pellet was re-suspended in 1 ml PBS. 100 µl of the single cell suspension was distributed in each well of a rounded bottom 96 well plate for flow cytometry. Afterwards, in separate wells cells were stained with individual antibodies (single staining) and parallel to that in other wells cells were stained for the isotype controls. The cells in one well were kept untouched for the unstained control. Some samples needed to be stained intracellularly as the antigen

to which the specific antibody could bind was intracellularly expressed like Pro-surfactant protein-C (proSP-C) as the well-known intracellular marker for the secreted surfactant of AECII. Other wells needed conventional surface staining as the antigens on the surfaces of the cells needed to be stained by the antibodies such as, α-F4/80, α-CD45, α-CD11b, α CD11c, α-CD19, α-Sca-1, α-CD31, α-T1α (Transmembrane) and Epithelial Cell Adhesion Molecule (EpCAM). For intracellular staining, the cells in the well were fixed and permeabilized with the Cytofix/Cytoperm solutions (Fixation/Permeabilization kit, BD) according to the manufacturer's protocol. Most antibodies were conjugated to fluorochromes except proSP-C. This staining had to be done with an extra step of adding an Alexa Fluor 488 coupled secondary antibody to the cells. All the primary antibodies were added 1:100 (between 1 to 2 µg) and the secondary antibody was added 1:500. Incubation was always performed for 15 minutes at 4°C. The washing steps, in case of the surface staining was done with 100 µl PBS and in case of the intracellular staining with 100 µl x1 perm/wash buffer from the mentioned kit. Centrifugation was done at 4 °C for 10 minutes and 250 G.

4.4 Proteomics

The analysis of the proteins was done with two strategies: the so called top down strategy in which the intact proteins were analyzed by 2D-DIGE (Section 4.4.1) and bottom up approach with which peptides were analyzed by LCMS (Section 4.4.2)

2D-DIGE was performed in rehydration loading manner and the proteins were labeled with saturation labeling technique in which all Cysteines were marked by fluorescent dye.

LCMS was done with label free strategy and the sample preparation was performed in the so called in solution digestion manner.

4.4.1 *A. fumigatus* infection kinetics/Fluorescence Difference Gel Electrophoresis (2D-DIGE)

AECII were isolated (section. 3.2) from C57Bl/6 mice after 30 minutes, 8 hours, 24 hours and 48 hours post *A. fumigatus* intratracheal infection. Isolated cells were lysed in lysis buffer for DIGE and were frozen at -80°C. Before starting the protein

concentration of the isolated AECII after different infection time points was measured by Bradford assay according to the manufacturer's protocol. Next, the two major steps of a conventional DIGE were performed. First, Iso Electric Focusing (IEF) and second, SDS-Polyacrylamide gel IEF was carried out by using IPG gel strips and rehydration loading approach. The pH gradient of the IPG gel strip was nonlinear from 3 to 11. The samples were initially labeled with spectrally resolvable fluorescent dyes Cy3 and Cy5. This labeling made it possible for us to load protein from *A. fumigatus* infected and mock infected (sterile tap water) isolated AECII on the same gel. This unique approach was performed so the comparison between the expressed proteins of the infected and control samples could finally be visualized. For that and to start with, a 200 pmol/µl working dye solution was generated in anhydrous DMF. 1 µl of the working dye solution Cy3 was added to the infected sample and Cy5 was used to label the mock infected sample. The 11 cm IPG strips were rehydrated with a mixture of 15 µg protein in 25 µl sample plus 10 mM DTT and 8 µl/ml IPG in 175 µl rehydration buffer, overnight. Next day, The IPGphor II manifold ceramic tray was placed on Ettan IPGphor II platform. The rehydrated IPG strips were placed on the ceramic tray. Two electrode pads were moistened with 150 µl water and were placed on both sides of the strip. The whole tray was covered by 110 ml oil. The IPGphor focusing program was run with voltages ranging from 0 to 1000 in the first 11 hours, from 1000 to 8000 in the next 3 hours and from 8000 to 24000 in the last 3 hours. Next day, Iin order for all the separated proteins to interact with SDS in the next step, the IPG strips were equilibrated with 0.25 g DTT (1%) and 0.625 iodoacetamide both in 25 ml equilibration buffer. The stripes were incubated with each of these solutions for 15 minutes separately with gentle agitation. This step helps the proteins to alkylate the sulfhydryl groups. For the second dimension 12.5% polyacrylamide gels were casted in Ettan Daltsix casting chamber and with the following recipe in Table 4.1:

Table 4.1 Polyacrylamide 12.5 % gel components

12.5% polyacrylamide gel components	amount
acrylamide/bis-acrylamide solution (30%)	189 ml
1.5 M Tris/Hcl, pH 8.8	113 ml
H_2O	139 ml
10% SDS	4.5 ml
Tetramethylethylenediamine (TEMED)	69 µl

Water saturated butanol (5 ml ddH_2O in 50 ml n-Butanol) was immediately added on top of the gel in order for the gel edges to polymerize and also removing the bubbles. Finally the IPG strip was placed on to the gel vertically and the Ettan Daltsix electrophoresis unit was ran. The gels together with the cast (3 mm) were scanned on Typhoon Variable Mode Imager with resolution of 100 pixels and 550 voltage.

4.4.1.1 2D-DIGE Data analysis

Data analysis was performed by Delta-2D software V4.3.2 from Decodon Company. In order to analyze the data first a project had to be set up and the images of the gels had to be imported and arranged in feasible replicate groups. The set up groups are mentioned in table 4.2.Then, group warping strategy was chosen and automatic warping was done. The spots were detected and quantified. Most number of spots

were detected from group number 3 therefore the 24 hours time point was picked as the time point post infection for the rest of the experiments.

Table 4.2 Set up groups for 2D-DIGE analysis with Delta-2D software

group no.	Gel one	Gel two
1	30 min post *A. fumigatus* infection	30 min post mock infection
2	8 hours post *A. fumigatus* infection	8 hours post mock infection
3	24 hours post *A. fumigatus* infection	24 hours post mock infection
4	48 hours post *A. fumigatus* infection	48 hours post mock infection
5	30 min post *A. fumigatus* infection	8 hours post *A. fumigatus* infection
6	8 hours post *A. fumigatus* infection	2 hours post *A. fumigatus* infection
7	24 hours post *A. fumigatus* infection	48 hourspost *A. fumigatus* infection
8	48 hours post *A. fumigatus* infection	30 min post *A. fumigatus* infection
9	30 min post mock infection	0 control
10	8 hours post mock infection	30 min post mock infection
11	24 hours post mock infection	8 hours post mock infection
12	48 hours post mock infection	24 hours post mock infection

4.4.2 Liquid chromatography mass spectrometry (LCMS)

Protein from isolated AECII were extracted and digested to peptides 24 hours after *A. fumigatus* and mock infection (Section. 4.4.2.1). 350 ng of tryptic peptides per sample was injected to an Ultimate 3000 RSLCnano HPLC System (Dionex, Idstein, Germany) online coupled to a Q-Exactive Orbitrap mass spectrometer (Thermo Scientific, Bremen, Germany). Peptides' pre-concentration was performed on a trap column (Acclaim PepMap 100, 100 μm x 2 cm, C18, 5 μm, 100 Å) in 7 minutes with

30 µl/min 0.1% TFA flow rate. Then, peptides were transferred to an analytical column for separation (Acclaim PepMap RSLC, 75 *µ*m x 50 cm, nano Viper, C18, 2 *µ*m, 100 Å) with a gradient from 5-40 % solvent B over 98 min at 400 nl/min at 60°C (solvent A: 0.1 % FA, solvent B: 0.1 % FA, 84 % acetonitrile). The Orbitrap analyzer's full scan mass spectra were obtained in profile mode with resolution of 70,000 and 400 m/z and within the mass range of 350-1400 m/z. Using a data dependent mode, the top 10 most abundant ions from the first MS were transferred to a second MS. The ions got fragmented there via Higher-energy collisional dissociation (HCD) technique. The ion fragments were measured by tandem MS (MS/MS) and the m/z ratio was detected.

4.4.2.1 Protein digestion

AECII from 24 hours *A. fumigatus* and mock infected C57Bl/6 mice was isolated and the pellet was kept at -80 °C. The experiment was done with 9 replicates from *A. fumigatus* infected and another 9 mock infected samples. Numbers of the isolated AECII from each mouse lung were about $5x10^5$. Cells were lysed by RAPIGEST SF Surfactant kit according to the protocol of the manufacturer. RAPIGEST power was re-suspended in 1 ml NH_4HCO_3 50 mM. 30 µl of the solution was added to each sample. After vortex and 1 minute sonication the sample was centrifuged for 10 minutes at 15,000 RPM. Next, the protein concentration was measured by Bradford kit. From each sample and for each measurement 4 µg protein was needed. The protein solution was filled up to 10 µl by NH_4HCO_3 and 5 mM DTT was added to each sample. After vortex and a short spin down, the samples were heated up to 60 °C for 30 minutes. The samples were cooled down to room temperature, 15 mM Iodoacetamide as an alkylating factor was added. The samples were incubated for 30 minutes in the dark. Lastly, the enzymatic digestion by trypsin was done. Trypsin concentration was 1:100 to 1:20, w/w. The trypsinization was performed at 37°C, overnight. The following day, in order to prepare the samples for HPLC and Mass Spectrometry (MS) 0.5 % Trifluoroacetic acid (TFA) (pH<2) was added and the samples were incubated in 37 °C for 30-45 minutes. Thereafter, centrifugation at 13,000 RPM for 10 minutes was done and the solution was carefully transferred to another tube.

4.4.2.2 Amino Acid Analysis (ASA)

For determination of the concentration and amino acid (AA) composition, amino acid analysis (ASA) was performed in two steps, first hydrolysis and second fluorescent derivatization. Hydrolysis was done by 6 M hydrogen chloride (HCL)/ Phenol at 15 °C. Derivatization was done by ACQ (6-Aminoqinolyl-N-Hydroxysuccinimidyl-carbamote). Next, Reversed Phase- High Performance liquid chromatography (RP-HPLC) was ran to separate the AAs. Lastly, detection with UV-spectrometer was performed.

4.4.2.3 Data analysis

As mentioned above, in a MS/MS process during the first mass spectrometry data for quantification of the proteins and during the second mass spectrometry data for identification of the proteins are obtained. Below the analysis of both types of data is explained.

4.4.2.3.1 Protein Identification

Proteome Discoverer 1.4 (Thermo Fisher Scientific) was the software used for protein identification. The acquired spectra from MS/MS found in the UniProtKB/Swiss-Prot database (Uniprot/Swissprot-Release 2013_10; 541,561 entries, 16641 after taxonomy 46rlenmeyer46) and Mascot (ver.2.5, Matrix Science, London, UK) search engine was used. The defined search criteria are mentioned in Table 4.3.

Table 4.3 Defined search criteria for Mascot

Mascot Search criteria	
Taxonomy	*Mus musculus*
mass tolerance	5 ppm for precursor ions
mass tolerance	0.4 Da for fragment ions
Dynamic modifications	46rlenmey (propionamide) & 46rlenmeyer (oxidation)

FDR (false discovery rate)	>1% was rejected
Peptide confidence	High

4.4.2.3.2 Protein quantification

Ion intensity was the basis for quantification analysis, which was performedby Progenesis QI *for proteomics* by Nonlinear Dynamics Ltd software. (ver.2.0.5387.52102, Newcastle upon Tyne, GB). A master mix was used as a reference for all the raw data and a master map for common set of features was created. Based on these features, m/z values of all peptides with a distinct retention time were determined and applied to all the experimental runs identically. Aligning the data from the same peptides of the different samples indicated the dissimilarities of the retention times, which is based on differences in RPLC performance. Ions with charges between +2 and +4 were only contemplated and three isotope peaks were the minima to be considered in the analysis. For protein quantification only unique peptides (peptides that certainly allocate to a protein) were taken into account. The total number of these unique peptide ions demonstrates the proteins profusion.

4.4.2.4 Statistical analysis

FDR-corrected ANOVA p-value (p-value) was the utilized approach for calculating the significance of the resulted analysis from Progenesis. P-values less than or equal to 0.05 was set as a filter. Another filter criterium was the fold changes of the protein's regulation resulting from the infected samples compare to mock infected samples. This filter was set on 2. Last but not least the proteins the most conceptual relevance was picked for further characterization and investigations.

4.5 Quantitative Polymerase Chain Reaction (qPCR)

AECII were isolated from mice 24 hours after *A. fumigatus* and mock (sterile tap water) infection. RNA was isolated from the primary AEC II following the protocol from the Qiagen Rneasy kit. According to the Qiagen reverse transcription protocol cDNA was generated from the isolated RNA. In this step cDNA is stable enough to be kept at -20 °C. Next, qPCR was performed based on Qiagen RT-PCR protocol.

4.6 SDS-Page and Western blot

4.6.1 Sample preparation

Primary AECII were isolated from mice 24 hours after *A. fumigatus* and mock infection. 50 µl TPNE buffer was added to the pellet of $1x10^6$ cells and incubated on ice for 30 minutes. Next, 15 minutes' centrifugation at 4°C and 14,000 RPM was done. The supernatant was kept at -20°C. The protein concentration was measured by BCA kit according to the protocol of the manufacturer.

4.6.2 Sodium Dodecyl Sulfate Polyacrylamide Gel Electrophoresis (SDS page)

20 µg of each sample was run on a 10% SDS gel. Before, the samples were mixed with 5X Laemmli buffer and boiled for 5 min at 95 °C. The samples were shortly mixed and centrifuged and loaded on the gel. 10 µl Pre-stained protein standard (Precision plus Protein All Blue Standards-Bio Rad) was loaded on the first slot of the gel as ladder. The whole system was connected to a power supply. The gel was run for the first 10 minutes 150 V, so the samples in all the stacking gel slots settled. The remaining electrophoresis was performed at 200 V for the separation. Table 4.4 indicates the recipe for 10% SDS separation gel and stacking gel.

Table 4.4 SDS 10% separation gel and stocking gel recipes

10%SDS gel	Separation gel	Stacking gel
Buffer A	2.5 ml	---------
Buffer B	--------	2.5 ml

Acrylamid	3.3 ml	1.1 ml
H_2O	4.2 ml	6.5 ml
TEMED	10 µl	20 µl
Ammonium Persulfate(APS)	25 µl	40 µl

4.6.2.1 SDS page silver staining

After electrophoresis, gel was fixed in 200 µl fixing solution for 30 minutes and protected from light. Then, the gel was washed 2 times each time 10 minutes with 200 ml 30 % (v/v) ethanol and 10 minutes with ddH_2O. Next, the gel was incubated in 0.02 % (w/v) thiosulfate solution exactly for 1 minute. Afterwards, it was washed in ddH_2O, 3 times and each time for 20 seconds. The gel was incubated for 20 minutes in 200 ml 0.2 % (w/v) silver nitrate solution on a shaker. Then, the gel was washed 3 times and each time 20 seconds in ddH_2O and incubated in 200 ml developing solution until color was visualized. Afterwards, a short wash with ddH_2O was performed and the gel was incubated for 10 minutes in 200 ml stop solution while shaking. Lastly the gel was washed 3 times and each time 10 minutes in ddH_2O.

4.6.3 Blotting

While the SDS gel was running, a piece of PVDF membrane was incubated in Methanol for 1 minute, then 5 minutes in ddH_2O and finally for 10 minutes in transfer buffer. When the gel was ready it was as well incubated for 10 minutes in transfer buffer at room temperature. Lastly, the blot was made using two pads and three whatmann papers, all pre-rinsed in transfer buffer on each side of the cassette and the membrane and gel were placed in the middle. The cassette was placed in a chamber filled with transfer buffer plus 10% methanol and was connected to a power supply with constant voltage of 100 V for 1 hour.

Blotting composition order

-

- 1 Pad
- 3 Whatmann papers
- PVDF Membrane
- Gel
- 3 Whatmann papers
- 1 Pad

4.6.3.1 Blot's staining and visualization

According to the chosen approach for visualization the blots were stained with different antibodies. Bellow two different used approaches are explained.

4.6.3.1.1 Chemiluminescence blot

After the transfer of the proteins from the gel to the PVDF membrane, the membrane was incubated in 3% BSA in TBS-Tween (0.1%) for 1 hour at room temperature on a shaker for blocking to prevent nonspecific binding of the antibodies. The membrane was incubated in 1 µg α-rabbit monoclonal IL4i1 antibody in 3% BSA in TBS-Tween overnight at 4°C. Next, 4 washing steps with TBS-T and each time 15 minutes at room temperature and on a shaker. Finally the incubation of the membrane by 1:10,000 α -rabbit HRP linked secondary antibody for 1 hour at room temperature was performed. After this step, The 4 washing steps just like before took place. Finally, ECL Chemiluminescence was used according to the manufacturer's protocol and the protein bands were visualized by Imagequant LAS-

4000, cooled CCD camera, gel documentation system (Sigma Aldrich, St. Louis, Missouri, United States).

4.6.3.1.2 Chromogenic blot

After the blotting was done and the membrane got blocked with 3 % BSA, the blot got stained in 1 µg α-rabbit monoclonal α-IL4i1 antibody in 3 % BSA in TBS-Tween. After the washing step (mentioned in section above) 1:10,000 AP conjugated α-rabbit secondary antibody in 3 % BSA in TBS-Tween was added to the blot for 1 hour at room temperature. The washing step was performed. The blot was incubated in AP-buffer for equilibration for the detection system. Nitro-blue tetrazolium (NBT) and 5-bromo-4-chloro-3'-indolyphosphate (BCIP) mixture, precipitate in contact with AP and results in an intense purple color. 33 µl BCIP and 60 µl NBT was mixed and added to 10 ml AP-buffer. The prepared solution was put on the blot and the blot was incubated at room temperature overnight in the dark until the signals of the protein appeared.

4.7 Immunohistochemistry

C57/Bl6 mice were infected with $5x10^6$ transgenic tdTomato conidia intratracheally and the mice were sacrificed by CO_2 asphyxiation 24 hours later. The lungs were perfused by ice cold PBS via the right ventricle of the heart. 1 ml 4 % paraformaldehyde (PFA) was instilled into the lung with a 22G IV catheter through the tracheae and the tracheae were tied with a piece of yarn. The complete lungs with tracheae were cut and incubated with2 ml 4 % PFA overnight at 4 °C for fixation. The next day, the tracheae were cut and the lung lobes were put in separate cassettes and in xylol and different ethanol gradients for dehydration (Table 4.5). Thereafter, the fixed, dehydrated lung lobes were embedded in paraffin wax. Finally, the paraffin embedded lung lobes were cut into 5 µm sections on Histobond slides (76x 26x 1 mm), (Marienfeld superior, Lauda-Königshofen, Germany).

Table 4.5Tissue processor program

Material	Incubation time
70% Ethanol	10 min
80% Ethanol	10 min
95% Ethanol	10 min
100% Ethanol	10 min
100% Ethanol	10 min
100% Ethanol	10 min
Xylol	20 min
Xylol	20 min
Xylol	20 min
Paraffin	1 hour
Paraffin	1 hour

4.7.1 Paraffin section De-paraffinization

Tissue section de-paraffinization was performed with incubation of the sections at room temperature in ethanol and xylol in the mentioned manner in Table 4.6.

Table 4.6 De-paraffinization process and steps

steps	1	2	3	4	5	6
Deparafinization	2x 10 min in xylin	2x 5 min 100 % Ethanol	2x3 min 70 % Ethanol	2x1 min 50 % Ethanol	Short incubation in tap water	Short incubation in ddH_2O

4.7.2 Antibody staining

In order to recover the epitopes of the antigens from the process of fixation antigen retrieval was performed with Tris (10 mM) EDTA (1 mM) solution at 98 °C for 30

minutes. The process was done in a beaker on a heater. Afterwards, the sections were cooled down in the Tris EDTA solution in the same beaker to room temperature. The sections were washed with ddH_2O and then TBS (pH, 7.6) and were blocked in 3 % BSA in TBS-Tween (0.1 %) for 1 hour in room temperature. Next, each section got stained by 100 µl rabbit α-mouse/ human monoclonal α-IL4i1 specific antibody in TBS-tween with the final concentration of 1 µg/ml. The primary antibody staining process was done overnight at 4 °C. The following day, for the removal of residual antibodies the slides were washed in TBS-Tween, 3 times. Next, the slides were incubated with biotinylated α-rabbit antibody (1:200) in TBS-Tween for 1 hour in room temperature. The next round of washing was done just like above. Lastly, 1:500 streptavidin-Alexa Fluor 488-conjugated antibody was added to the slides and the incubation was done in the dark and at room temperature. The last round of washing was performed like the other two times mentioned above. Adequate amount of mounting media DAPI Fluoromount was added to each slide.

With the exact same process of slide preparation, deparafinization and antigen retrieval the slides were stained with 2 µg/ml FITC conjugated rat mouse α- T1α antibody for AECI visualization. The incubation and washing steps were exactly as mentioned above.

Next antibody staining refers to proSP-C specifically for AECII visualization. 2 µg/ml α-proSP-C antibody was used for staining the slides exactly treated like mentioned above. Secondary antibody Alexa Fluor 488 with 4 µg/ml (1:500) concentration was added to the slides. All washing steps were performed as mentioned previously.

4.7.3 Microscopy

The slides were visualized with wide field microscope Leica DMI6000 and also Leica SP8 MP confocal microscope. Samples were analyzed using the wide field microscope Leica DMI6000, DFC295 color camera and with the objectives 10 x (HI PLAN I 10x/0.22 PH1, Leica), 20 x (HCX PL FL L 20x/0.40 CORR PH1, Leica), 40 x (HCX PL FL L 40x/0.60 CORR PH2, Leica) and 100 x oil objective (HCX PL APO 100x/1.40-0.70, Leica).

In addition Leica TCS SP8 confocal microscope was used. The system was installed with Argon Ion (65 mW), HeNe (10 mW) and DPSS (20mW) lasers and 5 X (HPLC

FLUOTAR), 25 x (N2.1HCX IRAPO) and 40 x (HC PL IRAPO) objectives. The system is installed with 2 PMT and 2 hybrid detectors (HyD).

For visualization of IL4i1 (AF488) Argon Ion laser (65 mW), objective 25 x (N2.1HCX IRAPO) and PMT2 (497 nm-539 nm) detector was set. For visualization of tdTomato conidia DPSS laser (20mW), 25 x (N2.1HCX IRAPO) objective and HyD (572 nm-654 nm) detector was set.

4.8 Analysis of branched-chain α-ketoacids

To analyze the content of branched-chain α-ketoacids (including 4HP and I3P), two different derivatization reagents were used (OPD: I3P; DMB: 4HP). 50 mg of homogenized lung tissue was extracted with 300 µl cold 1 M perchloric acid. Insoluble material was removed by centrifugation for 10 min at 25,000 G. For derivatization with OPD (o-phenylendiamine) reagent, 150 µl of the resulting supernatant were mixed with an equal volume of 25 mM OPD solution and derivatized by incubation at 50°C for 30 min. After centrifugation for 10 min, the derivatized ketoacids were separated by reversed phase chromatography on an Acquity HSS T3 column (100 mm x 2.1 mm, 1.7 µm, Waters) connected to an Acquity H-class UPLC system. Prior separation, the column was heated to 40 °C and equilibrated with 5 column volumes of solvent A (0.1 % formic acid in 10 % acetonitrile) at a flow rate of 0.55 ml/min. Separation of ketoacid derivates was achieved by increasing the concentration of solvent B (acetonitrile) in solvent A as follows: 2 min 2% B, 5 min 18% B, 5.2 min 22% B, 9 min 40% B, 9.1min 80% B and hold for 2min, and return to 2% B in 2 min.

For derivatization with DMB (1,2-diamino-4,5-methylendioxybenzene), 30 µl extract was mixed with 30 µl DMB reagent (5 mM DMB, 20 mM sodium hydrosulfite, 1 M 2-mercaptoethanol, 1.2 M HCl) and incubated at 100°C for 45 min. After 10 min centrifugation, the reaction was diluted with 240 µl 10% acetonitrile. UPLC system, column and solvent was used as described above. Baseline separation of DMB derivates was achieved by increasing the concentration of acetonitrile (B) in buffer A as follows: 2 min 2 % B, 4.5 min 15 % B, 10.5 min 38 % B, 10.6 min 90 % B, hold for 2 min, and return to 2 % B in 3.5 min. The separated derivates were detected by fluorescence (Acquity FLR detector, Waters, OPD: excitation: 350 nm, emission:

410 nm; DMB: excitation: 367 nm, emission: 446 nm) and quantified using ultrapure standards (Sigma). Data acquisition and processing was performed with the Empower3 software suite (Waters).

Analysis of branched-chain α-ketoacids was done in collaboration with Dr. Christiane Opitz, University hospital Heidelberg, Germany.

4.9 Qualification of lung's fungal burden by a colony forming unit (CFU) assay

Two days before the experiment *Aspergillus* minimal media (AMM) agar was prepared and autoclaved. The next day, 30 ml AMM agar was pipetted into 10 cm petri dishes and C57Bl/6 and IL4i1-deficient mice were infected with $5x10^6$ *A. fumigatus* conidia. 24 hours after infection the lungs were explanted from the animals and transferred to 2 ml PBS in a purple capped C-tube (Miltenyi Biotec, Bergisch Gladbach, Germany). The C-tube's lid was closed tightly and placed upside down into the gentleMACS dissociator (Miltenyi Biotec, Bergisch Gladbach, Germany). This instrument has two programs for dissociation of the lungs into single cells. Program one cuts the lung tissue into pieces by gentle rotation for 37 Seconds and program two turns the lung tissue pieces into a single cell suspension in 38 Seconds. After performing both programs one after the other single cell suspension was ready. At this point five PE 1.5 ml tubes numbered from 1 to 5 were filled with 180 µl PBS for the serial dilution of the single cell suspension. From the undiluted suspension, 100 µl was directly spread in a 10 cm petri dish. This step was done on a petriturn (Göttingen, Germany) with L shape spreader. Next, the single cell suspension was diluted 1:100 with PBS (20 µl undiluted suspension to180 µl PBS in tube 1). From this tube 20 µl suspension was pipetted to tube number 2 with 180 µl PBS. With the same fashion, 5 dilutions were prepared and all of them got spread on AMM agar of the prepared petri dishes. The plates got incubated in 37°C. Right after 24 hours the grown colonies on the plates were counted if possible (Fig4.2).

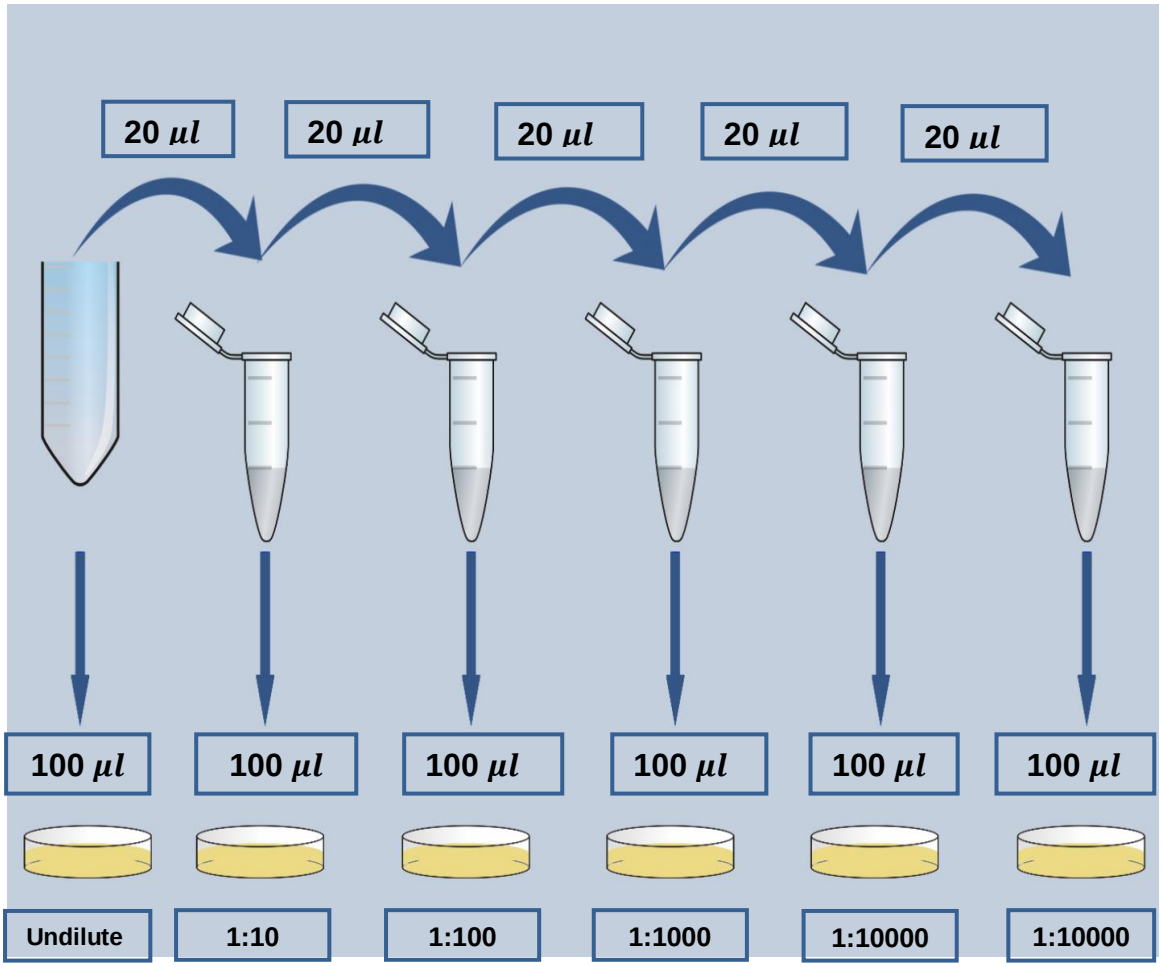

Figure 4.2 Fungal burden by Colony forming unit

4.9.1 CFU Calculation

The calculations were done as follow:

CFU $_{Lung}$ = CFU $_{counted}$ x dilution factor $_{plate}$ x dilution factor $_{suspension}$

Dilution factor $_{plate}$ = Undiluted (1), 10,100, 1000, 10000, 100000

$$\text{Dilution Factor}_{\text{Suspention}} = \frac{2000^{*}(\mu l) + \text{Volume}_{\text{plate}}}{\text{Volume}_{\text{plate}}}$$

* 2000 µl indicates the amount of PBS in which the lung tissue was dissociated in the C-tube initially. This value can be variable from experiment to experiment.

The plates with less than 3 and more than 300 colonies were not included in the results.

4.10 Mouse genotyping PCR

As mice were sacrificed for other experiments, about 0.5 mm from IL4i1-deficient and C57B/6 tails were cut. 5 µL Proteinase K (20 mg/mL) was added to 1 mL lysis buffer for each sample. The samples were incubated at 55 °C at 750 RPM speed for 2-3 minutes. Next, they were centrifuged at 13,500 RCF, RT, 20 -30 minutes. Supernatants were transferred to new tubes and 150 µL isopropanol was added to each with 4-6 minutes inversion. Samples got centrifuged in 12,500 RCF, RT, 20-30 minutes. Supernatant was removed and the pellet was left in RT to dry for 5-10 minutes. 100 µL sterile dH_2O was added to each tube and the pellet got dissolved in it. Samples got incubated in thermomixer with 300 RPM speed and at 37 °C so the DNA dissolves completely. The samples were centrifuged at 12,500 RCF at RT for 5-10 minutes. The supernatant was carefully removed and placed into new tubes. The master mix was prepared as mentioned in Table 4.7.

Table 4.7 Contents of the master mix for genotyping PCR

5xPCR-Mastermix	Primer(Forward)	Primer(Reverse)	DNA	Water
5 µl	1 µl	1 µl	1 µl	17 µl

IL4i1 primer sequence (forward): gcgaggctgaggactatgac

IL4i1 primer sequence (reverse): gcctctccccttcaggatac

PCR program:

1- Heat lid to 110 °C
2- 95°C for 5 minutes
3- Start loop 35x
4- 95°C for 30 seconds→Denaturation
5- 56°C for 30 seconds→Annealing
6- 72°C for 30 seconds→Elongation
7- Stop loop
8- 72°C for 5 minutes
9- Store forever at 4°C

4.10.1 Agarose gel electrophoresis

24 g agarose was dissolved in 100 ml Tris-Acetate-EDTA (TAE) buffer in an erlenmeyer flask in a microwave. When agarose was completely dissolved, the flask was left at room temperature until it was cooled down. To stain the DNA 7.5 µl Midori Green (nucleic acid labeling solution) was pipetted into the flask directly. The gel solution was casted into the gel tray. After 15 minutes incubation in room temperature the gel was formed and transferred to the container filled with TAE buffer. On the first slot 10 µl O'GeneRuler low range DNA ladder was loaded and 20 µl of the PCR product were loaded in the rest of the slots. The whole system was connected to a power supply. The voltage was set on 100 V and Amperage on 270 A. Proteins ran from Cathode (-) towards Anode (+) in 45-60 minutes.

4.11 *A. fumigatus* DNA extraction

100 µl $1x10^8$ *A. fumigatus* conidia was cultured in 200ml AMM medium and was incubated in 37 °C incubator with 180 RPM shaking speed for 20 hours. The grown mycelium was filtered with a filter paper and was completely dried between several tissues with hand force. The dried mycelium at this step should look like a sheet of paper. Next, the dried mycelium was grinded in a sterile set of mortar and pestle with liquid nitrogen. Here the mycelium turns into a powder that was collected in a PE 2 ml tube and incubated in 1 ml aspergillus lysis buffer for 10 minutes on ice. The PE 1.5 ml tube got centrifuged in 1300 g for 12 min in 4 °C and the supernatant was pipetted to another tube. In order to extract pure DNA from this *A. fumigatus* lysate Qiagen DNA extraction kit was used according to the manufacturer protocol.

4.12 Bronchoalveolar lavage (BAL)

C57bl/6 and IL4i1-deficient mice got infected with $5x10^6$ *A. fumigatus* conidia. 24 hours later all mice were sacrificed with CO_2 asphyxiation. The mice were fixed on a silicone pad on the bench top and the skin was cut opened. The salivary glands and the muscles around the tracheae was carefully removed. A 22 G IV catheter was placed into the trachea and 1 ml ice cold PBS + 5 m M EDTA was instilled into the lung with a 1 ml syringe and directly the PBS got aspirated and was collected in a 15 ml PE tube on ice. The same procedure was performed 5 times in order to

collect as many cells as possible from the lung. In the first round of aspiration the amount of returned liquid is normally less than the following times and the fact is that the main portion of the washed cells are collected during the first couple of aspirations.

4.13 TNF-α ELISA

As mentioned in the previous section, BAL was collected from IL4i1 k.o. and C57B/6 mice only in one time aspiration with 1 ml PBS to prevent dilution of the cytokine's level for a more efficient measurement. Mouse TNF-α was measured by special ELISA kit for this means from R&D systems. The experiment was done exactly as mentioned in the protocol from the manufacturer and the plate was measured by spectrometer (SpectraMax M5 plate reader, Molecular Devices, Sunnyvale, California, United States).

4.14 Neutrophil granulocytes isolation

For molecular investigations the next cells of the phagocytic network, which were isolate after *A. fumigatus* infection were neutrophil granulocytes. For this reason Catchup mice (Hasenberg, et al, 2014), a unique transgenic strain with tdTomato expressing neutrophils, was used as a tool for cell sorting. With this approach non antibody stained neutrophils which eventually were least activated during the process of isolation were prepared for proteomics studies.

4.14.1 Neutrophil sample preparation

Catchup mice were infected with $5x10^6$ transgenic Green Fluorescence protein (GFP) expressing *A. fumigatus* conidia (Krappmann et al., 2005) and another group of mice was infected with autoclaved tap water as negative control. Neutrophil granulocytes were sorted from three different sites of the same *A. fumigatus* infected mouse and two different sites of the same mock infected mouse. The three different sites from which neutrophils were sorted have been firstly bone marrow, secondly blood and thirdly BAL. So, from each infected mouse, three neutrophil samples had to be prepared. The BAL sample itself contained two populations for sorting and eventually analysis: The neutrophil population in direct and physical contact with *A. fumigatus* conidia and the population with no contact to conidia. As

there is almost no neutrophil recruitment to mice lungs after infection with sterile tap water, only two neutrophil populations were sorted for investigation from the mock infected group of animals which are bone marrow and blood neutrophils. All and all five samples and six different neutrophil populations were prepared. Bone marrow, blood, BAL and neutrophils from *A. fumigatus* infected Catchup mice and bone marrow and blood neutrophils from mock infected animal. Bone marrow, blood, BAL and BAL in contact with conidia neutrophil populations from *A. fumigatus* infected animals and bone marrow and blood neutrophil populations from mock infected animals.

4.14.1.1 Blood neutrophil preparation

24 hours after *A. fumigatus*/mock infection the mice were anesthetized by 100 µl/20 g mouse weight ketamine/xylazine solution intraperitoneal (IP) injection. When the mice were unconscious, 100 µl Heparin solution was injected retrobulbarly. After waiting for 5 minutes for heparin flowing into the blood, retrobulbar bleeding was performed. During this procedure at least 700 µl blood was collected into a PE 1.5 ml tubes, which initially contained 40 µl heparin. 700 µl blood was incubated on ice for 45 minutes in 3 ml erythrocyte lysis buffer in a 15 ml PE tube. The PE tube was filled with PBS to 15 ml and centrifuged for 10 minutes in 350 G in 4°C.

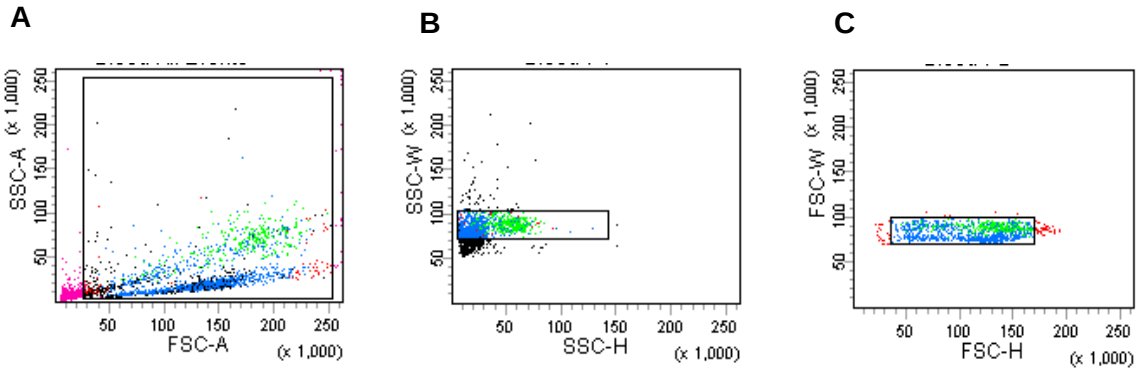

Figure 4.3 Gating strategy for FACS analysis of blood neutrophils A. Gate for all live cells B & C gate for excluding doublets

After the washing step, the supernatant was discarded and the pellet was re-

suspended in 1 ml sterile ice cold PBS. The cells were filtered and proceeded to FACS (Fig 4.3).

4.14.1.2 BAL neutrophil preparation

After the blood sample was obtained from the mice they were pinned to a silicone pad and BAL was performed as explained in section 3.12. As mentioned before, from the BAL sample two different populations of neutrophils were sorted: neutrophils in contact to conidia and neutrophils without conidia contact. The buffer used in this experiment for BAL was conventional PBS (contrary to section 3.12 in which PBS + 5 mM EDTA was used). The reason for this approach was that EDTA could wash away the physically connected conidia to the neutrophils and consequently the BAL in contact to conidia population would have been lacking. Regardless of the sample preparation protocol, observations indicated that number of cells from one animal for this population is inadequate. Therefore BAL in contact to conidia population was pooled from 3-5 animals. In the case of all the other sorted populations, the neutrophils were obtained from one animal. When the BAL was collected in a 15 ml PE tube it was centrifuged for 10 minutes in 350 G at 4°C. The pellet was re-suspended in 2 ml erythrocyte lysis buffer and incubated for 10 minutes on ice. After another washing step the pellet was re-suspended in 1 ml ice cold PBS and was filtered. The sample was proceeded to cell sorter for sorting the two mentioned populations of neutrophils (Fig 4.4).

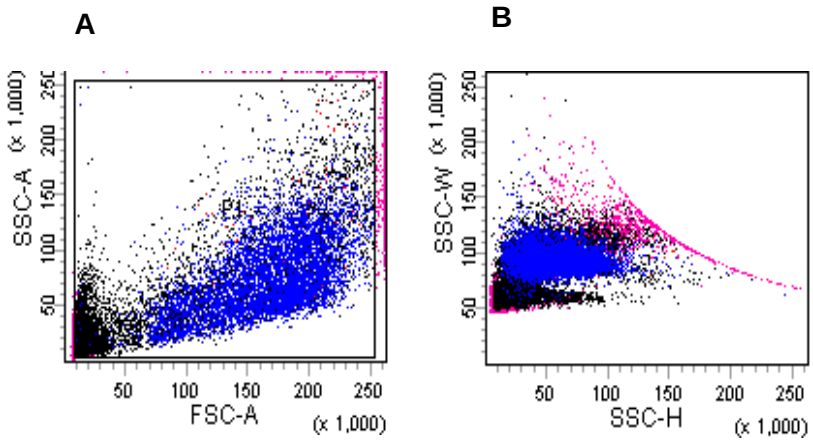

Figure 4.4 Gating strategy for FACS analysis of BAL neutrophils A. Gate for all live cells B. Doublets didn't get excluded so that no conidia bound to neutrophils were excluded.

4.14.1.3 Bone marrow neutrophil preparation

Finally, bone marrow was flushed and the erythrocytes were lysed as previously reported (Hasenberg et al., 2011). The cell pellet was re-suspended in 2 ml ice cold PBS and the sample was proceeded to cell sorter (Fig 4.5).

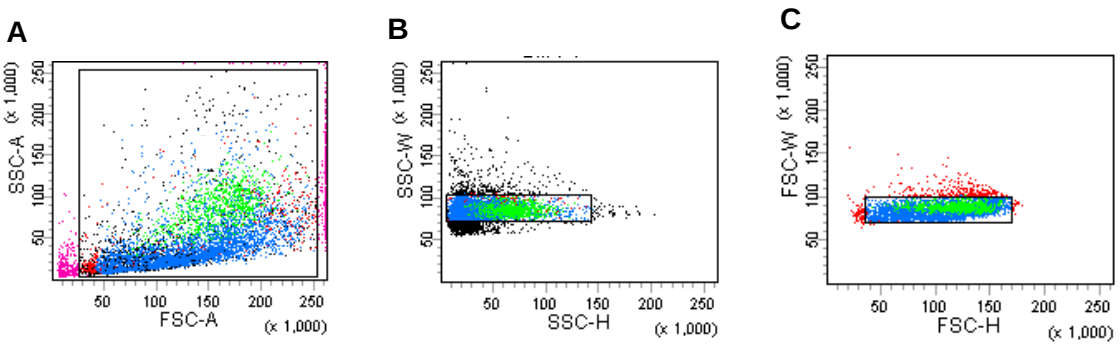

Figure 4.5 Gating strategy for FACS analysis of bone marrow neutrophils A. Gating for living cells B & C gate for excluding doublets

4.14.2 Fluorescence activated cell sorting (FACS) of neutrophil granulocytes

Neutrophil Sorting was performed in Imaging Center Essen (IMCES) using a BD FACS Aria III cell sorter. 488nm and 561 nm lasers were switched on to excite tdTomato expressing neutrophils of the Catchup mice and GFP of the transgenic conidia, respectively. The startup, drop delay adjustment, and compensation were performed according to the standard operating procedure of the machine. The used nozzle for neutrophil sorting was 100 micron with equivalent sheath pressure of 20 PSI. Frequency was fixed on 30, Amplitude was between 8 and 10 and Gap was between 10 and 12 in different measurements. Two 15 ml PE tubes filled with 2 ml PBS were placed into a two ways tube holder. The temperature unit was set on 4°C. “100,000” was entered to target event panel as the number of the neutrophils to be sorted and also the number of target events was adjusted on continuous. The precision mode was set on purity. In order to sort the neutrophils from bone marrow, BAL and blood, the positive population for phycoerythrin (PE) fluorophore was sorted as there was no direct tdTomato in the setting of the machine. To sort the population of neutrophils, which was in contact with conidia, the double positive population for PE (tdTomato neutrophils) and GFP (conidia) was chosen. When the sort of each sample was done, the 15 ml PE tube was completely filled with ice cold

PBS to collect all the sorted cells on the walls of the tube. The tube got centrifuged at 350 G, 4°C for 10 minutes. The supernatant was discarded and the pellet got frozen in -80°C freezer. After each round of sorting, the sorted sample was reanalyzed on the machine to make sure about the efficiency of the process.

4.15 Neutrophil granulocytes proteomics

In the first place minimum number of neutrophils that could be run on LCMS, for finding out the regulated proteins, was identified. Fig 3.6A shows a silver stained SDS gel. Gradient number of sorted neutrophils ran on this gel from 10k to 100k can be visualized. Running the gradient of sorted neutrophil numbers on LCMS revealed the fact that 100 k was the minimum number of cells for getting sensible results of the regulated proteins. Fig 3.6B indicates higher peptide concentrations and proteins groups with more number of cells. 100k cells demonstrate 1098 protein groups and 3713 identified peptides. Peptide spectrum matches (PSMs) resulted from 10k and 20k indicate that most of the detected spectra were identified poorly and this is in total contrast with the values of PSM from 100 k cells. Fig 3.6C shows the chromatogram from the 4 cell number conditions ran on LCMS. Taking a quick glance at the chromatograms one can obviously see better relative abundancy of peptides in 100k.

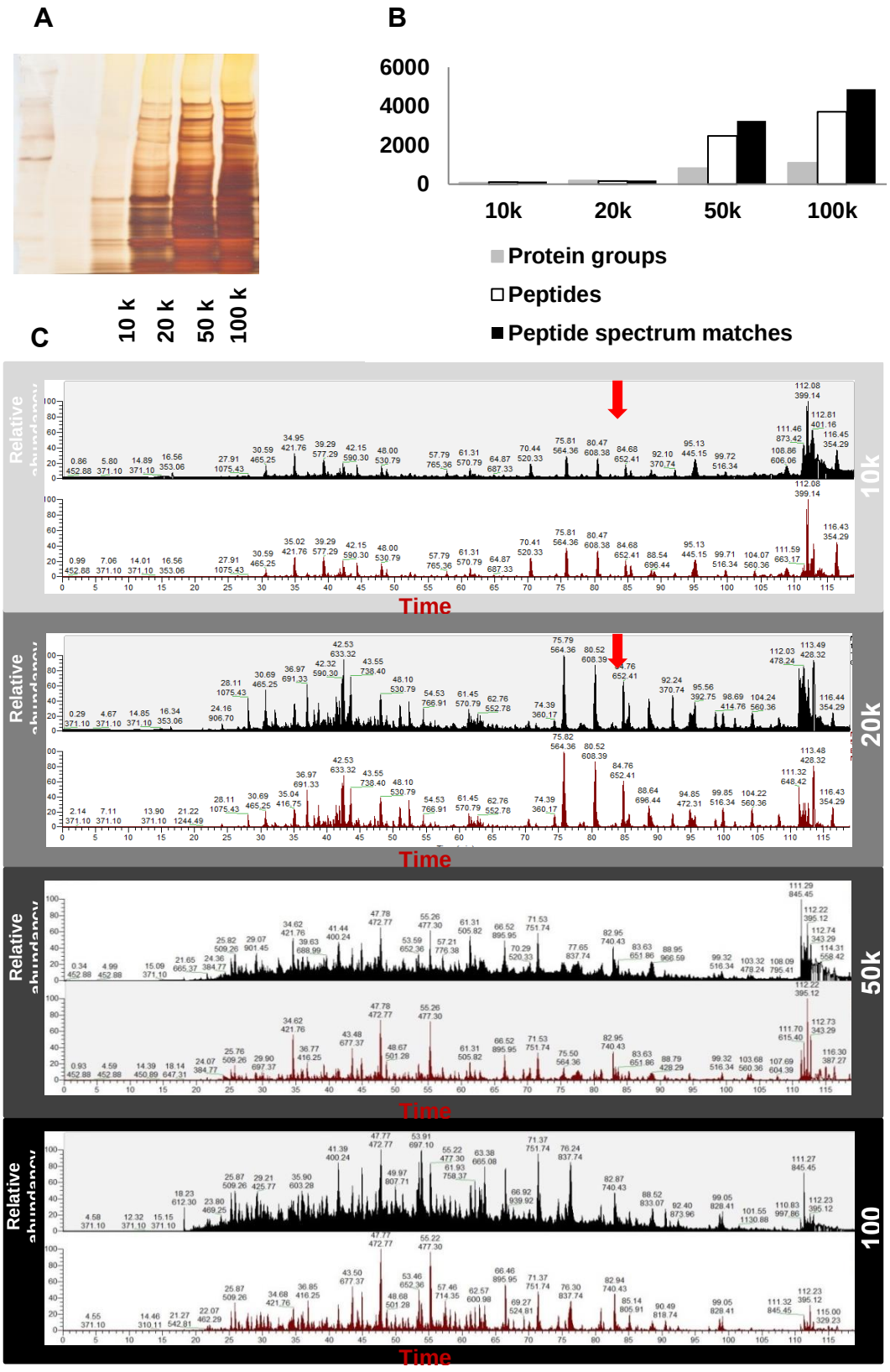

Figure 4.6 100k neutrophil granulocytes, minimum sensible cell number for LCMS analysis (A). 10k, 20k, 50k and 100k neutrophils were sorted from C57BL/6 mouse bone marrow and were analyzed on SDS gel and silver staining. (B). All four groups of neutrophils were analyzed on LCMS and different values were plotted. (C). Chromatograms of the analyzed10k to 100k neutrophils on LCMS; The X-axis represents retention time (minutes) and the Y-axis corresponds to relative abundancies of signals from the detected peptides. Red arrows indicate polymer contamination.

Protein digestion, ASA, data analysis, protein identification and quantification for performing LCMS on the sorted neutrophil granulocytes was done with the same procedures explained in section 3.4.2 for AECII proteomics except some adjustments. 100k neutrophils were lysed in 20 µl NH_4HCO_3 buffer containing 0.1 % RAPIGEST. DTT reduction, Iodoacetimide Alkylation and tryptic digestion were performed as in section 3.4.2. The samples were injected into an Ultimate 3000 RSLCnano system (Dionex, Idstein,Germany) coupled to an LTQ Orbitrap Elite mass spectrometer (Thermo Scientific, Bremen, Germany). For protein identification Proteome Discoverer 1.4 (Thermo Fisher Scientific) was the software used and for the peptide identification the mass spectra were searched against UniProtKB/Swiss-Prot database (Release 2015_11 of 11.11.2015); 549,832 entries) restricted to Mus musculus using the Mascot search engine (version 2.5)

5 Results

5.1 AECII respond to *A. fumigatus* infection

AEC type I and II coat the surface of alveoli. Fig 5.1A shows a scanning electron microscopy (SEM) image of a 24 hours *A. fumigatus* infected C57BL/6 mouse lung. AECII is highlighted in green. By definition, the entire surfaces of the alveoli, aside from AECII, are covered by AECI. According to this fact the grey surfaces are allegedly AECI. In this image neutrophil granulocytes are featured in blue and *A. fumigatus* conidia in pink. Neutrophils are in the process of phagocytosing conidia in a close proximity in AECI and II.

A

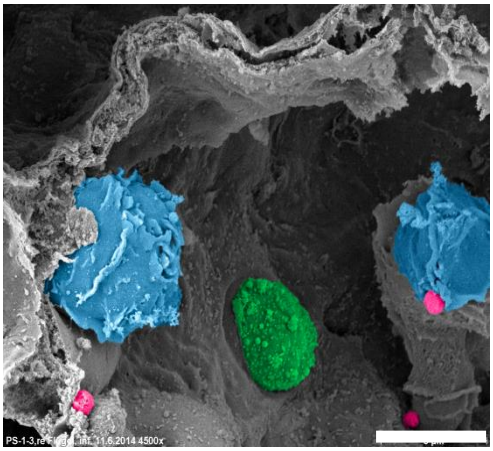

AECII

Lung phagocytes

A. fumigatus

B

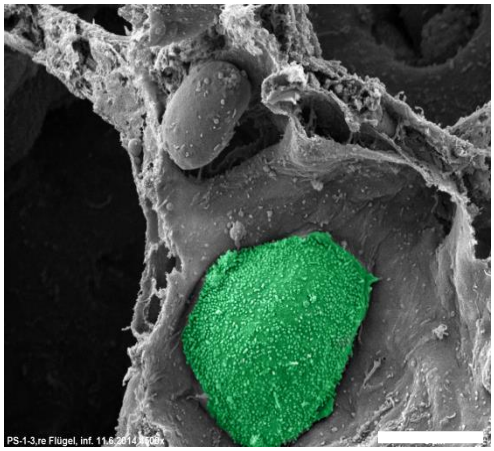

AECII

C

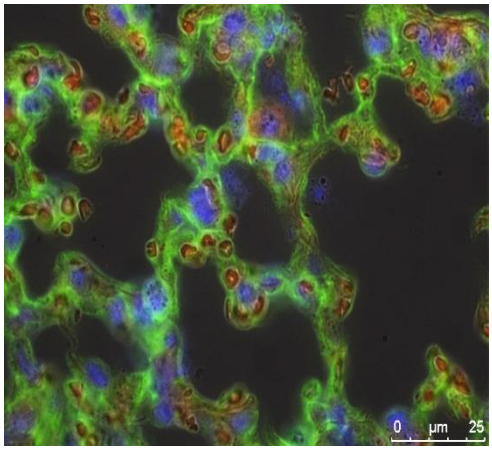

T1α

DAPI

A. fumigatus

D

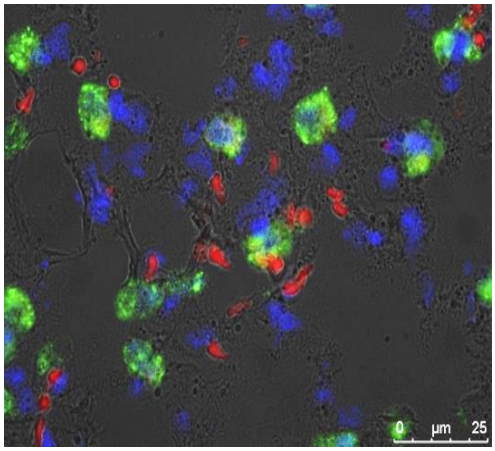

proSP-C

DAPI

A. fumigatus

Figure 5.1 Alveoli are covered by AECI & II (A). Scanning Electron Microscopy (SEM) image of an alveolus from an *A. fumigatus* infected lung. AECII is highlighted in green and the grey surface embracing this cell type is known to be AECI. Lung phagocytes are highlighted in blue. AECI, II and neutrophils are in juxtaposition. Neutrophil granulocytes phagocytose *A. fumigatus* conidia shown in pink. The scale bar represents 10 µm. (B). SEM image of the interior of an alveolus with a high magnification. The highlighted green cell is an AECII. The scale bar illustrates 5 µm. (C & D) show immunohistochemistry images of 5 µm paraffin slices of C57BL/6 mice lung (C) AECI stained by its known marker T1α, covers almost all surfaces. (D) AECII stained by Pro surfactant protein C. Nuclei are stained with DAPI.

Fig 5.1B also indicates the interior of an infected lung with a higher magnification. As a proved point, about 95% of the lung is covered by AECI and only 5% by AECII (Chen et al., 2004). Immunohistochemistry images of the lung in Fig5.1C and D confirm this feature. Taking a close look at these images, AECs interact excessively with *A. fumigatus* conidia.

5.2 AECII negative isolation by immune magnetic approach

Among the members of the phagocytic network AECs are the least investigated cell types upon *A. fumigatus* infection. Therefore, we first focused on this entity. To perform proteome analysis of AECs they first had to be isolated from murine lungs. A negative isolation protocol had to be applied as positive isolation techniques can activate cells by the labeling process only. According to the literature a protocol for negative isolation of AECI and II by immune magnetic approach does not exist. To finally establish this protocol first an enzyme mixture for lung dissociation had to be set up with which the target cell type could get detached from the tissue. Secondly, an antibody mixture had to be designed for exclusion of all the unwanted cells during the isolation.

As AECI are extremely thin for being physiologically efficient during gas exchange applying severe enzyme cocktails for lung digestion harmed these cells. For this reason either excessive number of dead cells resulted from applying harsh enzyme treatment or AECI were not released from basement membrane due to less severe enzyme mixtures. Additionally, designing an effective antibody mixture for negative isolation of AECI was not possible due to lack of commercial antibodies that can label surface markers of the unwanted cells for exclusion during the process of

isolation. Reasons above led us leave AECI negative isolation as an unsolved challenge and focus on AECII isolation.

Following the published protocol from Corti et al. (1996), murine lungs were digested by the enzyme dispase for AECII isolation. Then, lungs were dissociated and all cell types in the whole lysate were characterized following the published protocol for flow cytometric isolation of AECII by Gereke et al. (2009). This protocol suggests AECII purification by negative isolation with FACS approach which means the unwanted cell types get antibody labels and the untouched AECII with sideward scatter high (SSC^{high}) specification, due to the lamellar bodies, can be isolated by cell sorting. This protocol is mentioned as “the old protocol” in the following pages. Since FACS analysis could be too drastic for the cells, stress of the process might be a reason for activation of some biological pathways. However “The new protocol” suggests negative isolation of AECII by immune magnetic approach. The average result of three independent experiments indicated that after lung digestion by the enzyme dispase the lung lysate consisted of 10.64 % $CD11c^+$ cells, 21.75 % $CD11b^+$, 8 % $F4/80^+$, 8.58 % $T1\alpha^+$, 17.34 % $Sca\text{-}1^+$, 14.18 % $CD31^+$, 19.93 % $CD45^+$ and 2.95 % $CD19^+$ cells (Fig 5.2A). (As CD45 is the general marker for all leukocytes the following double positive populations were expected: $CD45^+/CD11c^+$, $CD45^+/CD11b^+$, and $CD45^+/F4/80^+$). With this knowledge a complete negative isolation antibody mixture for primary murine AECII isolation was newly designed.

As already mentioned above, components of the antibody mixture for AECII negative isolation were partly obtained from the old protocol The main difference of the new protocol were the additional antibodies against Sca1, T1α and CD31 to label mesenchymal and bronchiolar epithelial progenitor cells, AECI and endothelial cells, respectively (Bars shown in red in Fig 5.2B).

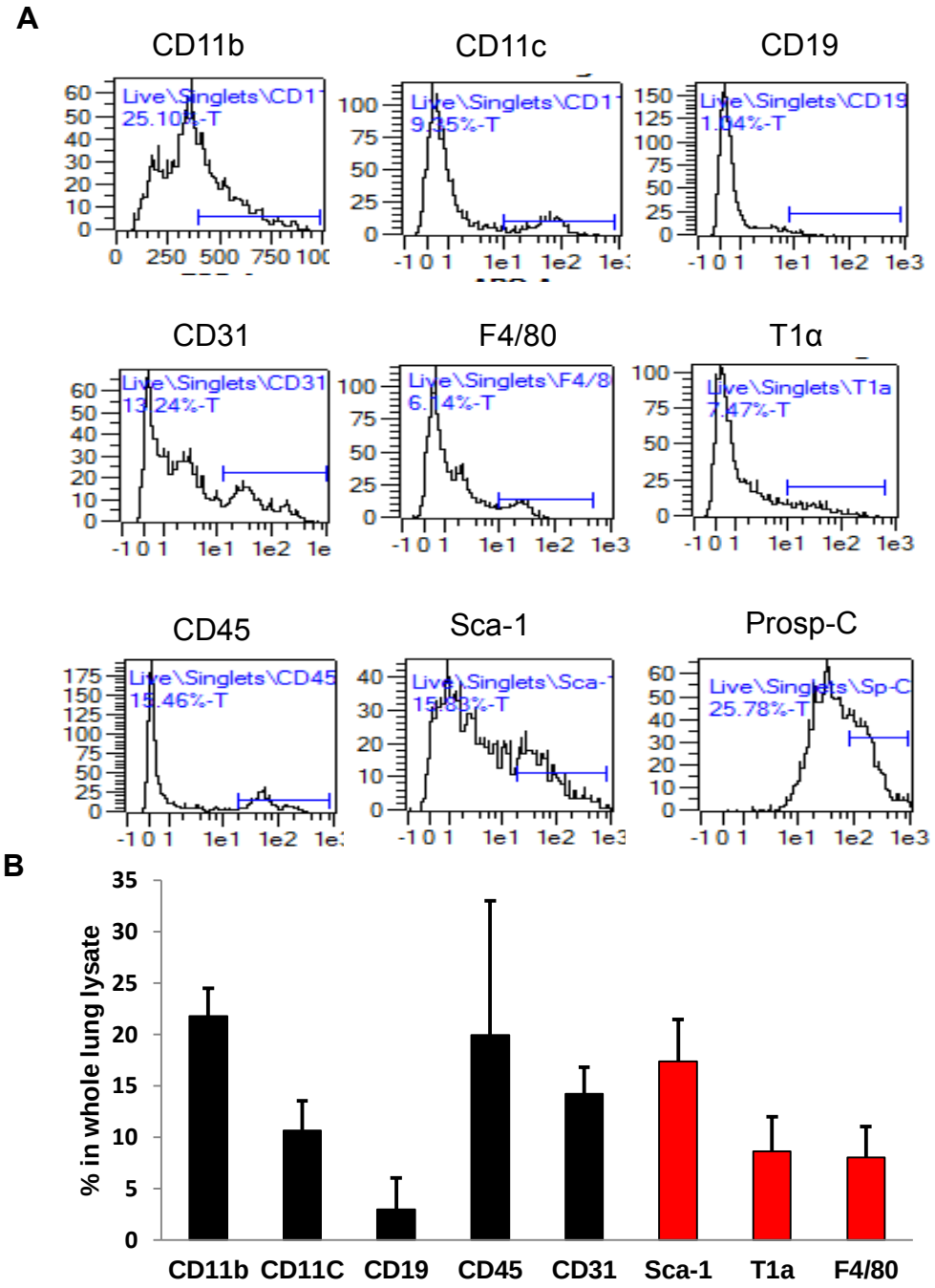

Figure 5.2 Murine lung cell components Whole lung single cell suspension antibody staining and flow cytometry reveals the main cell types existing in a mouse lung tissue digested by the enzyme dispase. (A) Histograms from staining of the different cell types inside the whole lung. (B) Bar graph shows the average of three independent analyses. Black bars refer to the members of the antibody mixture in the existing protocol for primary AECII isolation by flow cytometry. Red bars refer to the additional antibodies identified in the current work for setting up an exclusive negative isolation protocol for primary AECII from murine

.

Table 5.1 Comparison between the old protocol antibody mixture for primary AECII negative isolation and the new designed mixture

Corresponding cell type	Old protocol	New protocol	% in whole lung
Dendritic cells	α-CD11c	α-CD11c	10.64
Monocytes and macrophages	α-CD11b	α-CD11b	21.75
Macrophages	α-F4/80	α-F4/80	8.0
AECI	--------	α-T1α	8.58
bronchoalveolar stem cells (BASCs)	--------	α-Sca-1	17.34
Endothelial cells	--------	α-CD31	14.18
Leukocytes	α-CD45	α-CD45	19.93
B cells	α-CD19	α-CD19	2.95

Fig 5.3A shows a whole lung single cell suspension before negative isolation by immune magnetic approach (Pre-sort). Fig 5.3B indicates the pure isolated primary AECII (Post-sort). Gating strategies were according to isotype controls shown in Fig 5.3C. As shown in Fig 5.3D, the primary AECII isolation process yielded over 90% purity and AECII constitute over 25% of the non-purified lung lysate digested by the enzyme dispase.

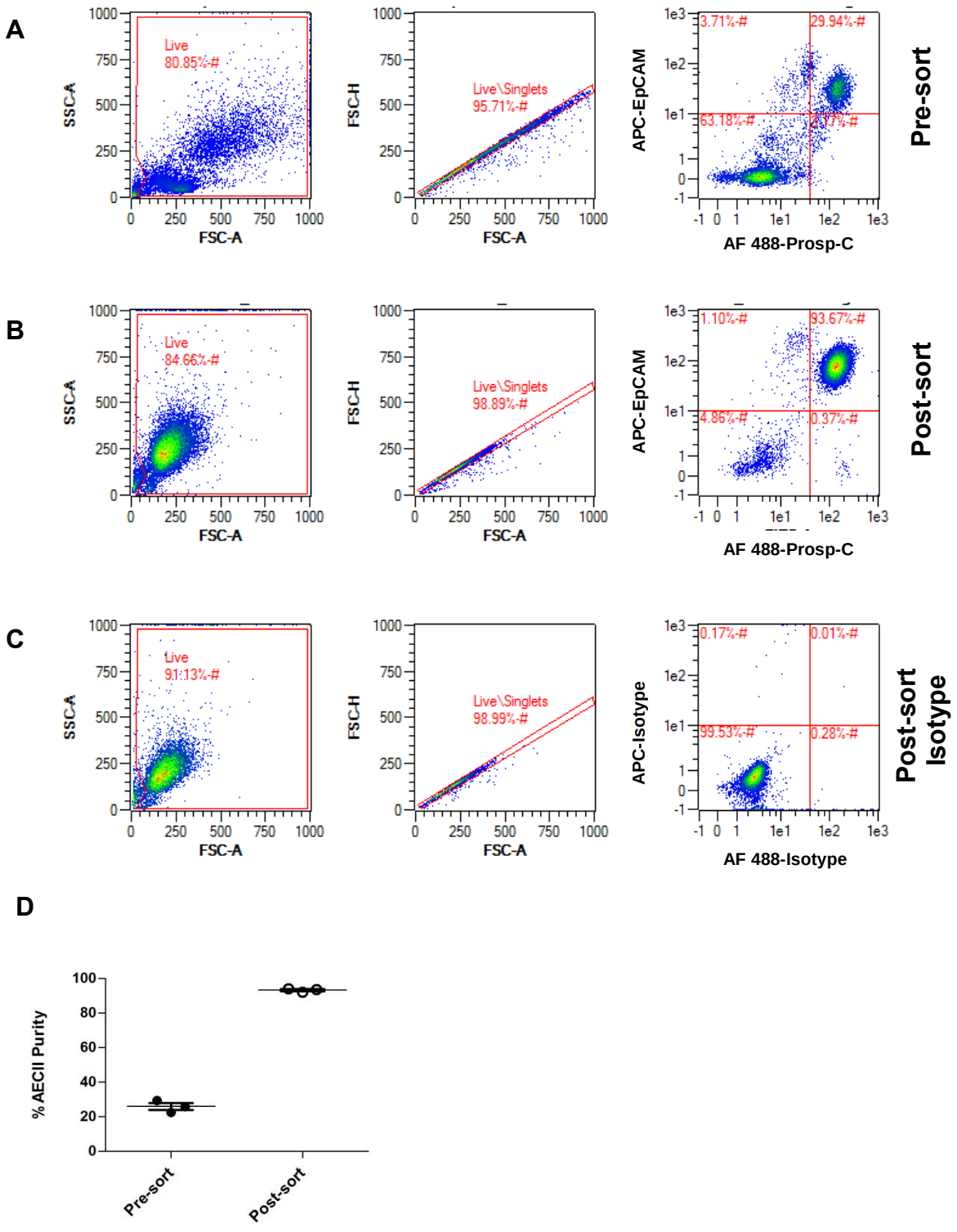

Figure 5.3 Primary AECII negative isolation by immune magnetic approach (A) Whole lung cell suspension resulting from dispase digestion. The applied gating strategy for A, B and C was equivalent and as follow: live cells, singlets and lastly gate for EpCAM, APC conjugated for all epithelial cells and Prosp-C – AF 488 (secondary antibody) specifically for AECII. (B) Primary AECII were isolated from mouse lungs by immune magnetic approach for negative isolation. (C) The isotype control was treated equally as the antibody staining for AECII sample. (D) Indicates that 25 % AECII exist in a whole lung lysate digested by the enzyme dispase (Pre-sort) and over 90 % AECII purity was reached after the immune magnetic based negative isolation (Post-sort). This data was highly reproducible as it was shown by three independent experiments.

Analyzing the proteome of the isolated pure population of AECII, 30 minutes, 8, 24 and 48 hours post *A. fumigatus* infection via 2D gel electrophoresis revealed that the time point 24 hours post fungal infection compared to sterile tap water (mock) infection showed the highest number of regulated proteins (Fig 5.4).

1.1.1 Primary AECII proteome analysis

As 2D gel electrophoresis is a time consuming technique and requires a high number of cells, in order to pinpoint the modified proteome of the isolated primary AECII 24 hours post *A. fumigatus* infection, Liquid Chromatography Mass Spectrometry (LCMS) was performed. Trypsin digested peptides of the isolated AECII from mock and fungal infected samples were run on liquid chromatographic column which was online coupled to a mass spectrometer. From this analysis 2256 proteins were identified as differentially regulated and quantified. Ten proteins were chosen for further studies according to a number of factors: In the first place all quantified proteins with minimum one unique peptide were chosen. Next, the statistical ANOVA test was performed and 121 proteins with P-values greater than/equal to 0.05 were selected. Significantly upregulated proteins were filtered for any max fold change greater than 2. These proteins were checked for their confidence score and the selection was done with the strategy “the higher the better”. Last but not least, all the remaining proteins were screened for their conceptual relevance. Taking into account all these factors, ten proteins were finally selected for further investigations. These ten proteins according to their fold changes from the highest (42.94 times) to the lowest (2.20 times) were as follows: Interleukin 4 induced 1 (IL4i1), Neutrophil gelatinase-associated lipocalin, Intercellular adhesion molecule 1(ICAM-1), Pendrin, Complement C3, Stimulator of interferon genes protein (TMEM 173), Resistin-like alpha (Retnla), Interleukin-33 (IL-33), Chitinase-3-like protein (CHI3L1) and Pulmonary surfactant-associated protein D. LCMS was performed two times independently. Once with 5 replicates and once with 9 replicates for both infected and mock conditions (Table 5.2).

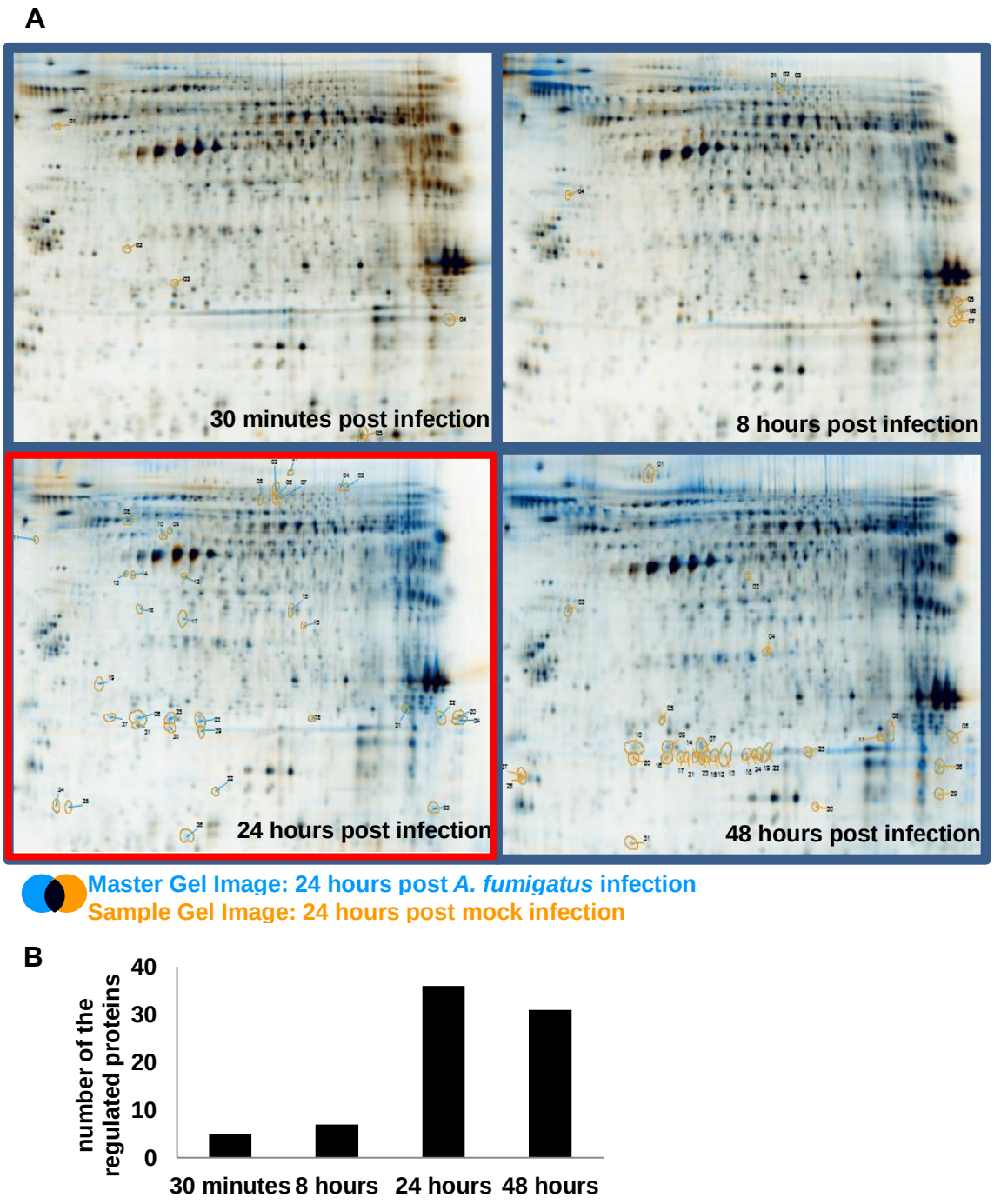

Figure 5.4 *A. fumigatus* infection kinetics (A) Scanned image of 2D gel electrophoresis of isolated primary AECII after 30 minutes, 8 hours, 24 hours and 48 hours *A. fumigatus* infection compared to mock infection. (B) Number of the regulated proteins in comparison to the isolated AECII from fungus infected and mock infected C57BL/6 mice. All mice were female and between 8-12 weeks.

Seven out of these ten proteins (Lcn 2, SFTPD, CHI3L1, Pendrin, C3, IL33 and ICAM-1) were found in both experiments with the difference that the resulted proteins from the experiment with 9 replicates showed better significance, higher

peptide number for quantification, higher confidence scores and also higher fold changes.

Analyzing the proteins down regulated in AECII during *A. fumigatus* infection with the same strategies for filtering as mentioned, turned out lower numbers of conceptually relevant proteins with less fold changes. Therefore we focused on the upregulated proteins resulting from the analysis of the list we acquired from the LCMS measurement.

Table 5.2 Top ten upregulated proteins resulting from two independent LCMS runs of isolated primary AECII, during *A. fumigatus* infection The list resulting from the LCMS run was put through different filters: quantified proteins with minimum one unique peptide were filtered firstly. Next they were selected for statistical significance (p-Anova≤0.05). These proteins were filtered for any max fold change greater than 2. Among those proteins the top ten with the highest confidence score and best conceptual relevance are shown here.

Proteins	P-Value	Max fold change	Confidence score	Peptides used for quantification
IL4i1	$2.91x10^{-10}$	42.94	491.13	8
Lcn 2	$1.08x10^{-10}$	8.05	517.48	9
ICAM-1	$2.06x10^{-7}$	3.94	555.72	12
Pendrin	$1.95x10^{-5}$	3.41	87.5	2
C3	$4.6x10^{-4}$	3.1	1372.26	25
Tmem173	$2.92x10^{-7}$	3.01	113.78	2
Retnla	$5.6x10^{-3}$	2.64	169.72	3

IL33	$5.08x10^{-5}$	2.28	685.24	11
CHI3L1	$2.25x10^{-10}$	2.24	1349.8	21
SFTPD	$1.07x10^{-7}$	2.20	654.52	10

1.1.1.1 Verification of IL4i1 regulation

Among the ten mentioned upregulated proteins, IL4i1 was selected for further investigation. IL4i1 with the highest record of max fold change (42.9 times) among all the other proteins showed importance. The second highest max fold change between these ten proteins belonged to Lcn 2 which was about 5 times less than IL4i1.

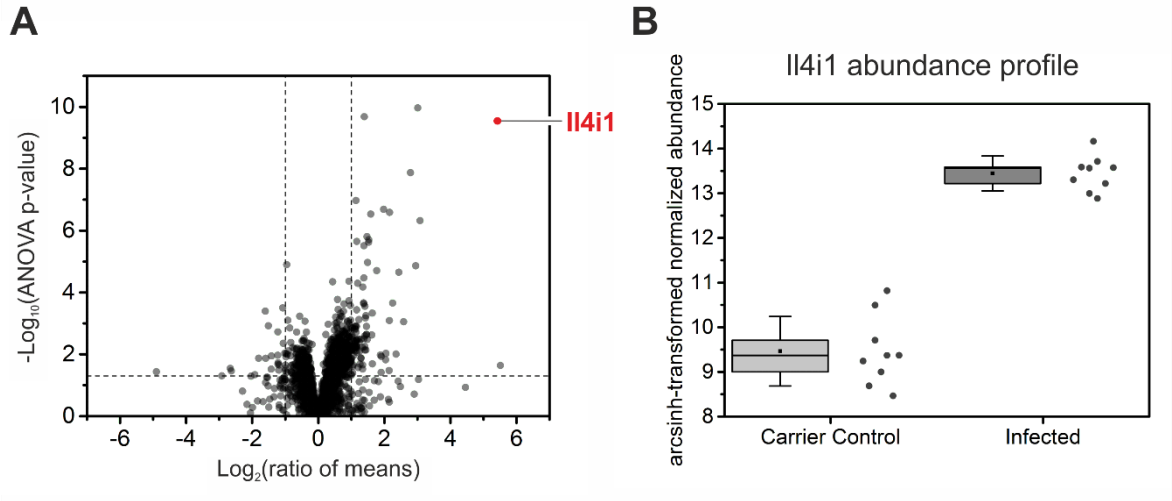

Figure 5.5 IL4i1, the top candidate for further verification (A) Volcano plot indicates Log2 fold change on the X axis and –log10 P-value on the Y axis for 2256 proteins. On the X axis positive values represent positive fold changes for the infected group and negative values correspond to increased expression in the mock infected group. Dashed lines indicate the threshold of significance for both axes. (B) The abundance profile of IL4i1 represents the 25th percentile with the first box and the 75th percentile with the second. The lines inside the boxes indicate the median and the small squares appear for average. The experiment was done with 9 replicates and each dot stands for one sample.

On the other hand, the calculated p-value for IL4i1 was $2.91x10^{-10}$ which was one of the most significant values of all. The confidence score and number of peptides

used for quantification were 491.31 and 8, respectively. With this information IL4i1 which is an L-amino acid oxidase was selected for additional analysis. Fig 5.5A clearly demonstrates that IL4i1 was the most significant protein according to the two above mentioned values and compared to all the 2256 proteins. The abundance profile of the 9 replicates of both infected and a control sample in Fig 5.5B demonstrates a significant upregulation of IL4i1 expression in the infected sample compared to the control. Next, the LCMS results were confirmed by performing real time PCR (qPCR) and Western blot on isolated primary AECII from 24 hours *A. fumigatus* infected and mock infected C57BL/6 animals. Average results of three independent qPCR experiments showed 199.1 fold upregulation of IL4i1 in isolated AECII from fungus infected lungs compared to mock infected samples (Fig 5.6A). Additionally, the Western blot showed a signal 24 hours after *A. fumigatus* infected isolated AECII sample and no bands for the mock infected sample. The appeared two bands on the Western blot for IL4i1 represented the two isoforms of this protein. ERK bands for both samples appeared almost equal (Fig 5.6B). In order to visualize the expression of IL4i1 during infection *in situ*, immunohistochemistry on fungus infected and mock infected murine lung samples was performed and analyzed by wide field microscopy. A specific staining for IL4i1 was shown on the fungus infected slides and no staining was detected on mock infected lungs. The IL4i1 signal was discovered to be in cells that morphologically and size-wise are similar to AECII (Fig 5.6C). Next, the same slides were used for analysis by a confocal microscope to investigate the localization of IL4i1. Fig 5.6D indicates the localization of IL4i1 in AECII in vesicle shaped structures. According to literature these vesicles are lysosomes (Mason et al., 2004).

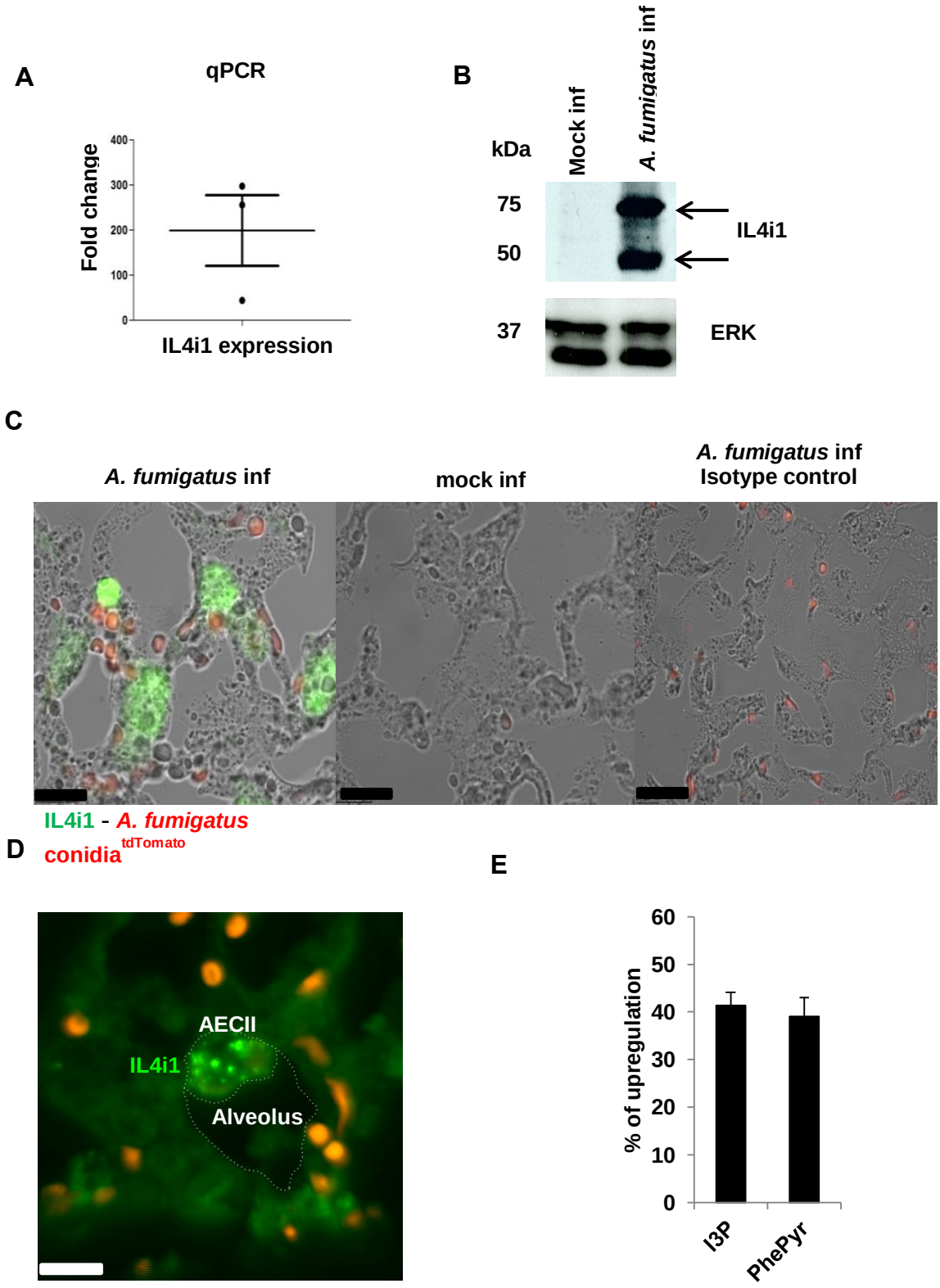

Figure 5.6 IL4i1 upregulates in AECII during *A. fumigatus* infection (A) qPCR results on isolated infected AECII from C57BL/6 mice showed an average of 199.1 fold upregulation of the IL4i1 mRNA compared to mock infected animals. The analysis of the data was performed by ΔΔ CT calculation. The negative control was the mock infected sample and the housekeeping gene was GAPDH. The shown results are generated from three independent experiments (B) The Western blot shows two bands for the infected AECII and no signal for mock infected. These two bands represent the two isoforms of the

protein. ERK control shows the same signal for both conditions. (C) 5 µm paraffin embedded histology slides from fungus infected and mock infected lungs, stained with monoclonal anti rabbit IgG antibody and the equivalent isotype control were visualized on a fluorescent wide field microscope and demonstrated specific staining for IL4i1 on the fungus-infected slides and no staining on mock-infected or isotype control. Transgenic tdTomato conidia can be seen in in the infected samples. (D) HPLC performance on whole lungs demonstrated the upregulation of the metabolites of IL4i1 enzyme activity. Indole 3-pyruvate (I3P) and Phenylpyruvate (PhePyr) are produced while IL4i1 oxidases tryptophan and phenylalanine, respectively. These two amino acids are known as main substrates for IL4i1. This data result from 5 replicates per condition. (E) Confocal image of a 5 µm paraffin embedded *A. fumigatus* infected lung section stained with an IL4i1 specific monoclonal antibody shows positive vesicles in cells similar to AECII in an alveolus. Conidia can be seen in tdTomato. All used animals were female C57BL/6 J mice and between 8-12 weeks.

After confirming the upregulation of IL4i1 in mRNA (qPCR) and protein levels (Western blot) and also with visualization of the expression by wide field and confocal microscopy, the metabolites of the enzyme IL4i1 were measured by HPLC in a collaboration with Dr. Christiane Opitz, Heidelberg University. L - Phenylalanine and L - Tryptophan are the main amino acid substrates for IL4i1 and the upregulation in their metabolism indicates an increase in IL4i1 activity. Fig 5.6E illustrates 41% and 39% upregulation, for indole-3-pyruvate (I3P) and Phenylpyruvate (PhePyr) respectively, 24 hours post *A. fumigatus* infection compared to control in a whole lung. I3P and PhePyr are the main metabolites produced during tryptophan and Phenylalanine metabolism by IL4i1.

To find out the importance of IL4i1 during *A. fumigatus* infection, first New Zealand White (NZW) mice were used. The NZW mouse is a model for studying Systemic Lupus Erythematous (SLE) and, interestingly, the IL4i1 gene with three substitutions in its amino acid sequence is exactly located in the same area of the NZW genome as the gene corresponding to SLE susceptibility (Mason et al., 2004). Therefore this mouse line could be defective in the production of functional IL4i1 and a model for IL4i1 deficiency or dysfunctionality, but it has not been proven yet by any research group. To check the expression of IL4i1 in NZW compared to C57BL/6 mice, AECII were isolated from *A. fumigatus* infected and control animals and real time PCR was performed. The mRNA level of IL4i1 in NZW mice was slightly less than C57BL/6 animals but it didn't show a significant difference (Fig 5.7)

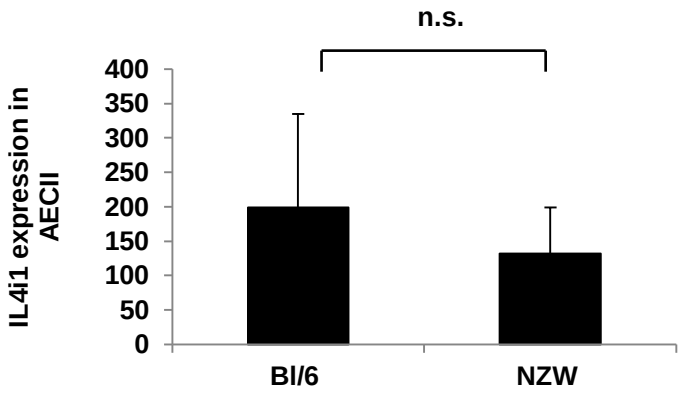

Figure 5.7 IL4i1 expression in NZW compared to C57BL/6 mice Real time PCR of isolated primary AECII from *A. fumigatus* infected NZW and C57BL/6 animals. The fold changes were calculated with the ΔΔ CT method. GAPDH was measured as housekeeping gene and mock infected sample measurements were counted as negative control. This result is the outcome of three replicates per condition. All mice were females and between 8-12 weeks.

Next, NZW mice were set down into a survival experiment. Fig 5.8A demonstrates 100% survival for NZW mice during *A. fumigatus* infection. On the first day after infection NZW, C57BL/6 and C57BL/6 neutropenic animals lost between 7 to 10% of their weight. C57BL/6 animals started recovering from the infection from the second day post infection but neutropenic C57BL/6 animals and NZW increased weight loss percentage. On day three post infection NZW started recovering from the infection but neutropenic animals all died. From day 4 to 7 C57BL/6 animals recovered from the infection completely but NZW did not go back to their initial weight (Fig 5.8B). Culturing mashed lung tissue from NZW, C57BL/6 and C57BL/6 neutropenic animals on AMM agar showed a slight increase in colony numbers in NZW compared to C57BL/6 mice but the difference was not significant and the NZW mice could clear the fungal infection equal to controls (Fig 5.9).

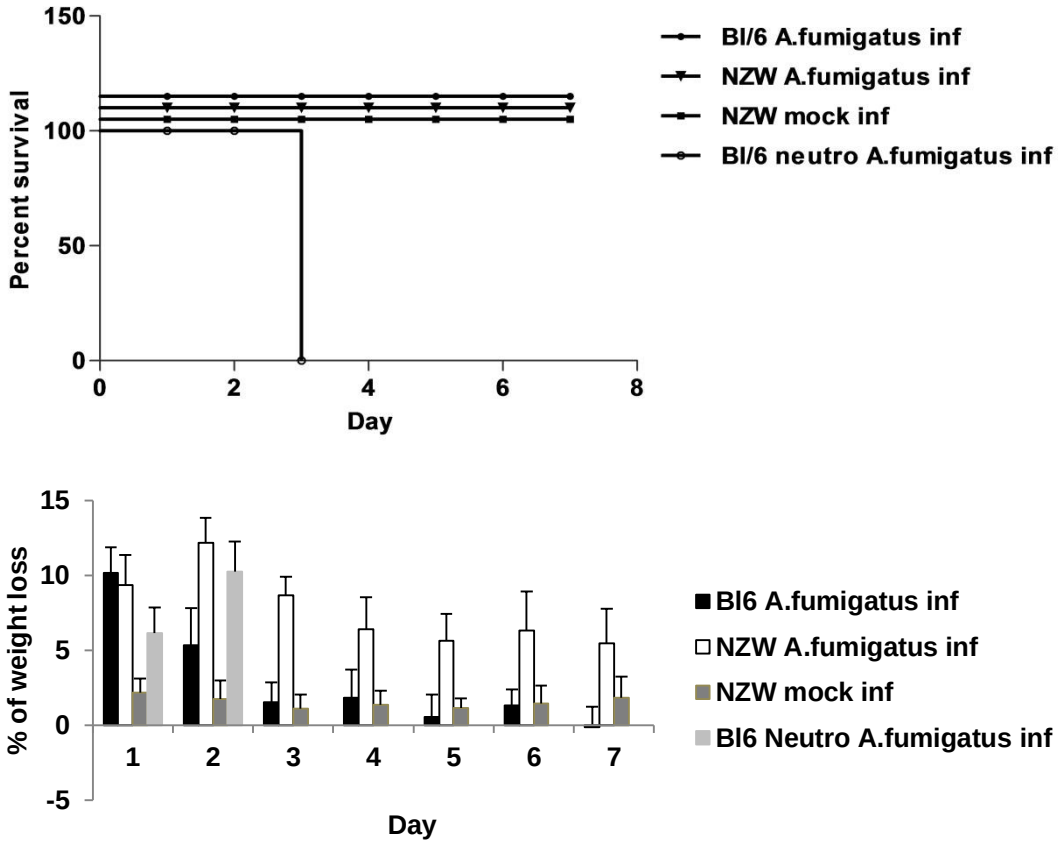

Figure 5.8 NZW mice survived *A. fumigatus* infection to 100% 5x10^6 *A. fumigatus* conidia was instilled into NZW, C57BL/6 and neutropenic C57BL/6 animals and during a course of 7 days (A) survival and (B) percentage of weight loss was measured. All animals were female and between 8-12 weeks.

Not finding any phenotype in NZW mice during *A. fumigatus* infection and to show the importance of IL4i1, the knock out mice for IL4i1 which were available at this time point (Cousin et al., 2015), were put into the different experiments. This mouse was generated in The Texas A&M Institute for Genomic Medicine (TIGM) by deletion of exons 2 to 8 by substitution with a lacZ/neo cassette. As the first step, the deletion of the IL4i1 gene was confirmed by performing Western blot on the isolated AECII from IL4i1 k.o. and C57BL/6 mice. The AECII were isolated from both *A. fumigatus* and mock infected conditions in both mouse lines. Among all the four samples only a signal was observed for *A. fumigatus* infected C57BL/6 mice (Fig 5.10A).

After confirmation of IL4i1 knock out (Fig 5.10A), they were put into a survival experiment. However, all IL4i1 k.o. animals survived the *A. fumigatus* infection. Neutropenic C57BL/6 animals died to 100% within 4 days after infection (Fig 5.10B). IL4i1 k.o. and C57B/6 animals showed similar patterns for weight loss after fungus infection. These two groups both lost about 10% of their weight during day 1 post infection and right after this day the animals started recovering slowly.

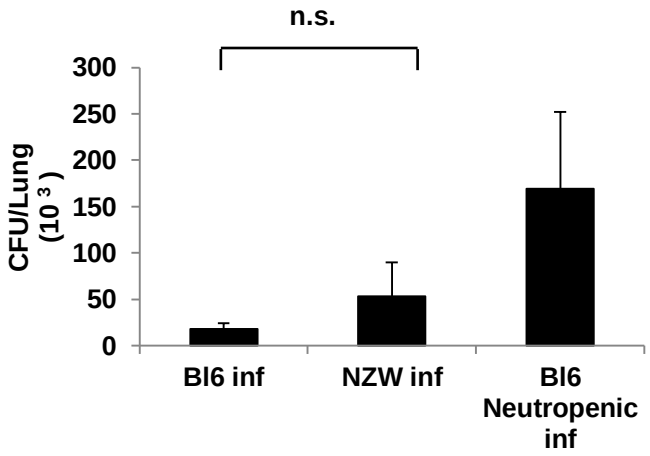

Figure 5.9 CFU number in NZW mice 24 hours post *A. fumigatus* infection mashed lung tissue from NZW, C57BL/6 and C57BL/6 neutropenic animals were cultured on AMM agar. After a 24 hours incubation time the colonies were counted. This experiment was performed with three replicates per condition. All mice were female and between 8-12 weeks.

During the second day post infection both groups gained weight up to 5% compared to the day before. After seven days all animals of both groups were completely healthy again. The IL4i1 k.o. mock infected group was considered as the negative control group and all animals of this group showed almost no weight loss. Neutropenic C57BL/6 animals were counted as positive control. This group of animals lost about 10% of their weight one day after infection and the weight loss reached 25% of the initial weight on the animals (Fig5.10C).

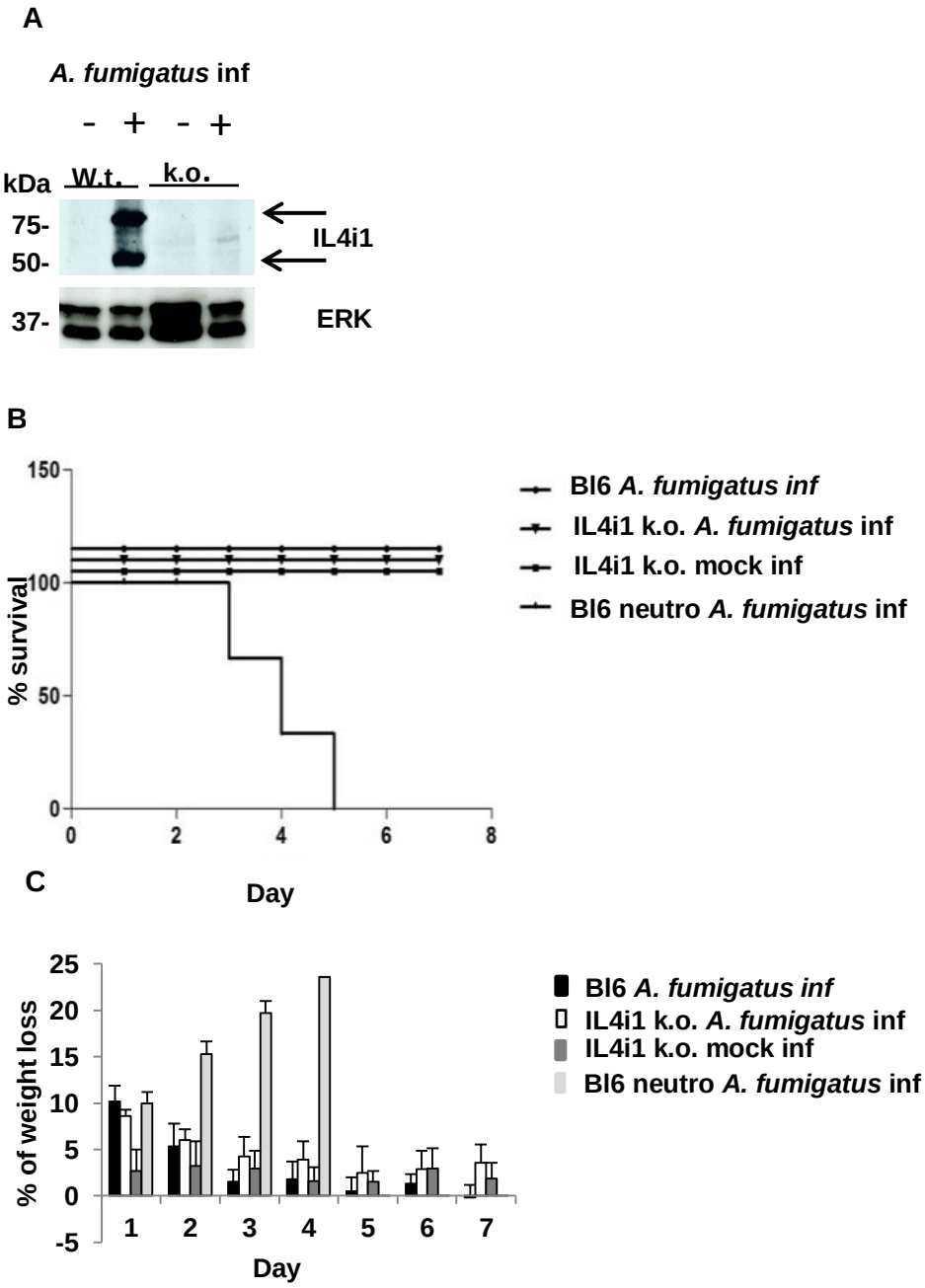

Figure 5.10 IL4i1 k.o. mice survived *A. fumigatus* infection (A) Western blot results showed signal for the expression of IL4i1 in *A. fumigatus* infected C57BL/6 mice and no band for IL4i1 k.o. (B). 100% of the C57BL/6 and IL4i1 k.o. mice survived *A. fumigatus* infection. All neutropenic C57Bl/6 mice died after *A. fumigatus* infection. (C). *A. fumigatus* infection resulted in similar weight loss behavior in C57Bl/6 and IL4i1 k.o. animals. IL4i1 k.o. mice with mock infection showed almost no weight loss. C57Bl/6 neutropenic animals showed dramatic weight loss and they all died within four days. This experiment was done with 5 animals per group. All mice were between 8-14 weeks. Male and female mice were equally distributed between the groups.

Further experiments were performed for finding a phenotype in IL4i1 k.o. mice. CFU were counted from IL4i1 k.o. and C57BL/6 mice after 24 hours cultivation of mashed lungs on AMM agar. The number of CFU per lung of IL4i1 k.o animals showed no significant difference compared to C57BL/6 animals (Fig 5.11A). Next, the absolute number of neutrophils recruited to lungs of IL4i1 k.o. mice and C57BL/6 was measured by flow cytometry. However, no significant difference was detected (Fig 5.11B).

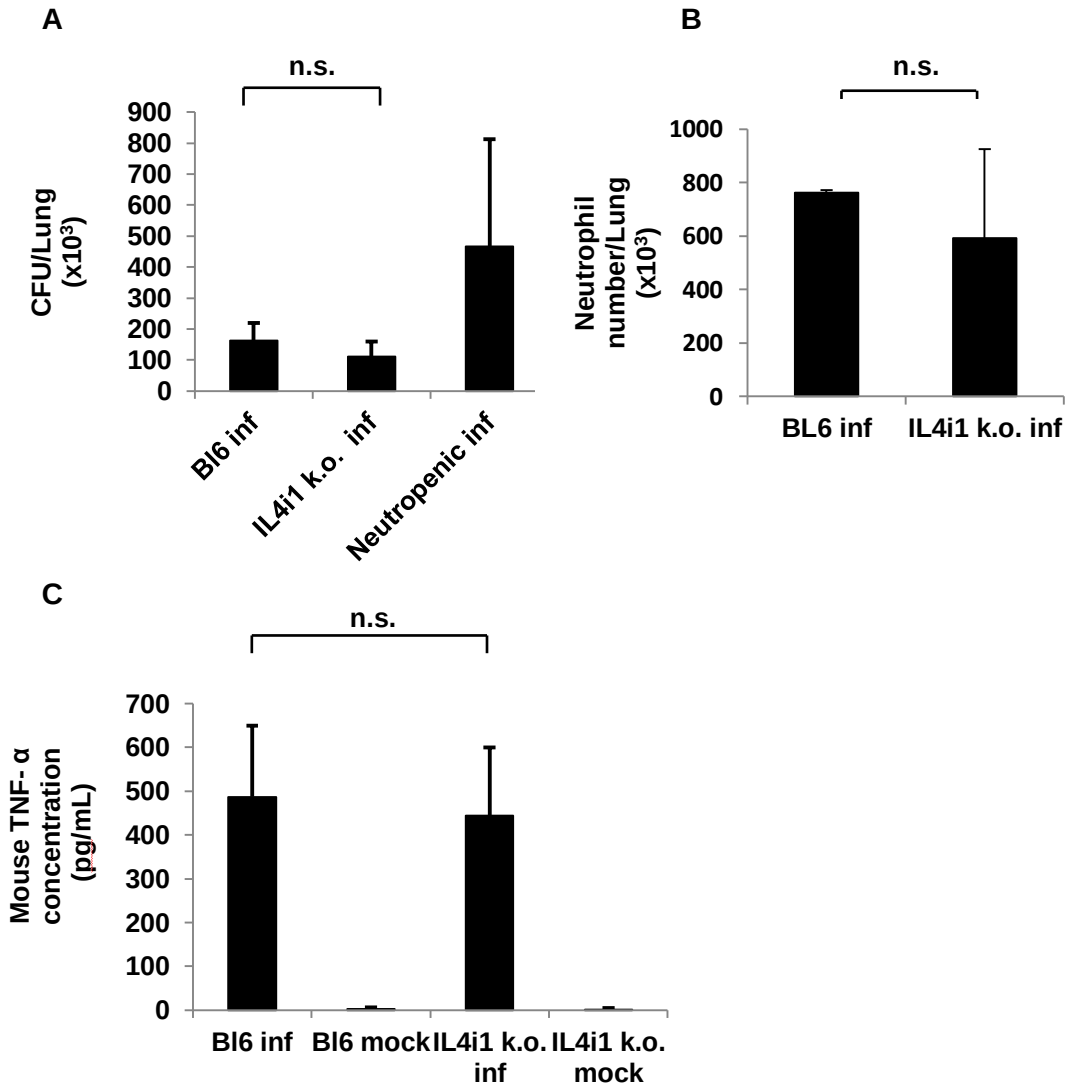

Figure 5.11 IL4i1 k.o. mice showed no phenotype upon *A. fumigatus* infection (A) IL4i1 k.o. mice showed no significant difference in CFU per lung compared to C57BL/6. This experiment was performed on three animals per group. (B) The absolute number of the recruited neutrophils in IL4i1 k.o. mice was not significantly lower than the recruited neutrophils to C57BL/6 mice's lungs. This data result from three animals per group. (C) The expression level of TNF-α indicated no significant regulation in IL4i1 k.o. mice compared to C57BL/6 mice. This data is based on seven animals per group. All three experiments were performed 24 hours post infection.

Next, expression of the pro-inflammatory cytokine TNF-α was measured. It is known that IL4i1 is an immunosuppressive enzyme (Cousin et al., 2015) and it has been reported that IL4i1 knock down enhances TNF-α expression in LPS treated M1 macrophages (Yue et al., 2015). Due to these facts up-regulation of TNF-α in IL4i1 k.o. mouse lung during *A. fumigatus* infection was hypothesized. Therefore, TNF-α expression in BAL collected from fungus infected and mock infected IL4i1 k.o and C57BL/6 animals was measured by ELISA. No significant difference was detected as seen in Fig 5.11C

1.2 Neutrophil granulocytes, the most influential phagocytes during *A. fumigatus* infection

Lack of neutrophils is associated with a high increase in susceptibility to *A. fumigatus* infection (Fig 5.8A, 5.10C). Thus, it was important to get a molecular understanding of the changes in neutrophils recruited to the infected lung. Fig 5.12 is a scanning electron microscopy image of the interior of an *A. fumigatus* infected lung, 24 hours post infection. In this image conidia covered in neutrophil extracellular traps (NET) (shown in yellow) are obvious. According to presence of NETs, occupancy of the infected lung 24 hours post infection by neutrophil granulocytes is concluded.

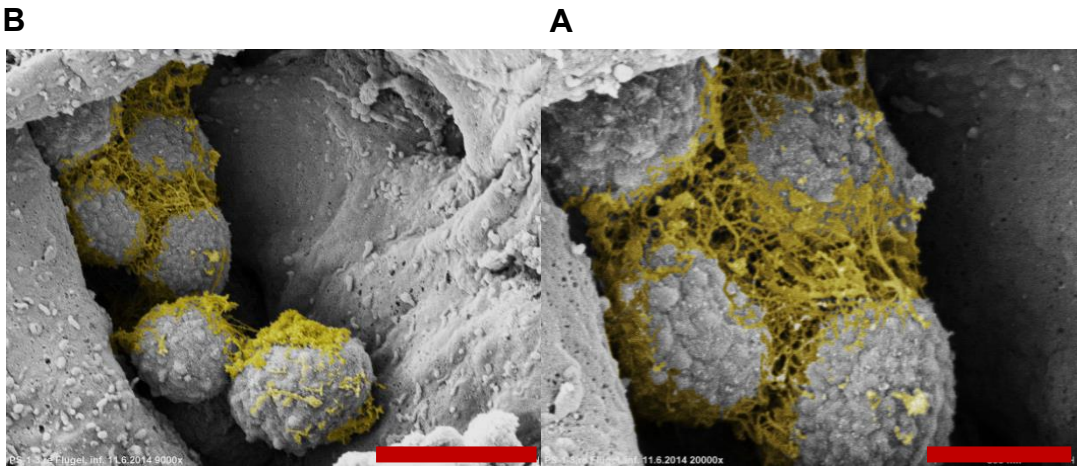

Figure 5.7 Neutrophil granulocytes existence 24 hours post *A. fumigatus* infection structures resembling NETs (in yellow) are identified covering the conidia.(A) The scale bar represents 2 µm. (B) Demonstrates a higher magnification of the same spot as A. The scale bar illustrates 1 µm.

In an infected lung various types of immune cells exist in order to clear the invaded pathogen. Fig 5.13 indicates that the recruited neutrophil granulocytes form the biggest portion of leukocytes inside the lung 24 hours post *A. fumigatus* infection. Ly6G positive cells make up to 48.03% while CD45 positive cells appeared to be 51.4%. Both percentages refer to the whole lung lysate. In other words Ly6G positive cells configure over 90% of the leukocytes inside murine lung in this time point.

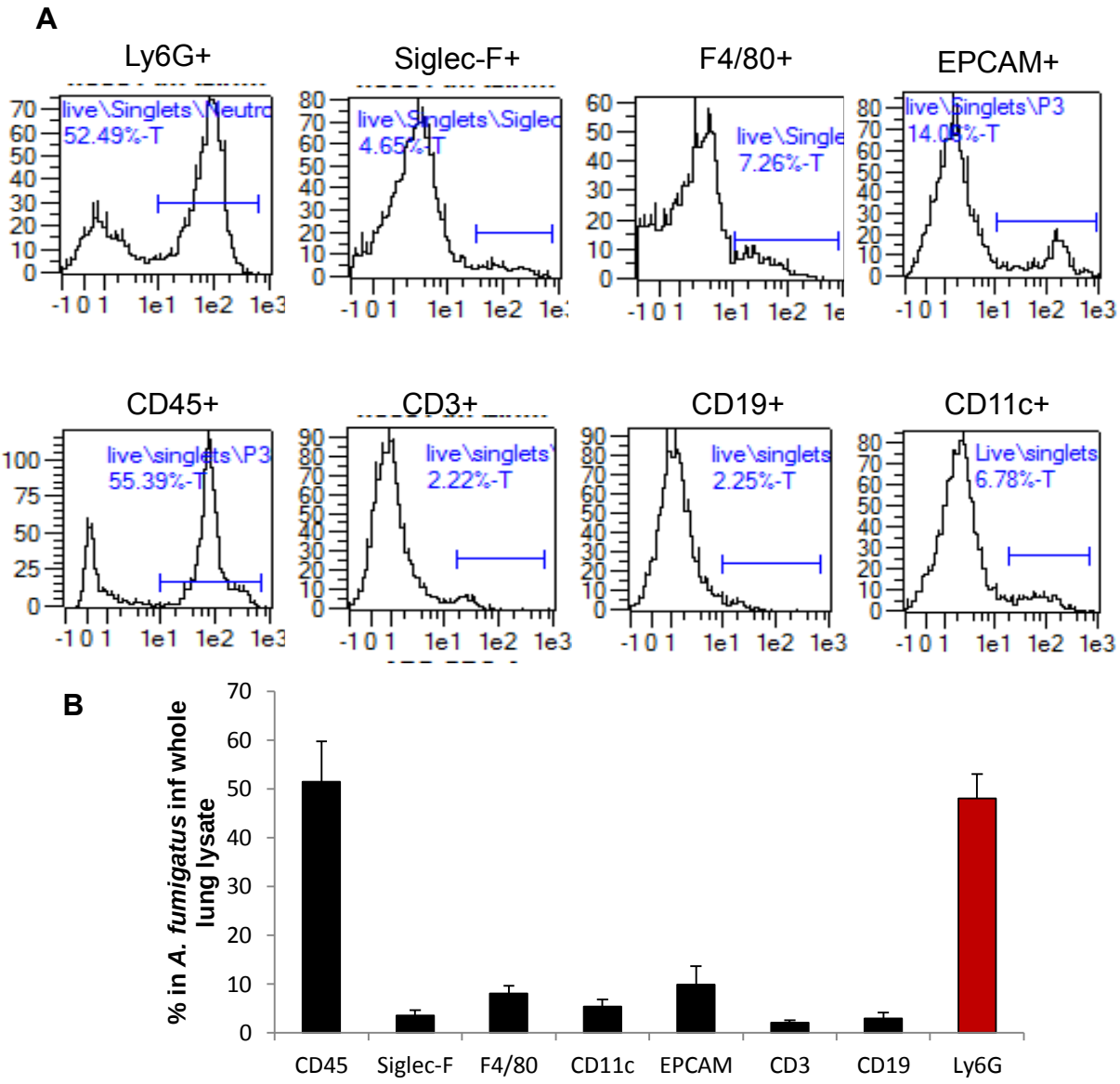

Figure 5.8 Neutrophil granulocytes are the most abundant leukocytes inside the lung 24 hours post *A. fumigatus* infection (A) Dispase digested lungs from C57BL/6 mice were analyzed by flow cytometry. (B) The bar graph is the average result of three independent experiments. All mice were between 8-12 weeks, male and female.

1.2.1 Neutrophil granulocyte isolation

Neutrophils from bone marrow (P1), blood (P2) and lungs (BAL) of *A. fumigatus* infected Catchup mice were sorted. Catchup mice express tdTomato under the Ly6G promoter, therefore having red fluorescent neutrophils (Hasenberg et al., 2015). Neutrophils from the BAL were sorted into two groups: Neutrophils with no physical contact to *A. fumigatus* conidia (P3) and neutrophils with physical contact to conidia (P4). Groups could be discriminated as the used conidia expressed GFP

(Krappmann et al., 2005). With equivalent conditions neutrophils from bone marrow (P5) and blood (P6) of the mock infected catchup mice were also sorted as negative controls. Fig 5.14A illustrates the experimental procedure by a schematic image.

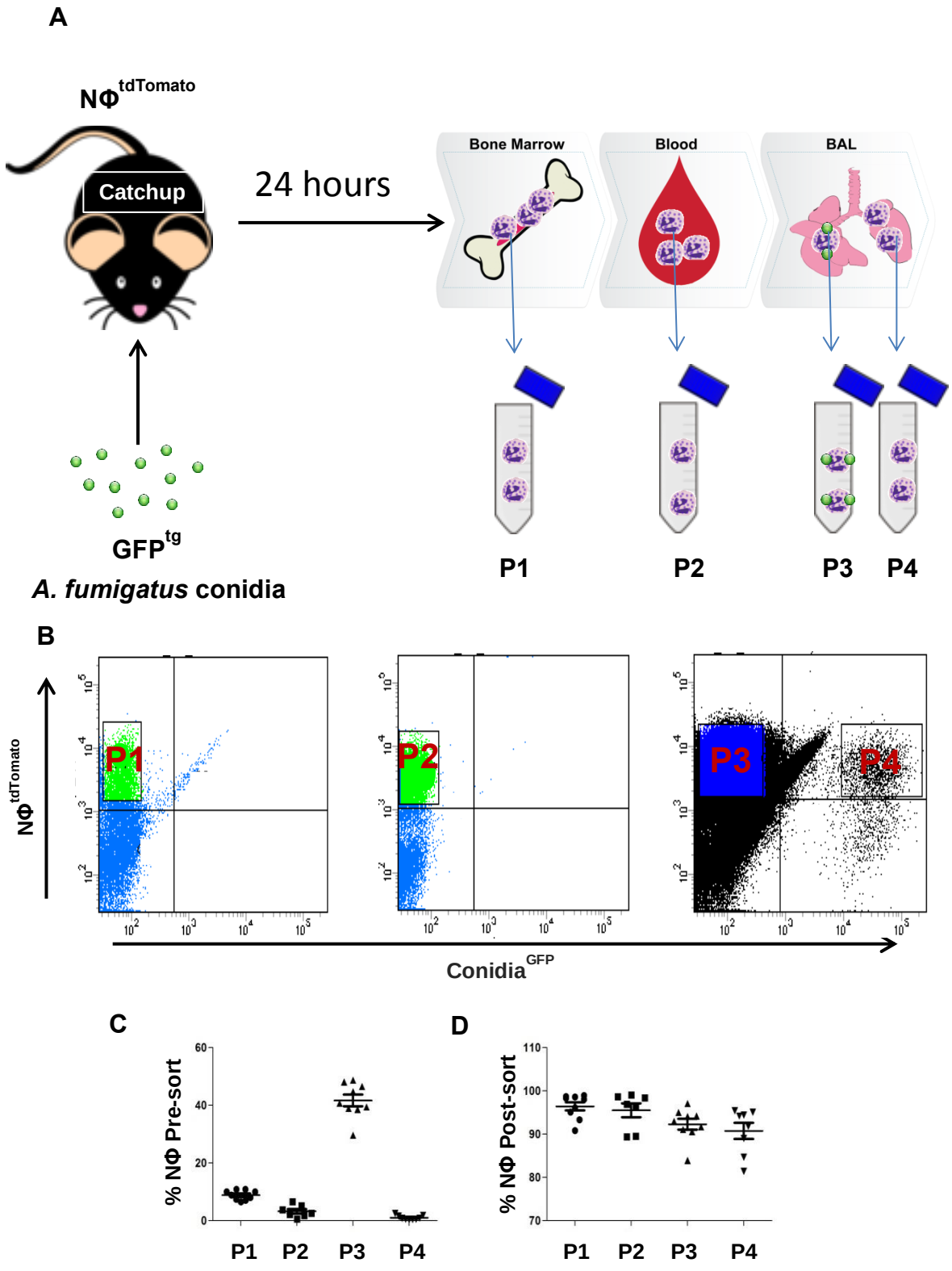

Figure 5.9 Neutrophil granulocytes FACS analysis (A) Schematic image of the experimental procedure; Catchup mice with tdTomato expressing neutrophil granulocytes were infected with GFP^{tg} *A. fumigatus* conidia. (B) P1 represents the sorted bone marrow neutrophils while P2, P3 and P4 illustrate blood, BAL and BAL in contact to conidia, respectively. (C) Neutrophils of P1 to P4 constitute 8.8%, 3.2%, 41.68% and 0.7% of their niche. (D) All populations were over 90% pure neutrophils post-sort. P1 to P4 were calculated from 9 independent replicates. All Catchup mice were between 8-12 weeks, male and female.

Fig 5.14B illustrates the sorted populations. The amount of neutrophil granulocytes in whole sorted bone marrow equals 8.8% (P1) and in whole sorted blood 3.2% (P2). BAL neutrophils from 24 hours infected lungs constitute 41.68% (P3) and the neutrophils in direct contact to conidia represent only 0.7% (P4) of the whole BAL (Fig5.14C). Results from sorted bone marrow (P5) and blood (P6) of the mock infected animals are equivalent to P1 and P2 and are not shown here. All populations were over 90% pure neutrophil granulocytes post-sort (Fig 5.14D)

1.2.1.1 Primary neutrophil granulocytes proteome analysis

The six mentioned groups of neutrophils were sorted and eventually their differential protein expressions were measured by LCMS. This measurement resulted in characterization of 3868 regulated proteins, 850 of which belong to *A. fumigatus* and 3018 to mouse. 2289 of these proteins were identified by minimum one unique peptide. Performing an ANOVA p_{FDR}-value of ≤ 0.05 and a fold change ≥ 2 was counted as significant. In order to analyze the expression profile of over 2000 proteins in six experimental groups, Principal Components Analysis (PCA) was used. PCA is a descriptive statistical method with an ability in finding directions for maximal variance in the data set. PC means principal component and is the result of the principal component analysis. From each data set more than one PC can be calculated. PCs are hierarchically ordered regarding the variance they explain in the data set (Pearson, 1901).

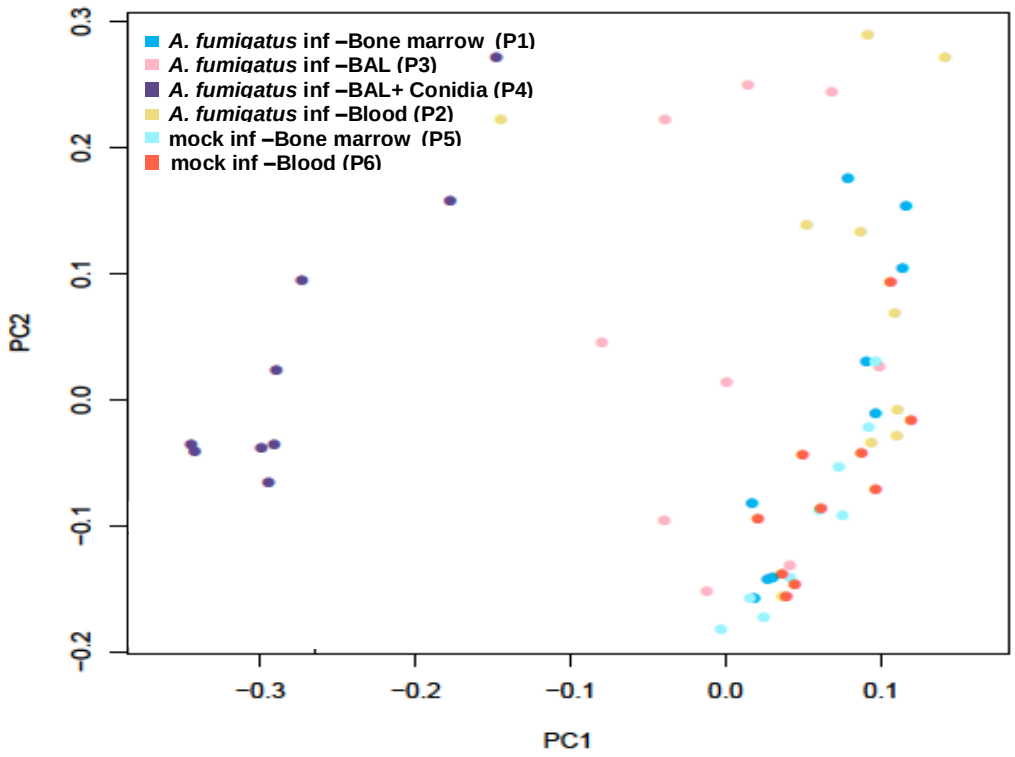

Figure 5.10 Neutrophil granulocytes of different site's protein abundancies P4 has divergent protein abundancies compared to the other groups. This PC scatter plot corresponds to the data analysis from 6 groups of neutrophils with over 2000 variables (protein abundancies). Purple dots (9 replicates) represent P4, pink dots (9 replicates) demonstrate P3, yellow dots (9 replicates) P2, light blue (9 replicates) P1, red dots (10 replicates) show protein abundancies of P5 and turquious (9 replicates) P6. Catchup mice were both male and female and between 8-12 weeks.

In this study abundancy of over 2000 proteins in 6 experimental groups has been analyzed in a PC-scatter, resulting from plotting PC1 against PC2. This PC-scatter plot shows only the mouse proteins. Interestingly enough, this plot indicated divergent protein abundancies for P4 (purple dots) compared to all the other five experimental groups.

Taking a closer look at the scatter plot, it shows that P3 has similarities to P4 in the abundancy of the expressed proteins as the pink dots have a tendency towards the purple dots. The scatter plot also shows that protein abundancy of P2 is slightly similar to P3 and P4 as some of the yellow dots has tendency towards the purple and pink dots. Neutrophils from P1, P5 and P6 showed almost the same pattern for the abundancy of their expressed proteins, which was in total contrast to P4.

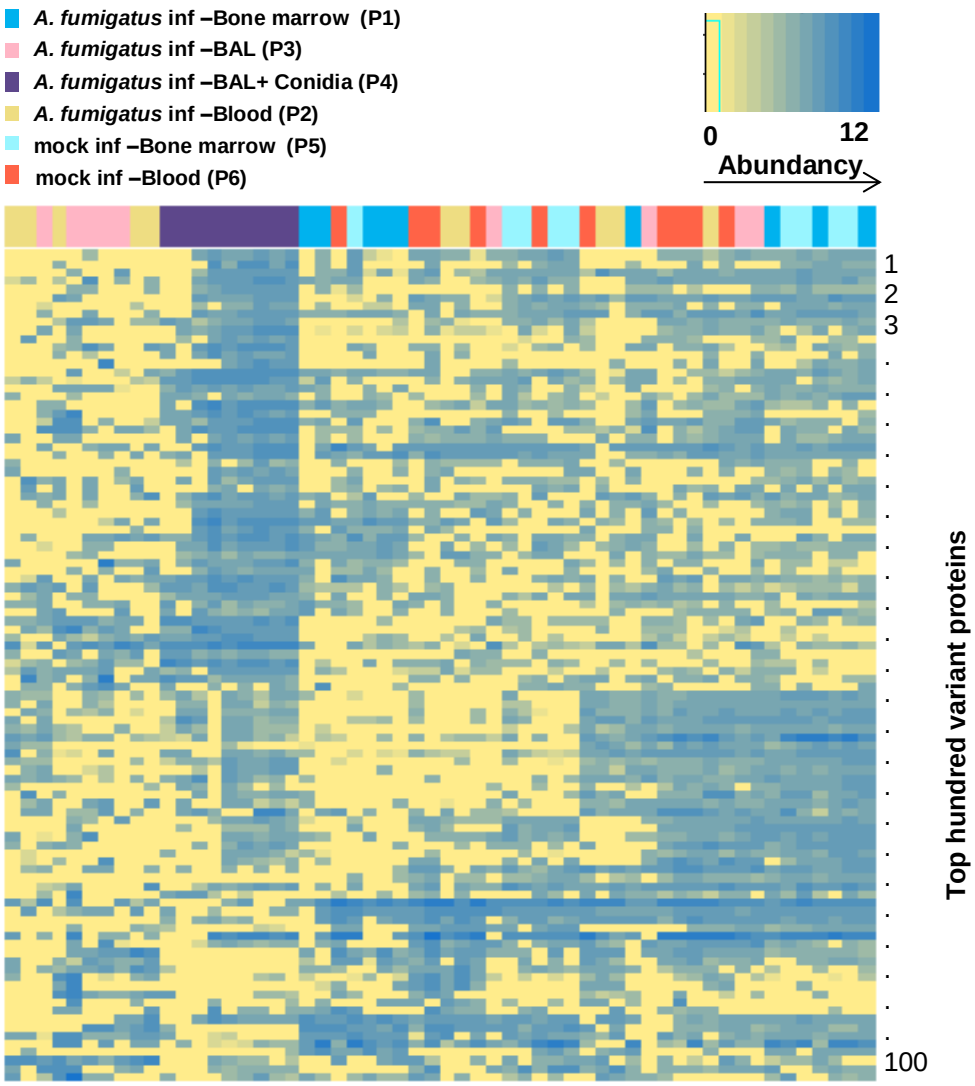

Figure 5.11 heatmap of the top 100 variant proteins The applied algorithm was unsupervised clustering. P4 structures a cluster and the visual intuition indicates that this group shows upregulation for about half of the proteins with colour code purple. Color codes light blue , torquious and red which correspond to P1, P5 and P6, demonstrate opposite regulation compared to P4. In this graph dark blue shows highest protein abundancies and light yellow shows the opposite.

To sum up the obtained data from this plot, P4 protein content has the most dramatic variance compared to all the other experimental groups, which suggests that an *A. fumigatus* infection has a considerable effect on the expression of the neutrophil's proteins (Fig 5.15).

In Fig 5.16 the top 100 most variant proteins, resulting from running the 6 mentioned groups of neutrophils on LCMS, were plotted on a heat map. Observing the heat map shows that, although it was plotted with unsupervised clustering algorithm (the algorithm does not know the experimental groups), P4 has formed a cluster. According to the visual impression of the heat map, about half of the proteins show upregulation in P4 while the other half indicates upregulation mainly in P1, P5 and P6. This data is compatible with the extracted information from Fig 5.15. For

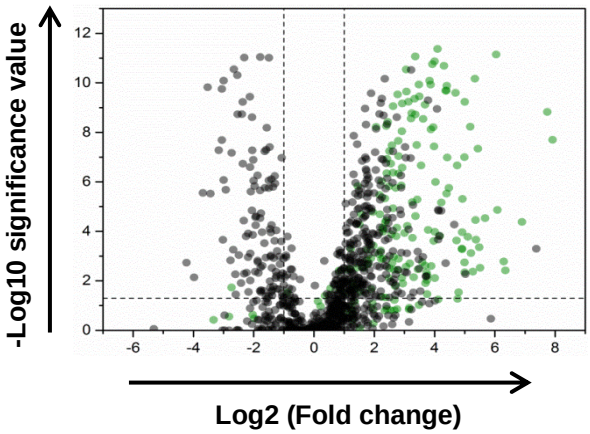

Figure 5.12 Volcano plot demonstrates P3 against P4 with highlights for the murine and the fungal proteins The X-axis refers to fold change and the Y-axis corresponds to significance. On this plot positive values demonstrate upregulation and negative values represent down regulation. *A. fumigatus* proteins are highlighted in green and murine proteins are in grey

Since the number of the differentially expressed proteins between P3 and P4 was found to be the highest among all the other experimental groups, expressed proteins in P3 were plotted against all the expressed proteins of P4 (murine and fungal proteins) on a volcano plot. Volcano plot is a type of scatter plat that demonstares the changes in large data sets at a glance (Li et al., 2014). In Fig 5.17 *A. fumigatus* proteins are high lighted in green and murine proteins are in grey. In this plot positive values represent upregulation and negative values represent down

regulation of the proteins compared to control. According to this fact, most fungal proteins show upregulation while murine proteins have been regulated to higher abundancies or lower compared to control but again the upregulated proteins are visually much more in number.

6 Discussion

6.1 Phagocytic network

A. fumigatus infections are a common global issue for immunosuppressed patients that can lead to invasive aspergillosis and death. Immunocompetent individuals on the other hand, encounter this infection very efficiently (M. K. Mansour et al., 2012). During an *A. fumigatus* infection different phagocytes play a decisive role in clearing up the fungus. From an immunological perspective, these cells can be divided into two groups: professional and non-professional phagocytes. Classical innate immune cells such as monocytes/macrophages, neutrophil granulocytes and dendritic cells are placed in the first group of phagocytes whereas pulmonary epithelial cells are regarded to belong to the second group (Rabinovitch, 1995).

The phagocyte mediated immune response towards inhaled conidia of *A. fumigatus* is predominantly described as interaction of conidia with alveolar macrophages (Schaffner et al., 1982). This contact subsequently leads to the cytokine mediated recruitment of neutrophil granulocytes (Bonnett et al., 2006) and the collaborative action of these innate immune cells is regarded to reliably eliminate the pulmonary occurrence of the pathogenic mold. However, inside the alveoli AECI and II as phagocytic cell types, probably get into contact with inhaled spores much faster than alveolar macrophages (Croft et al., 2016).

Assuming the interactions between these phagocytes and *A. fumigatus*, we suggest the general name of phagocytic network for them. This thesis has focused on the isolation of the primary phagocytes from murine lung in the setting of pulmonary invasive aspergillosis and further molecular characterization of these cells on the protein level. The aim was to isolate cell types with the least possible direct touch on them to prevent any kind of cellular process activation. To reach this goal, negative isolation protocols for the different phagocytes had to be set up.

6.1.1 AECI

Although several hundred published papers exist investigating the contact of professional phagocytes with inhaled *A. fumigatus* conidia, only about 40 publications characterize the interaction of epithelial cells and conidia (Osherov, 2012).This is despite the fact that, AECI number-wise and also due to their enormously large surface have a much higher likelihood to encounter conidia rather than any other phagocyte. Because of these reasons we have first focused on primary AECI isolation and consequently investigation of their role during infection.

In order to be able to study AECI we first had to set up a protocol for negative isolation of this cell type. As the main task of AECI is gas exchange at the blood-air barrier, they need to be extremely thin and extensively stretched along the alveolus for being functionally efficient (Ward et al., 1984). On the other hand, AECI have a tight bound to the basal membrane of alveoli in collagen, laminin and fibronectin fibers and to adjacent AECI and also AECII by tight junction proteins like claudins (Lwebuga-Mukasa, 1991) (Overgaard et al., 2012). Therefore, to isolate this cell type, they had to be dissociated from the basement membrane, from each other and also from AECII. Chen et al. (2004) have successfully isolated AECI from rat lungs by using the enzyme elastase for lung tissue digestion. This protocol did not function effectively for murine lung. Although a T1α/EpCAM double positive population appeared in flow cytometric analysis, the number of the dead cells was excessive and the positive population was too small compared to the whole lung lysate. Next, lung digestion by different enzyme mixtures and under different conditions such as the incubation temperature and time point was performed but, as AECI are very fragile a rigorous enzyme treatment harmed the cell. Next, lower concentration of the enzymes was applied which was ineffective for the lung digestion. This vicious circle made it difficult to isolate AECI. During lower respiratory tract complications, like *A. fumigatus* infection, where lung tissue is damaged due to pathogen/host interaction, AECI isolation is even less probable. Due to the mentioned reasons AECI isolation and investigation remained as an unsolved problem in this project.

6.1.2 AECII

The next cell type of the phagocytic network to be investigated was AECII. AECII secrete surfactant protein not only to prevent lung lobes from collapsing. It is known that these proteins also possess antimicrobial effects. Therefore AECII contribute to the innate immune responses towards an invading pathogen (Wright, 2005). It has also been reported that isolated primary rat AECII are able to synthesize and release complement proteins like C5 which can lead to pulmonary inflammation and eventually immune cell recruitment and innate immune response to pathogens (Strunk et al., 1988). Besides, it has been observed that isolated rat primary AECII, , could internalize conidia 24 hours after culture (Paris et al., 1997). Simultaneously, another study demonstrated conidial uptake by the A549 cell line (DeHart et al., 1997). It has also been suggested that conidia can escape from the immune responses in A549 cells. Conidia are taken up by these cells and live for another 6 hours inside them (Wasylnka et al., 2002). A year later, the same group announced the localization of conidia in phagosomes and further investigation indicated that the internalized conidia in A549 cells can survive the acidic condition and are able to germinate and breakout of the phagosomes (Wasylnka et al., 2003). It has also been proven that primary AECII isolated from mice lung could internalize mycobacteria and subsequently present antigens to T-cells. Checking cytokine and chemokine secretion upon stimulation of AECII revealed that these cells can trigger different pathways (Chuquimia et al., 2012). Taking into account all above published data, it is a fair rationale to set AECII into the innate immune system and not just considering them as a physical barrier in the lung.

More than 10 studies indicate the interaction between AECII and conidia but almost all of them refer to *in vitro* studies using A549 cell line (Osherov, 2012). In this study we concentrated on establishing a negative isolation protocol for AECII with the least distress and best purity for cells. Contradictory to AECI, several publications report successful AECII isolation. In order to isolate AECII, murine lung was digested based on the Corti et al. (1996) protocol. The main challenge for setting up a negative isolation protocol was designing a biotinylated antibody mixture that would label all the unwanted cells, while leaving AECII untouched. To achieve this goal, the suggested antibody mixture by Gereke et al. (2012) for isolation of AECII with flow cytometric approach was considered as the basis. This mixture includes

α-CD11b, α-CD1c1, α-F4/80, α-CD45, and α-CD19 antibodies which all bind to immune cell types. According to this protocol all the unwanted cell types undergo antibody labeling and AECII are enriched by FACS analysis as the non-labeled, scatter high (SSC^{high}) cell population. Although the suggested AECII isolation by this protocol follows negative isolation, still the process of FACS analysis can be too rigorous for the cells. Therefore the need for an AECII negative isolation protocol with a less severe experimental process was still unmet. However "The new protocol" suggests AECII isolation with an immune magnetic separation approach. This protocol provides a much smoother experimental process but it does not allow side scatter based isolation. Therefore, next to immune cell types also endothelial cells, epithelial cells and many different types of resident cells in bronchi, intralobular bronchioles and the bronchoalveolar duct junction (BADJ) like Clara cells, Basal cells, ciliated cells, neuroendocrine cells, Goblet cells, and epithelial progenitor cells (Rock et al., 2011) had to be excluded. For labeling all these different cell types with biotinylated antibodies for negative isolation process, antibodies which could bind to specific antigens on the surfaces of these cells didn't exist. To overcome this complication, bronchi were cut out by very fine surgery scissors after the lung digestion step by the enzyme dispase and before lung dissociation with forceps; with this simple approach many of the contaminating cell types efficiently got excluded. Additionally, some cells which are big in size like Goblet and ciliated cells (~50 µm) were eliminated during cell straining process. Subsequently, biotinylated α-CD31, α-T1α and α-Sca-1were added to the existing antibody mixture to exclude contaminating endothelial cells, AECI and bronchoalveolar stem cells (BASCs) respectively. BASCs reside in bronchoalveolar duct junction (BADJ) (Kim et al., 2005) and have stem cell like properties and can differentiate to Clara cells, AECI and also AECII independently (Dovey et al., 2008). Adding these strategies to the existing protocols for AECII isolation, a negative isolation protocol with over 90 % pure AECII was generated.

The final target of this thesis was the investigation of murine lung phagocytes during *A. fumigatus* infection at the protein level. To obtain that, the best time point post infection had to be pin pointed. Knowing the advantages of 2D-DIGE as a powerful tool for proteomics, it was used for this means. Isolated AECII 30 minutes, 8 hours, 24 hours and 48 hours post *A. fumigatus* infection were analyzed by 2D-DIGE. 24

hours post infection was confirmed to show the most protein regulations; therefore this time point was used throughout the whole study.

Although 2D-DIGE with the ability to visualize substantial number of proteins with differential presentation is a widely used method, some disadvantages are also involved in using this technique (Verrills, 2006). 2D-DIGE is not only very time consuming but also running one round of this technique needs excessive amount of material. However isolation of the primary cells usually, does not lead to a big purified population (Haynes et al., 2000). Taking the mentioned disadvantages into account, after the analysis of AECII by 2D-DIGE for finding the time point post infection with the most differentially regulated proteins, the rest of the study was pursued by liquid chromatography mass spectrometry (LCMS) technique focusing on sensitivity, specificity and throughput (Grebe et al., 2011).

Running the prepared trypsin digested peptides from isolated AECII, 24 hours post *A. fumigatus* versus mock infection on LCMS, 2703 proteins were detected. Among these proteins, 2256 of them were recognized by at least 1unique peptide. Next means of filtering was an ANOVA statistical test. 121 proteins were detected to have a p value of ≤ 0.05 and a fold change of ≥ 2. Among these proteins, 100 of them showed upregulation compared to the control during *A. fumigatus* infection and the top candidate found was interleukin 4- induced gene 1(IL4i1) with an ANOVA p-value of 2.91^{-10} and a fold change of 42.94.

As a next step, IL4i1 upregulation 24 hours post *A. fumigatus* infection was confirmed by further molecular experiments. qPCR showed a 199.1 fold upregulation of IL4i1 expression compared to the control. The Western blot with a specific IL4i1 antibody demonstrated a clear signal for IL4i1 in the infected sample while no signal was seen for the mock infected sample. Immunohistology of the infected lung slices revealed a specific staining for IL4i1 on the cells that according to morphology and size are AECII. Confocal microscopy indicated that IL4i1 is localized in vesicles inside AECII. According to the literature theses vesicles are lysosomes (Mason et al., 2004). With these affirmations we continued the study focusing on IL4i1.IL4i1 belongs to the family of L-amino acid oxidases (Mason et al., 2004). The general function of this family of enzymes is known to be catalysis of L-amino acid oxidative deamination. The amino acid which IL4i1 catalyzes most is reported to be Phenylalanine (Boulland et al., 2007). IL4i1 initially was reported to be secreted from B-cells through STAT6 activation (Schroder et al., 2002). In

addition to B-cells IL4i1 was proven to be secreted from antigen presenting cells like dendritic cells and macrophages (Chu et al., 2004; Sahara et al., 2003). Furthermore, it was reported that IL4i1 expression is restricted to immune tissues (Chu et al., 1997). Along with the deamination of L-amino acids by IL4i1 or any other member of the L-amino acid oxidase family, H_2O_2 and ammonia together with keto-acids are produced. With this knowledge, it has been proven that IL4i1 both *in vivo* and *in vitro* obstructs bacterial growth. It is shown that this effect is due to accumulation of H_2O_2 and environmental basification which is related to collection of ammonia (Puiffe et al., 2013). Another proven role for IL4i1 due to its enzymatic activity and H_2O_2 production is the inhibition of $CD3^+$ T-cell proliferation (Boulland et al., 2007) In contrast to the inhibitory effect of IL4i1 on $CD3^+$ T-cells, it stimulates the growth of $FoxP3^+$ regulatory T lymphocytes (Cousin et al., 2015).

According to the mentioned findings in the paragraph above it is clear that IL4i1 is an immunoregulatory enzyme and has a high conceptual relevance for further investigation. The important point is that we are reporting the expression of IL4i1in AECII for the first time.

Because the knock out mouse for IL4i1 was not available at this time, we used the New Zealand White (NZW) mice to study the relevance of IL4i1 *in vivo*. This mouse line was suggested to have a defect in expression of IL4i1 According to previous findings IL4i1 alleles in NZW mouse has three amino acid substitutions (Chavan et al., 2002) which can lead to deficiency of the protein. The lack of IL4i1 in NZW mice has not been investigated so far but the probability of the shortage for this enzyme in NZW mice is being suggested (Mason et al., 2004). With this ground we first checked for mRNA level of IL4i1 expression in NZW mice. Compared to C57BL/6 mice we didn't see a significant difference but this was no direct proof that the enzyme is defect in protein level so we set NZW mice in survival and CFU experiments with *A. fumigatus* infection. The results from this experiment showed that all animals survived. Monitoring the weight loss of the animals 7 days post infection demonstrated 4.3 % more weight loss for NZW compared to C57BL/6 mice and a lower rate for recovery but not significantly. The mean number of colonies growing from NZW mice's lungs was 53.4 which was elevated compared to a CFU count of 18.1 in C57BL/6 mice but this difference was not significant either.

Next, we moved on with performing survival and CFU experiments on IL4i1 knock out mice which by this time were available. After the verification of IL4i1 deletion in

the .knockout mice they were put into survival experiments post *A. fumigatus* infection. Although mice went through a weakness period they recovered soon and survived the infection eventually. Animal weight loss and recovery observation showed the same pattern for IL4i1 k.o. and C57BL/6 mice. Furthermore, number of colony forming units, neutrophil recruitment to the lung and TNF-α expression in BAL fluid in IL4i1 k.o. mice did not reveal significant contrast to C57BL/6 animals. Although, in all three experiments a tendency for reduced capability of IL4i1 k.o. mice for encountering the infection compared to C57BL/6 mice was identified, these tendencies were minimal. These results suggest that having a greater statistical power might lead to a significant phenotype in the k.o. animals compared to C57BL/6 mice.

As mentioned above, IL4i1 as an L-amino acid oxidase catalyzes the oxidative deamination of L amino acids and produces H_2O_2, ammonia and the corresponding α-keto acid (Zeller et al., 1944). The collection of excessive amounts of H_2O_2 by the activity of this enzyme has a bactericidal effect. With this knowledge it was expected to find higher fungal burden or slower recovery from *A. fumigatus* infection in IL4i1 k.o. mice. However no significant phenotype was revealed. This can be due to the fact that D-amino acid oxidases also produce the same products during their catalytic reactions as L-amino acid oxidases do.(Zhang et al., 2004) Therefore bactericidal activity of the D-amino acid oxidases could offset the lack of IL4i1 in the k.o. mice during *A. fumigatus* infection.

After IL4i1, the next interesting protein candidate for more profound investigation could be Lipocalin 2 (Lcn 2) with a p-value of $1.08x10^{-10}$ and a max fold change of 8.05. This protein was the second highest upregulated protein in the isolated primary AECII during fungal infection. Moreover it has been reported that Lcn 2 inhibits mycobacterial growth in AECII (Saiga et al., 2008). Therefore, it is a good potential candidate for further investigation during *A. fumigatus* infection.

ICAM-1 with a p-value of $2.06x10^{-7}$ and a max fold change of 3.94 could be the next potential protein candidate for deeper investigation. ICAM-1 is known for the process of leukocyte / endothelial transmigration (Sans et al., 2001). Therefore, the leukocytes / alveolar epithelial transmigration during fungal infection could be studied.

In order to fully investigate the importance of each of the detected differential proteins from this study, an *in vivo* approach should be followed which is too time consuming and too expensive. Therefore an innovative high throughput method for investigation of all these proteins can be generated in the future.

6.1.3 Neutrophil granulocytes

In this thesis the next phagocyte to isolate and investigate during *A. fumigatus* infection was neutrophil granulocytes. During an *A. fumigatus* infection in the lung the invading conidia that have not been removed by alveolar macrophages germinate and produce hyphae. During this time neutrophil granulocytes are recruited to the infected lung and phagocytose the produced hyphae. It is reported that during this infection neutropenia is the main reason for developing IA (Schaffner et al., 1982). With our experience, scanning electron microscopy images of an interior of a mouse lung 24 hours after infection revealed NET formation around the conidia which is a direct sign for the presence of neutrophils. At the same time point flow cytometric analysis of a whole lung showed that among all the other cell types neutrophil granulocytes are the most numerous. Actually, more than 90 % of the existing leukocytes inside an infected lung 24 hours post infection are neutrophil granulocytes. With the rationale above, here we emphasize on this cell type. In order to isolate neutrophil granulocytes, the novel transgenic Catchup mice with tdTomato expressing neutrophils were used (Hasenberg et al., 2015). Neutrophils from bone marrow blood and lungs of the Catchup mice were sorted and eventually regulation of the proteins were investigated by LCMS. With this experimental design an excessive amount of unknown facts concerning neutrophil's journey from their bone marrow niche to circulating blood and finally site of infection was revealed. To be more specific, two populations of neutrophils from lung were sorted: Neutrophils without contact to conidia (P3) and neutrophils in physical contact to conidia (P4). To the best of our knowledge there is currently no comparable set of differentially sorted phagocytes reported, with which a complex proteome analysis has been obtained. According to P4, the effect of the occurring interaction between neutrophils and conidia on the protein level was investigated. In order to get enough cells for LCMS analysis this population was pooled from 3 to 5 mice as the number of the neutrophils in direct contact to conidia was rare. To be able to run one round

of LCMS on neutrophils, it was found out that 100000 is the minimum acceptable cell number.

3868 proteins were detected, 850 of which belong to *A. fumigatus* and 3018 of them were mouse proteins. The *A. fumigatus* proteins were only found in P4 which confirms the efficiency of the sorting protocol. 2289 proteins with minimum one unique peptide were identified. After performing the statistical tests an ANOVA p_{FDR}-value of ≤ 0.05 and a fold change ≥ 2 was counted as significant.

Finally, the abundancy of these 2289 proteins in the different experimental groups was analyzed. This analysis was done by a principal component plot (Fig 5.15). Interestingly, the abundancy of the proteins in P4 indicated the most variations compared to all the other groups. This unique pattern demonstrates highly up and down regulations which can be due to recruitment to the lung and phagocytosis. The abundancy of the proteins in P3 showed a tendency towards P4 which might result from the recruitment of the neutrophils to the lung. The abundancy of the proteins of P2 also has a slight shift towards P3 and P4 which can be due to the preparation of the neutrophils for recruitment.

P1, P5 and P6 showed similar protein abundancies among each other but differed from the other three groups. The explained patterns can also be seen in the heat map (Fig 5.16). Although this heat map was set to be unsupervised (the algorithm cannot distinguish the experimental groups) the proteins from P4 generated a cluster. This again indicates the differential protein abundancies in P4 compared to the other groups.

To make the analysis of the experimental groups more substantial, numbers of the regulated proteins among the different groups are mentioned in Fig 6.1. Between P1 and P2 19 upregulated and 21 down regulated proteins were detected. From P2 to P3 23 upregulated and 17 down regulated proteins were noticed. From P3 to P4 414 upregulated and 116 down regulated proteins are recognized. This immense difference between the numbers of the regulated proteins from P3 to P4 compared to the other groups indicates the importance of the direct contact of the neutrophils to conidia inside the lung. Among the top ten of these proteins, molecules related to actin polymerization were detected as a direct consequence of phagocytosis. In contrast, the number of the detected regulated proteins between P1 and P5 is so low that it can be concluded that an *A. fumigatus* infection in the lung has almost no

effect on the expression of the proteins in bone marrow neutrophils. Differential proteins between P5 and P6 also were so few that it can be concluded that under physiological conditions the expression of the proteins does not change dramatically among the neutrophil's journey from bone marrow to blood circulation.

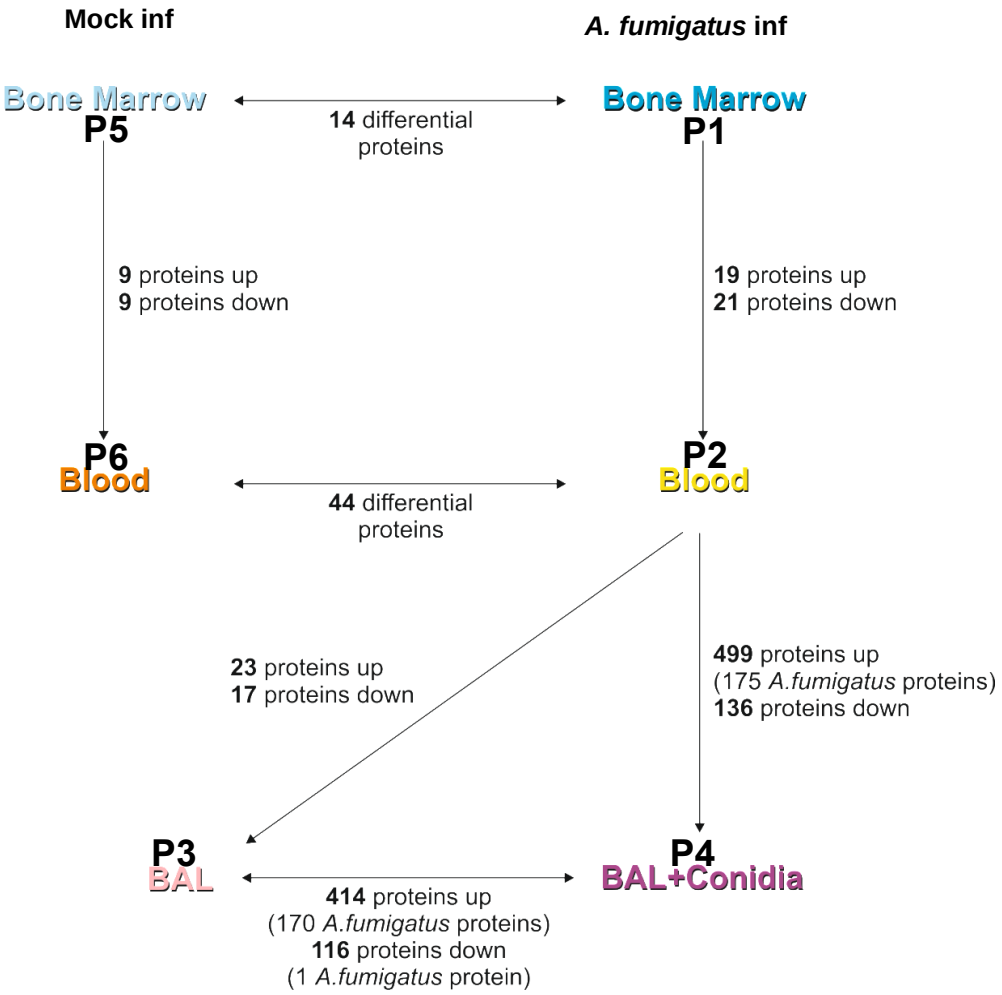

Figure 6.2 Number of the regulated proteins among different neutrophil groups From P1 to P2 and from P2 to P3 an increasing number of the regulated proteins can be seen. The number of regulated proteins between P3 and P4 was excessively high. Few proteins showed regulation between P1 and P5 and also between P5 and P6.

Having a long list of proteins, as a next step, they have to be investigated in detail and their functions need to be studied in knock out mice during *A. fumigatus* infection. This approach will help us to understand the mechanisms which make neutrophil granulocytes such important factors during infection. Investigation of the protein regulations in neutrophils of the different sites during *A. fumigatus* infection indeed opens up a whole new platform for further studies which can help us improve

our understanding about the importance of these cells during IA and could be an initiation for finding new medications for neutropenic patients who are in risk of IA.

7 Conclusion and outlook

In this thesis two cell types of the phagocytic network during *A. fumigatus* infection have been isolated and characterized in protein level.

The first cell type to be investigated in this study was the AECII which is a so called non-professional member of the phagocytic network in murine lung during *A. fumigatus* infection. We have successfully purified AECII with over 90 % purity applying immune magnetic based negative isolation technique. This population was analyzed by LCMS and 2256 proteins were characterized. With this data it can be concluded that AECII is not just a physical barrier for invading pathogens. As an innate immune cell, AECII actively secretes different molecules for encountering conidia. Amongst all the detected proteins in this study IL4i1 was further investigated as the top candidate. The k.o. animals for this protein showed no significant phenotype during *A. fumigatus* infection. Investigation of the other detected proteins upon infection such as ICAM-1 or Lcn 2 in detail is left to be done.

The second isolated and investigated cell type in this thesis was the neutrophil granulocytes. These cells got sorted from different sites of Catchup mice 24 hours post *A. fumigatus* infection. The proteome of the sorted cells was analyzed by LCMS. Over 3000 proteins were detected which generates a platform for further studies. The importance of the most interesting proteins could be investigated in the k.o. animals. As this approach is too expensive and time consuming generation of gene deletions in cell lines by CRISPR/Cas could be substituted. In case of observing compelling behaviors in the gene deleted cell types, .knockout mice could be further examined upon *A. fumigatus* infection.

Last but not least, establishment of AECI isolation which was started in this thesis ended up very challenging due to the fact that this cell type is tightly bound to basal membrane and adjacent AECI and II. In order to overcome this problem a bachelor project is running with the aim of finding the most efficient enzyme mixture for AECI isolation without harming the cells.

8 References

Aderem, A. (2003). Phagocytosis and the inflammatory response. *Journal of Infectious Diseases, 187 Suppl 2*, S340-345. doi:10.1086/374747

Alberts, B. (2002). *Molecular biology of the cell* (4. ed. ed.). New York, NY: Garland Science.

Andriole, V. T. (1993). Infections with Aspergillus species. *Clin Infect Dis, 17 Suppl 2*, S481-486. Retrieved from http://www.ncbi.nlm.nih.gov/pubmed/8274614

Ariizumi, K., Shen, G. L., Shikano, S., Xu, S., Ritter, R., Kumamoto, T., . . . Takashima, A. (2000). Identification of a novel, dendritic cell-associated molecule, dectin-1, by subtractive cDNA cloning. *Journal of Biological Chemistry, 275*(26), 20157-20167. doi:DOI 10.1074/jbc.M909512199

Beavis, R. C., & Chait, B. T. (1989). Matrix-assisted laser-desorption mass spectrometry using 355 nm radiation. *Rapid Commun Mass Spectrom, 3*(12), 436-439. doi:10.1002/rcm.1290031208

Ben-Ami, R., Lasala, P. R., Lewis, R. E., & Kontoyiannis, D. P. (2010). Lack of galactomannan reactivity in dematiaceous molds recovered from cancer patients with phaeohyphomycosis. *Diagn Microbiol Infect Dis, 66*(2), 200-203. doi:10.1016/j.diagmicrobio.2009.09.015

Betts, J. G., Desaix, P., Johnson, E. W., Johnson, J. E., Korol, O., Kruse, D., . . . Wise, J. (2013). *Anatomy and Physiology*: OpenStax College.

Bonnett, C. R., Cornish, E. J., Harmsen, A. G., & Burritt, J. B. (2006). Early neutrophil recruitment and aggregation in the murine lung inhibit germination of Aspergillus fumigatus conidia. *Infection and Immunity, 74*(12), 6528-6539. doi:10.1128/Iai.00909-06

Boon, A. P., Obrien, D., & Adams, D. H. (1991). 10 Year Review of Invasive Aspergillosis Detected at Necropsy. *Journal of Clinical Pathology, 44*(6), 452-454. doi:DOI 10.1136/jcp.44.6.452

Borregaard, N., & Cowland, J. B. (1997). Granules of the human neutrophilic polymorphonuclear leukocyte. *Blood, 89*(10), 3503-3521. Retrieved from http://www.ncbi.nlm.nih.gov/pubmed/9160655

Boulland, M. L., Marquet, J., Molinier-Frenkel, V., Moller, P., Guiter, C., Lasoudris, F., . . . Castellano, F. (2007). Human IL4I1 is a secreted L-phenylalanine oxidase expressed by mature dendritic cells that inhibits T-lymphocyte proliferation. *Blood, 110*(1), 220-227. doi:10.1182/blood-2006-07-036210

Braem, S. G., Rooijakkers, S. H., van Kessel, K. P., de Cock, H., Wosten, H. A., van Strijp, J. A., & Haas, P. J. (2015). Effective Neutrophil Phagocytosis of Aspergillus fumigatus Is Mediated by Classical Pathway Complement Activation. *J Innate Immun, 7*(4), 364-374. doi:10.1159/000369493

Brown, G. D., & Gordon, S. (2001). Immune recognition - A new receptor for beta-glucans. *Nature, 413*(6851), 36-37. doi:Doi 10.1038/35092620

Brown, M. J., Worthy, S. A., Flint, J. D. A., & Muller, N. L. (1998). Invasive aspergillosis in the immunocompromised host: Utility of computed tomography and bronchoalveolar lavage. *Clinical Radiology, 53*(4), 255-257. doi:Doi 10.1016/S0009-9260(98)80122-0

Caillot, D., Casasnovas, O., Bernard, A., Couaillier, J. F., Durand, C., Cuisenier, B., . . . Guy, H. (1997). Improved management of invasive pulmonary aspergillosis in neutropenic patients using early thoracic computed

tomographic scan and surgery. *Journal of Clinical Oncology, 15*(1), 139-147. Retrieved from <Go to ISI>://WOS:A1997WB90700020

Carlos, T. M., & Harlan, J. M. (1994). Leukocyte-endothelial adhesion molecules. *Blood, 84*(7), 2068-2101. Retrieved from http://www.ncbi.nlm.nih.gov/pubmed/7522621

Chavan, S. S., Tian, W. Z., Hsueh, K., Jawaheer, D., Gregersen, P. K., & Chu, C. C. (2002). Characterization of the human homolog of the IL-4 induced gene-1 (Fig1). *Biochimica Et Biophysica Acta-Gene Structure and Expression, 1576*(1-2), 70-80. doi:Pii S0167-4781(02)00295-6

Doi 10.1016/S0167-4781(02)00295-6

Chazalet, V., Debeaupuis, J. P., Sarfati, J., Lortholary, J., Ribaud, P., Shah, P., . . . Latge, J. P. (1998). Molecular typing of environmental and patient isolates of Aspergillus fumigatus from various hospital settings. *J Clin Microbiol, 36*(6), 1494-1500. Retrieved from http://www.ncbi.nlm.nih.gov/pubmed/9620367

Chen, J., Chen, Z., Narasaraju, T., Jin, N., & Liu, L. (2004). Isolation of highly pure alveolar epithelial type I and type II cells from rat lungs. *Lab Invest, 85*(9), 1181-1181. Retrieved from http://dx.doi.org/10.1038/labinvest.3700318

Chu, C. C., Chavan, S. S., Naidu, M. D., Mason, J. M., Porti, D., Barcia, M., & Teichberg, S. (2004). Interleukin-four induced gene-1 (I14i1 or Fig1) expressed primarily in antigen presenting cells. *Faseb Journal, 18*(4), A37-A37. Retrieved from <Go to ISI>://WOS:000220470600178

Chu, C. C., & Paul, W. E. (1997). Fig1, an interleukin 4-induced mouse B cell gene isolated by cDNA representational difference analysis. *Proceedings of the National Academy of Sciences of the United States of America, 94*(6), 2507-2512. doi:DOI 10.1073/pnas.94.6.2507

Chuquimia, O. D., Petursdottir, D. H., Rahman, M. J., Hartl, K., Singh, M., & Fernandez, C. (2012). The Role of Alveolar Epithelial Cells in Initiating and Shaping Pulmonary Immune Responses: Communication between Innate and Adaptive Immune Systems. *PLoS One, 7*(2). doi:ARTN e32125

10.1371/journal.pone.0032125

Cooper, G. M., & Hausman, R. E. (2013). *The cell : a molecular approach* (6. ed. H1 - E31 VOH4301(6) ed.). Sunderland, Mass.: Sinauer Assoc.

Corti, M., Brody, A. R., & Harrison, J. H. (1996). Isolation and primary culture of murine alveolar type II cells. *Am J Respir Cell Mol Biol, 14*(4), 309-315. doi:10.1165/ajrcmb.14.4.8600933

Cousin, C., Aubatin, A., Le Gouvello, S., Apetoh, L., Castellano, F., & Molinier-Frenkel, V. (2015). The immunosuppressive enzyme IL4I1 promotes FoxP3(+) regulatory T lymphocyte differentiation. *Eur J Immunol, 45*(6), 1772-1782. doi:10.1002/eji.201445000

Croft, C. A., Culibrk, L., Moore, M. M., & Tebbutt, S. J. (2016). Interactions of Aspergillus fumigatus Conidia with Airway Epithelial Cells: A Critical Review. *Front Microbiol, 7*, 472. doi:10.3389/fmicb.2016.00472

Daniels, C. C., Rogers, P. D., & Shelton, C. M. (2016). A Review of Pneumococcal Vaccines: Current Polysaccharide Vaccine Recommendations and Future Protein Antigens. *J Pediatr Pharmacol Ther, 21*(1), 27-35. doi:10.5863/1551-6776-21.1.27

DeHart, D. J., Agwu, D. E., Julian, N. C., & Washburn, R. G. (1997). Binding and germination of Aspergillus fumigatus conidia on cultured A549 pneumocytes.

Journal of Infectious Diseases, 175(1), 146-150. Retrieved from <Go to ISI>://WOS:A1997WA93700021

Denning, D. W. (1998). Invasive aspergillosis. *Clinical Infectious Diseases, 26*(4), 781-803. doi:Doi 10.1086/513943

Dovey, J. S., Zacharek, S. J., Kim, C. F., & Lees, J. A. (2008). Bmi1 is critical for lung tumorigenesis and bronchioalveolar stem cell expansion. *Proceedings of the National Academy of Sciences of the United States of America, 105*(33), 11857-11862. doi:10.1073/pnas.0803574105

Drummond, R. A., & Brown, G. D. (2011). The role of Dectin-1 in the host defence against fungal infections. *Current Opinion in Microbiology, 14*(4), 392-399. doi:10.1016/j.mib.2011.07.001

Dyer, P. S., & Paoletti, M. (2005). Reproduction in Aspergillus fumigatus: sexuality in a supposedly asexual species? *Med Mycol, 43 Suppl 1*, S7-14.

Ene, I. V., & Bennett, R. J. (2014). The Cryptic Sexual Strategies of Human Fungal Pathogens. *Nature reviews. Microbiology, 12*(4), 239-251. doi:10.1038/nrmicro3236

Fenn, J. B., Mann, M., Meng, C. K., Wong, S. F., & Whitehouse, C. M. (1989). Electrospray ionization for mass spectrometry of large biomolecules. *Science, 246*(4926), 64-71. Retrieved from http://www.ncbi.nlm.nih.gov/pubmed/2675315

Geginat, J., Nizzoli, G., Paroni, M., Maglie, S., Larghi, P., Pascolo, S., & Abrignani, S. (2015). Immunity to pathogens taught by specialized human dendritic cell subsets. *Frontiers in Immunology, 6*. doi:UNSP 527

10.3389/fimmu.2015.00527

Geissmann, F., Manz, M. G., Jung, S., Sieweke, M. H., Merad, M., & Ley, K. (2010). Development of monocytes, macrophages, and dendritic cells. *Science, 327*(5966), 656-661. doi:10.1126/science.1178331

Gereke, M., Autengruber, A., Grobe, L., Jeron, A., Bruder, D., & Stegemann-Koniszewski, S. (2012). Flow cytometric isolation of primary murine type II alveolar epithelial cells for functional and molecular studies. *J Vis Exp*(70). doi:10.3791/4322

Gereke, M., Jung, S., Buer, J., & Bruder, D. (2009). Alveolar type II epithelial cells present antigen to CD4(+) T cells and induce Foxp3(+) regulatory T cells. *Am J Respir Crit Care Med, 179*(5), 344-355. doi:10.1164/rccm.200804-592OC

Ginhoux, F., & Jung, S. (2014). Monocytes and macrophages: developmental pathways and tissue homeostasis. *Nat Rev Immunol, 14*(6), 392-404. doi:10.1038/nri3671

Golubovskaya, V., & Wu, L. (2016). Different Subsets of T Cells, Memory, Effector Functions, and CAR-T Immunotherapy. *Cancers (Basel), 8*(3). doi:10.3390/cancers8030036

Gordon, S. (2016). Phagocytosis: An Immunobiologic Process. *Immunity, 44*(3), 463-475. doi:10.1016/j.immuni.2016.02.026

Gordon, S., & Taylor, P. R. (2005). Monocyte and macrophage heterogeneity. *Nat Rev Immunol, 5*(12), 953-964. Retrieved from http://dx.doi.org/10.1038/nri1733

http://www.nature.com/nri/journal/v5/n12/pdf/nri1733.pdf

Grebe, S. K., & Singh, R. J. (2011). LC-MS/MS in the Clinical Laboratory - Where to From Here? *Clin Biochem Rev, 32*(1), 5-31. Retrieved from http://www.ncbi.nlm.nih.gov/pubmed/21451775

Gross, O., Gewies, A., Finger, K., Schafer, M., Sparwasser, T., Peschel, C., . . . Ruland, J. (2006). Card9 controls a non-TLR signalling pathway for innate anti-fungal immunity. *Nature, 442*(7103), 651-656. doi:10.1038/nature04926

Guilliams, M., Ginhoux, F., Jakubzick, C., Naik, S. H., Onai, N., Schraml, B. U., . . . Yona, S. (2014). Dendritic cells, monocytes and macrophages: a unified nomenclature based on ontogeny. *Nat Rev Immunol, 14*(8), 571-578. doi:10.1038/nri3712

Haines, J. (1995). Aspergillus in Compost - Straw Man or Fatal Flaw. *Biocycle, 36*(4), 32-35. Retrieved from <Go to ISI>://WOS:A1995QU25900005

Hasenberg, A., Hasenberg, M., Mann, L., Neumann, F., Borkenstein, L., Stecher, M., . . . Gunzer, M. (2015). Catchup: a mouse model for imaging-based tracking and modulation of neutrophil granulocytes. *Nature Methods, 12*(5), 445-+. doi:10.1038/Nmeth.3322

Hasenberg, M., Kohler, A., Bonifatius, S., Borucki, K., Riek-Burchardt, M., Achilles, J., . . . Gunzer, M. (2011). Rapid immunomagnetic negative enrichment of neutrophil granulocytes from murine bone marrow for functional studies in vitro and in vivo. *PLoS One, 6*(2), e17314. doi:10.1371/journal.pone.0017314

Haynes, P. A., & Yates, J. R., 3rd. (2000). Proteome profiling-pitfalls and progress. *Yeast, 17*(2), 81-87. doi:10.1002/1097-0061(20000630)17:2<81::AID-YEA22>3.0.CO;2-Z

Hearn, V. M., & Mackenzie, D. W. R. (1980). Mycelial Antigens from 2 Strains of Aspergillus-Fumigatus - an Analysis by Two-Dimensional Immunoelectrophoresis. *Mykosen, 23*(10), 549-562. Retrieved from <Go to ISI>://WOS:A1980KQ55600001

Heath, W. R., & Carbone, F. R. (2001). Cross-presentation, dendrttic cells, tolerance and immunity. *Annual Review of Immunology, 19*, 47-64. doi:DOI 10.1146/annurev.immunol.19.1.47

Horvath, J. A., & Dummer, S. (1996). The use of respiratory-tract cultures in the diagnosis of invasive pulmonary aspergillosis. *American Journal of Medicine, 100*(2), 171-178. doi:Doi 10.1016/S0002-9343(97)89455-7

Jakubzick, C., Tacke, F., Ginhoux, F., Wagers, A. J., van Rooijen, N., Mack, M., . . . Randolph, G. J. (2008). Blood monocyte subsets differentially give rise to CD103+ and CD103- pulmonary dendritic cell populations. *J Immunol, 180*(5), 3019-3027. Retrieved from http://www.ncbi.nlm.nih.gov/pubmed/18292524

http://www.jimmunol.org/content/180/5/3019.full.pdf

Kelly, M., Hwang, J. M., & Kubes, P. (2007). Modulating leukocyte recruitment in inflammation. *J Allergy Clin Immunol, 120*(1), 3-10. doi:10.1016/j.jaci.2007.05.017

Khan, N., Vidyarthi, A., Javed, S., & Agrewala, J. N. (2016). Innate Immunity Holding the Flanks until Reinforced by Adaptive Immunity against Mycobacterium tuberculosis Infection. *Front Microbiol, 7*, 328. doi:10.3389/fmicb.2016.00328

Kim, C. F., Jackson, E. L., Woolfenden, A. E., Lawrence, S., Babar, I., Vogel, S., . . . Jacks, T. (2005). Identification of bronchioalveolar stem cells in normal lung and lung cancer. *Cell, 121*(6), 823-835. doi:10.1016/j.cell.2005.03.032

Kindt, T. J., Goldsby, R. A., Osborne, B. A., & Kuby, J. (2007). *Kuby immunology*. New York: W.H. Freeman.

Kobayashi, S. D., Malachowa, N., & DeLeo, F. R. (2015). Pathogenesis of Staphylococcus aureus Abscesses. *The American Journal of Pathology, 185*(6), 1518-1527. doi:http://dx.doi.org/10.1016/j.ajpath.2014.11.030

Krappmann, S., Bayram, Ö., & Braus, G. H. (2005). Deletion and Allelic Exchange of the Aspergillus fumigatus veA Locus via a Novel Recyclable Marker Module. *Eukaryotic Cell, 4*(7), 1298-1307. doi:10.1128/EC.4.7.1298-1307.2005

Kwon-Chung, K. J., & Bennett, J. E. (1992). Medical mycology. *Revista do Instituto de Medicina Tropical de São Paulo, 34*, 504-504.

Latgé, J.-P. (1999). Aspergillus fumigatus and Aspergillosis. *Clinical Microbiology Reviews, 12*(2), 310-350. Retrieved from http://www.ncbi.nlm.nih.gov/pmc/articles/PMC88920/

http://www.ncbi.nlm.nih.gov/pmc/articles/PMC88920/pdf/cm000310.pdf

Latge, J. P. (1995). Tools and trends in the detection of Aspergillus fumigatus. *Curr Top Med Mycol, 6*, 245-281. Retrieved from http://www.ncbi.nlm.nih.gov/pubmed/8724248

Lee, K. H., Gordon, A., & Foxman, B. (2016). The role of respiratory viruses in the etiology of bacterial pneumonia: An ecological perspective. *Evol Med Public Health, 2016*(1), 95-109. doi:10.1093/emph/eow007

Li, W. T., Freudenberg, J., Suh, Y. J., & Yang, Y. N. (2014). Using volcano plots and regularized-chi statistics in genetic association studies. *Computational Biology and Chemistry, 48*, 77-83. doi:10.1016/j.compbiolchem.2013.02.003

Lominadze, G., Ward, R. A., Klein, J. B., & McLeish, K. R. (2006). Proteomic analysis of human neutrophils. *Methods Mol Biol, 332*, 343-356. doi:10.1385/1-59745-048-0:343

Lwebuga-Mukasa, J. S. (1991). Matrix-driven pneumocyte differentiation. *American Review of Respiratory Disease, 144*(2), 452-457. doi:10.1164/ajrccm/144.2.452

Mansour, M. K., Tam, J. M., & Vyas, J. M. (2012). The cell biology of the innate immune response to Aspergillus fumigatus. *Annals of the New York Academy of Sciences, 1273*(1), 78-84. doi:10.1111/j.1749-6632.2012.06837.x

Mansour, M. K., Tam, J. M., & Vyas, J. M. (2012). The cell biology of the innate immune response to Aspergillus fumigatus. *Advances against Aspergillosis Ii, 1273*, 78-84. doi:10.1111/j.1749-6632.2012.06837.x

Mantovani, A., Cassatella, M. A., Costantini, C., & Jaillon, S. (2011). Neutrophils in the activation and regulation of innate and adaptive immunity. *Nat Rev Immunol, 11*(8), 519-531. Retrieved from http://dx.doi.org/10.1038/nri3024

http://www.nature.com/nri/journal/v11/n8/pdf/nri3024.pdf

Margalit, A., & Kavanagh, K. (2015). The innate immune response to Aspergillus fumigatus at the alveolar surface. *Fems Microbiology Reviews, 39*(5), 670-687. doi:10.1093/femsre/fuv018

Martino, P., Raccah, R., Gentile, G., Venditti, M., Girmenia, C., & Mandelli, F. (1989). Aspergillus Colonization of the Nose and Pulmonary Aspergillosis in Neutropenic Patients - a Retrospective Study. *Haematologica, 74*(3), 263-265. Retrieved from <Go to ISI>://WOS:A1989AD72300004

Mason, J. M., Naidu, M. D., Barcia, M., Porti, D., Chavan, S. S., & Chu, C. C. (2004). IL-4-induced gene-1 is a leukocyte L-amino acid oxidase with an unusual

acidic pH preference and lysosomal localization. *J Immunol, 173*(7), 4561-4567. Retrieved from http://www.jimmunol.org/content/173/7/4561.full.pdf

Megger, D. A., Bracht, T., Meyer, H. E., & Sitek, B. (2013). Label-free quantification in clinical proteomics. *Biochim Biophys Acta, 1834*(8), 1581-1590. doi:10.1016/j.bbapap.2013.04.001

Middleton, J., Patterson, A. M., Gardner, L., Schmutz, C., & Ashton, B. A. (2002). Leukocyte extravasation: chemokine transport and presentation by the endothelium. *Blood, 100*(12), 3853-3860. doi:10.1182/blood.V100.12.3853

Muller, W. A. (2013). Getting leukocytes to the site of inflammation. *Vet Pathol, 50*(1), 7-22. doi:10.1177/0300985812469883

Murphy, K. P., & Janeway, C. (2012). *Janeway's immunobiology* (8. ed. ed.). London [u.a.]: Garland Science.

Murray, P. J., & Wynn, T. A. (2011a). Obstacles and opportunities for understanding macrophage polarization. *Journal of Leukocyte Biology, 89*(4), 557-563. doi:10.1189/jlb.0710409

Murray, P. J., & Wynn, T. A. (2011b). Protective and pathogenic functions of macrophage subsets. *Nat Rev Immunol, 11*(11), 723-737. Retrieved from http://dx.doi.org/10.1038/nri3073

Nalesnik, M. A., Myerowitz, R. L., Jenkins, R., Lenkey, J., & Herbert, D. (1980). Significance of Aspergillus Species Isolated from Respiratory Secretions in the Diagnosis of Invasive Pulmonary Aspergillosis. *Journal of Clinical Microbiology, 11*(4), 370-376. Retrieved from <Go to ISI>://WOS:A1980JP90000013

Neyt, K., & Lambrecht, B. N. (2013). The role of lung dendritic cell subsets in immunity to respiratory viruses. *Immunological Reviews, 255*(1), 57-67. doi:10.1111/imr.12100

Nichols, B. A., Bainton, D. F., & Farquhar, M. G. (1971). Differentiation of monocytes. Origin, nature, and fate of their azurophil granules. *J Cell Biol, 50*(2), 498-515. Retrieved from http://www.ncbi.nlm.nih.gov/pubmed/4107019

O'Farrell, P. H. (1975). High resolution two-dimensional electrophoresis of proteins. *Journal of Biological Chemistry, 250*(10), 4007-4021. Retrieved from http://www.ncbi.nlm.nih.gov/pubmed/236308

O'Gorman, C. M., Fuller, H., & Dyer, P. S. (2009). Discovery of a sexual cycle in the opportunistic fungal pathogen Aspergillus fumigatus. *Nature, 457*(7228), 471-474. doi:10.1038/nature07528

Osherov, N. (2012). Interaction of Aspergillus fumigatus with host cells. *Mycoses, 55*, 8-8. Retrieved from <Go to ISI>://WOS:000305069800024

Overgaard, C. E., Mitchell, L. A., & Koval, M. (2012). Roles for claudins in alveolar epithelial barrier function. *Barriers and Channels Formed by Tight Junction Proteins I, 1257*, 167-174. doi:10.1111/j.1749-6632.2012.06545.x

Paris, S., Boisvieux-Ulrich, E., Crestani, B., Houcine, O., Taramelli, D., Lombardi, L., & Latgé, J. P. (1997). Internalization of Aspergillus fumigatus conidia by epithelial and endothelial cells. *Infection and Immunity, 65*(4), 1510-1514. Retrieved from http://www.ncbi.nlm.nih.gov/pmc/articles/PMC175160/

http://iai.asm.org/content/65/4/1510.full.pdf

Pearson, K. (1901). Statistical investigations on variability and heredity. *Nature, 64*, 102-102. doi:DOI 10.1038/064102b0

Pitsillides, C. M., Runnels, J. M., Spencer, J. A., Zhi, L., Wu, M. X., & Lin, C. P. (2011). Cell labeling approaches for fluorescence-based in vivo flow cytometry. *Cytometry A, 79*(10), 758-765. doi:10.1002/cyto.a.21125

Pitt, J. J. (2009). Principles and applications of liquid chromatography-mass spectrometry in clinical biochemistry. *Clin Biochem Rev, 30*(1), 19-34. Retrieved from http://www.ncbi.nlm.nih.gov/pubmed/19224008

Price, P. (1991). Standard definitions of terms relating to mass spectrometry : A report from the committee on measurements and standards of the American society for mass spectrometry. *J Am Soc Mass Spectrom, 2*(4), 336-348. doi:10.1016/1044-0305(91)80025-3

Puiffe, M. L., Lachaise, I., Molinier-Frenkel, V., & Castellano, F. (2013). Antibacterial properties of the mammalian L-amino acid oxidase IL4I1. *PLoS One, 8*(1), e54589. doi:10.1371/journal.pone.0054589

Rabinovitch, M. (1995). Professional and non-professional phagocytes: an introduction. *Trends Cell Biol, 5*(3), 85-87. Retrieved from http://www.ncbi.nlm.nih.gov/pubmed/14732160

Raiser, D. M., & Kim, C. F. (2009). Sca-1 and Cells of the Lung: A Matter of Different Sorts. *Stem cells (Dayton, Ohio), 27*(3), 606-611. doi:10.1002/stem.10

Ribaud, P., Esperoubourdeau, H., Devergie, A., & Gluckman, E. (1994). Invasive Aspergillosis and Allogeneic Bone-Marrow Transplantation. *Pathologie Biologie, 42*(7), 652-655. Retrieved from <Go to ISI>://WOS:A1994PN02900005

Ricevuti, G., Mazzone, A., Fossati, G., Mazzucchelli, I., Cavigliano, P. M., Pasotti, D., & Notario, A. (1993). Assay of phagocytic cell functions. *Allerg Immunol (Paris), 25*(2), 55-66. Retrieved from http://www.ncbi.nlm.nih.gov/pubmed/8385468

Rivollier, A., He, J. P., Kole, A., Valatas, V., & Kelsall, B. L. (2012). Inflammation switches the differentiation program of Ly6C(hi) monocytes from antiinflammatory macrophages to inflammatory dendritic cells in the colon. *Journal of Experimental Medicine, 209*(1), 139-155. doi:10.1084/jem.20101387

Rock, J. R., & Hogan, B. L. (2011). Epithelial progenitor cells in lung development, maintenance, repair, and disease. *Annu Rev Cell Dev Biol, 27*, 493-512. doi:10.1146/annurev-cellbio-100109-104040

Rogers, T. R. (1995). Epidemiology and Control of Nosocomial Fungal-Infections. *Current Opinion in Infectious Diseases, 8*(4), 287-290. doi:Doi 10.1097/00001432-199508000-00014

Rozycki, H. J. (2014). Potential contribution of type I alveolar epithelial cells to chronic neonatal lung disease. *Front Pediatr, 2*, 45. doi:10.3389/fped.2014.00045

Sahara, H., & Shastri, N. (2003). Second class minors: Molecular identification of the autosomal H46 histocompatibility locus as a peptide presented by major histocompatibility complex class II molecules. *Journal of Experimental Medicine, 197*(3), 375-385. doi:10.1084/jem.20021961

Saiga, H., Nishimura, J., Kuwata, H., Okuyama, M., Matsumoto, S., Sato, S., . . . Takeda, K. (2008). Lipocalin 2-Dependent Inhibition of Mycobacterial Growth in Alveolar Epithelium. *Journal of Immunology, 181*(12), 8521-8527. Retrieved from <Go to ISI>://WOS:000261583000040

Sans, E., Delachanal, E., & Duperray, A. (2001). Analysis of the roles of ICAM-1 in neutrophil transmigration using a reconstituted mammalian cell expression

model: Implication of ICAM-1 cytoplasmic domain and Rho-dependent signaling pathway. *Journal of Immunology, 166*(1), 544-551. Retrieved from <Go to ISI>://WOS:000166012400068

Savina, A., & Amigorena, S. (2007). Phagocytosis and antigen presentation in dendritic cells. *Immunological Reviews, 219*, 143-156. doi:DOI 10.1111/j.1600-065X.2007.00552.x

Schaffner, A., Douglas, H., & Braude, A. (1982). Selective Protection against Conidia by Mononuclear and against Mycelia by Polymorphonuclear Phagocytes in Resistance to Aspergillus - Observations on These 2 Lines of Defense Invivo and Invitro with Human and Mouse Phagocytes. *Journal of Clinical Investigation, 69*(3), 617-631. doi:Doi 10.1172/Jci110489

Schroder, A. J., Pavlidis, P., Arimura, A., Capece, D., & Rothman, P. B. (2002). Cutting edge: STAT6 serves as a positive and negative regulator of gene expression in IL-4-stimulated B lymphocytes. *J Immunol, 168*(3), 996-1000. Retrieved from http://www.ncbi.nlm.nih.gov/pubmed/11801631

Sheshachalam, A., Srivastava, N., Mitchell, T., Lacy, P., & Eitzen, G. (2014). Granule protein processing and regulated secretion in neutrophils. *Frontiers in Immunology, 5*, 448. doi:10.3389/fimmu.2014.00448

Shi, C., & Pamer, E. G. (2011). Monocyte recruitment during infection and inflammation. *Nat Rev Immunol, 11*(11), 762-774. Retrieved from http://dx.doi.org/10.1038/nri3070

http://www.nature.com/nri/journal/v11/n11/pdf/nri3070.pdf

Si, Y., Tsou, C. L., Croft, K., & Charo, I. F. (2010). CCR2 mediates hematopoietic stem and progenitor cell trafficking to sites of inflammation in mice. *Journal of Clinical Investigation, 120*(4), 1192-1203. doi:10.1172/JCI40310

Sibille, Y., & Reynolds, H. Y. (1990). Macrophages and Polymorphonuclear Neutrophils in Lung Defense and Injury. *American Review of Respiratory Disease, 141*(2), 471-501. Retrieved from <Go to ISI>://WOS:A1990CN84500034

Soehnlein, O., & Lindbom, L. (2009). Neutrophil-derived azurocidin alarms the immune system. *J Leukoc Biol, 85*(3), 344-351. doi:10.1189/jlb.0808495

Strunk, R. C., Eidlen, D. M., & Mason, R. J. (1988). Pulmonary Alveolar Type-Ii Epithelial-Cells Synthesize and Secrete Proteins of the Classical and Alternative Complement Pathways. *Journal of Clinical Investigation, 81*(5), 1419-1426. doi:Doi 10.1172/Jci113472

Summers, C., Rankin, S. M., Condliffe, A. M., Singh, N., Peters, A. M., & Chilvers, E. R. (2010). Neutrophil kinetics in health and disease. *Trends Immunol, 31*(8), 318-324. doi:10.1016/j.it.2010.05.006

Takeda, K., & Akira, S. (2005). Toll-like receptors in innate immunity. *Int Immunol, 17*(1), 1-14. doi:10.1093/intimm/dxh186

Verrills, N. M. (2006). Clinical proteomics: present and future prospects. *Clin Biochem Rev, 27*(2), 99-116. Retrieved from http://www.ncbi.nlm.nih.gov/pubmed/17077880

Ward, H. E., & Nicholas, T. E. (1984). Alveolar Type-I and Type-Ii Cells. *Australian and New Zealand Journal of Medicine, 14*(5), 731-734. doi:DOI 10.1111/j.1445-5994.1984.tb04928.x

Wasylnka, J. A., & Moore, M. M. (2002). Uptake of Aspergillus fumigatus Conidia by Phagocytic and Nonphagocytic Cells In Vitro: Quantitation Using Strains

Expressing Green Fluorescent Protein. *Infection and Immunity, 70*(6), 3156-3163. doi:10.1128/IAI.70.6.3156-3163.2002

Wasylnka, J. A., & Moore, M. M. (2003). Aspergillus fumigatus conidia survive and germinate in acidic organelles of A549 epithelial cells. *J Cell Sci, 116*(Pt 8), 1579-1587. Retrieved from http://www.ncbi.nlm.nih.gov/pubmed/12640041

Wright, J. R. (2005). Immunoregulatory functions of surfactant proteins. *Nature Reviews Immunology, 5*(1), 58-68. doi:10.1038/nri1528

Wysocka, J., Lipartowska, R., & Lipska, A. (2001). [Granules of neutrophils]. *Postepy Hig Med Dosw, 55*(1), 177-188. Retrieved from http://www.ncbi.nlm.nih.gov/pubmed/11355531

Xiang, W., Chao, Z. Y., & Feng, D. Y. (2015). Role of Toll-like receptor/MYD88 signaling in neurodegenerative diseases. *Rev Neurosci, 26*(4), 407-414. doi:10.1515/revneuro-2014-0067

Yue, Y., Huang, W., Liang, J., Guo, J., Ji, J., Yao, Y., . . . Wang, J. (2015). IL4I1 Is a Novel Regulator of M2 Macrophage Polarization That Can Inhibit T Cell Activation via L-Tryptophan and Arginine Depletion and IL-10 Production. *PLoS One, 10*(11), e0142979. doi:10.1371/journal.pone.0142979

Zeller, E. A., & Maritz, A. (1944). A new l-amino acid-oxidasis. *Helvetica Chimica Acta, 27*, 1888-1902. doi:DOI 10.1002/hlca.194402701241

Zhang, H., Yang, Q., Sun, M., Teng, M., & Niu, L. (2004). Hydrogen peroxide produced by two amino acid oxidases mediates antibacterial actions. *J Microbiol, 42*(4), 336-339. Retrieved from http://www.ncbi.nlm.nih.gov/pubmed/15650691

Zhu, J., & Paul, W. E. (2008). CD4 T cells: fates, functions, and faults. *Blood, 112*(5), 1557-1569. doi:10.1182/blood-2008-05-078154

Zumla, A., Rao, M., Wallis, R. S., Kaufmann, S. H., Rustomjee, R., Mwaba, P., . . . Host-Directed Therapies Network, c. (2016). Host-directed therapies for infectious diseases: current status, recent progress, and future prospects. *Lancet Infect Dis, 16*(4), e47-63. doi:10.1016/S1473-3099(16)00078-5

"The biography is not included in the online version for reasons of data protection".

Acknowledgemen

Firstly, I would like to express my sincere gratitude to my advisor Prof. Matthias Gunzer for the continuous support of my Ph.D study and related research, for his patience, motivation, and immense knowledge. His guidance helped me in all the time of research and writing of this thesis.

I would like to thank Prof. Axel Brakhage for giving me the chance to be a member of the International Leibniz Research School and for his insightful comments and encouragement during the annual ILRS symposia and also thesis committee meetings.

My sincere thanks and appreciation also goes to Dr. Mike Hasenberg. You have been a wonderful mentor for me. Your scientific guidance throughout these four years was priceless.

Thanks to Prof. Barbara Sitek and Dr. Thilo Bracht for their permanent scientific input during the past three years. Without the proteomics studies story of my thesis wouldn't have been round.

I would like to thank all the past and present members of the group specially Dr. Juliane Weski, Dr. Marc Schuster and Dr. Anja Hasenberg for their scientific support. Thanks to Andreas Kraus for his intuitive tips in the lab. Thanks to Dr. Eloho Etemire for his words of encouragement. Thanks to Djamschid Soluk for cheering me up every time I was down. Without you it would have been even harder. Thanks to Kamilla Wierzchowski for filling out the German forms for me. Thanks to Lukas Otto for being highly motivated even for cell sorting. Thanks to Feten Hajji for her good mood even on the busy days.

I thank Dr. Anthony Squire and Alexandra Brenzel for their support at Imaging Center Essen (IMCES).

I thank Dr. 'valerie Molinier-Frenkel and Dr. Flavia Castellano for their helpful collaboration during the last one year. I also thank Dr. Christiane Opitz for providing us with her expertise in the collaboration.

I would like to Thank Dr. Olaf Kniemeyer and Dr. Christine Vogler for their extensive support during the three weeks of my work in Jena.

Finally and most importantly I want to thank my parents. Words cannot express how grateful I am for all the sacrifices that you've made on my behalf. Thanks to my brothers for never stop believing in me. I would also want to thank all my friends who warmed my heart during the past four years.

Erklärung:

Hiermit erkläre ich, gem. § 6 Abs. 2, g der Promotionsordnung der Fakultät für Biologie zur Erlangung der Dr. rer. nat., dass ich das Arbeitsgebiet, dem das Thema *„Titel der Dissertation“* zuzuordnen ist, in Forschung und Lehre vertrete und den Antrag von *(Name des Doktoranden)* befürworte.

Essen, den _____ _____

_____

Name des wissenschaftl. Betreuers/Mitglieds der Universität Duisburg-Essen	Unterschrift d. wissenschaftl. Betreuers/ Mitglieds der Universität Duisburg-Essen

Erklärung:

Hiermit erkläre ich, gem. § 7 Abs. 2, d und f der Promotionsordnung der Fakultät für Biologie zur Erlangung des Dr. rer. nat., dass ich die vorliegende Dissertation selbständig verfasst und mich keiner anderen als der angegebenen Hilfsmittel bedient habe und alle wörtlich oder inhaltlich übernommenen Stellen als solche gekennzeichnet habe.

Essen, den _____ _____

Unterschrift des/r Doktoranden/in

Erklärung:

Hiermit erkläre ich, gem. § 7 Abs. 2, e und g der Promotionsordnung der Fakultät für Biologie zur Erlangung des Dr. rer. nat., dass ich keine anderen Promotionen bzw. Promotionsversuche in der Vergangenheit durchgeführt habe, dass diese Arbeit von keiner anderen Fakultät abgelehnt worden ist, und dass ich die Dissertation nur in diesem Verfahren einreiche.

Essen, den _____ _____

Unterschrift des/r Doktoranden/in